Investigation into the Structure of Collagen in Mineralizing Tissues

Joanne Benton

Degree of Ph.D

The University of Edinburgh

1999

Declaration

I declare that all the work presented in this thesis is the sole work of the author and has not been presented in any previous application for a degree. Help given by others has been acknowledged and all sources of information have been specifically referenced.

Joanne Benton

Acknowledgements

I would like to thank Professor W.P.T. James and the board of Governors of the Rowett Research Institute and also the University of Edinburgh for the facilities provided. I also gratefully acknowledge the financial support provided by SOAFD.

I would especially like to thank Dr. Simon Robins at the Rowett Research Institute and Dr. Tim Wess at Stirling University for their supervision and encouragement throughout my Ph.D. I also thank Dr. Jim Allan for his supervision and help in the latter stages.

I would also like to express my gratitude to the following friends and colleagues for their expert help and support:

Mr. Sandy Duncan and Mrs. Nicola Wilson for their help with HPLC and the running of the ASPEC, a special thank-you to Nicola for the washing-up.
Mrs. Phyllis Nicol for her help with cell culture.
Dr. Barry Thorpe and Dr. Paul Hocking at the Roslin Institute for providing the turkey leg tendons.
Everyone at the Daresbury Laboratory, Warrington and ESRF, Grenoble for their assistance with X-ray Diffraction.
Dr. Steve Yewdall for his help with computing at the University of Edinburgh.
All my friends, past and present from the Rowett Research Institute and the Biochemistry Department who have provided me with much help and even more laughter.
Finally I would like to thank John and my Mum and Dad for their love and support throughout this project.

Abstract

The packing of type I collagen molecules in mineralized tissues is different to those found in nonmineralized tissues. Many studies have been carried out to investigate the structures in these two environments, with turkey leg tendon being used as a model system in which to study both nonmineralized and mineralized tissue. Previously published studies using crosslink analyses in turkey leg tendon and bovine bone presented two hypotheses:

1) The post-translational chemistry and molecular environments of collagen fibrils are different in the nonmineralized and mineralized portions of turkey leg tendon.

2) The crosslink changes observed in mineralized tissue are brought about as a consequence of the mineral crystal itself, distorting the collagen packing, breaking existing crosslinks and forming alternative crosslinks.

The aim of the present study was to further investigate the structure of collagen in mineralized tissues and to elucidate which of the hypotheses is true.

Crosslink data collected for different ages of turkey leg tendon at the edge of mineralization showed no changes in the mature crosslink levels except those associated with mineralization. The reducible crosslink levels in the small sections of tissue analysed were below detection limits. X-ray diffraction analysis of different ages of turkey leg tendon also showed no changes in the axial and lateral structure except those associated with mineralization. Studies of the mineral crystal size with age showed that the crystal size increases from 12-week-old turkey leg tendon to 44-week-old turkey leg tendon and decreases in size from 44 weeks of age to 60 weeks of age, possibly due to a resorption of the mineral with age. These data together with the crosslink analysis data on different ages of tendon indicate that there is no change in the crosslink profile

accompanying the increase in size of the mineral crystal which would be expected if the growing mineral crystal distorted the collagen structure. Telopeptide organisation studies in turkey leg tendon also showed that there are no differences in the nonmineralized and mineralized portions. Again this suggests that no crosslinks are being formed with lysine residues that are not normally involved in crosslinking as a result of collagen distortion. Other studies investigating the collagen production in mineralizing and nonmineralizing portions of turkey leg tendon *in vivo* suggest that collagen is being produced at a greater rate in the mineralizing portions than in the nonmineralizing portions.

An *in vitro* study of lysine hydroxylation in bone cell culture showed no changes in the crosslinking profile in cells kept in growth media. Only after the addition of mineralizing media were changes seen. The newly synthesized collagen had high levels of a compound with the properties of HLNL (hydroxylysinonorleucine) after reduction with borohydride.

The data collected in this study suggest that the collagen being produced in early mineralization has less lysine hydroxylation in either the telopeptide or helical residues than nonmineralized tissue. An accompanying resorption of nonmineralized collagen takes place and a higher rate of production of the newly synthesized collagen. These data agree with the hypothesis that there is a different post-translational chemistry in mineralized tissue.

Contents

1. Introduction

The mechanism of mineralization of collagen type I in connective tissues is one which is not well understood. It has been established that collagen type I forms fibrils which are arranged in a specific axial array (Hodge & Petruska, 1962, 1963). Intermolecular crosslinks are thought to be important in stabilizing this molecular packing which is also essential for the organised growth of carbonated calcium phosphate (apatite) crystals within this matrix.

At the onset of mineralization of collagen, changes occur in the shape of the fibrils (Lee & Glimcher, 1989; Landis *et al.*, 1991), and in the geometry of the organisation of the molecules within a fibril (Bigi *et al.*, 1988; Katz *et al.*, 1989). Analysis of the crosslinks also indicates that there are changes in molecular packing brought about by mineralization of the collagen fibrils (Otsubo *et al.*, 1992; Yamauchi and Katz, 1993). The aim of the present study was to determine how the structure of collagen influences mineralization and whether the changes in the packing of the collagen observed with mineralization are a consequence of the mineralization itself or whether these changes occur prior to mineralization and perhaps play a role in allowing the process.

1.1 The Biochemistry of Collagen

The collagens are the most abundant structural proteins in the animal kingdom. This group of proteins is located within the extracellular matrix of connective tissue and provides an insoluble scaffold responsible for support, the attachment of macromolecules, glycoproteins, hydrated polymers and inorganic ions and also for cell attachment. This introductory section is intended to review the genetically

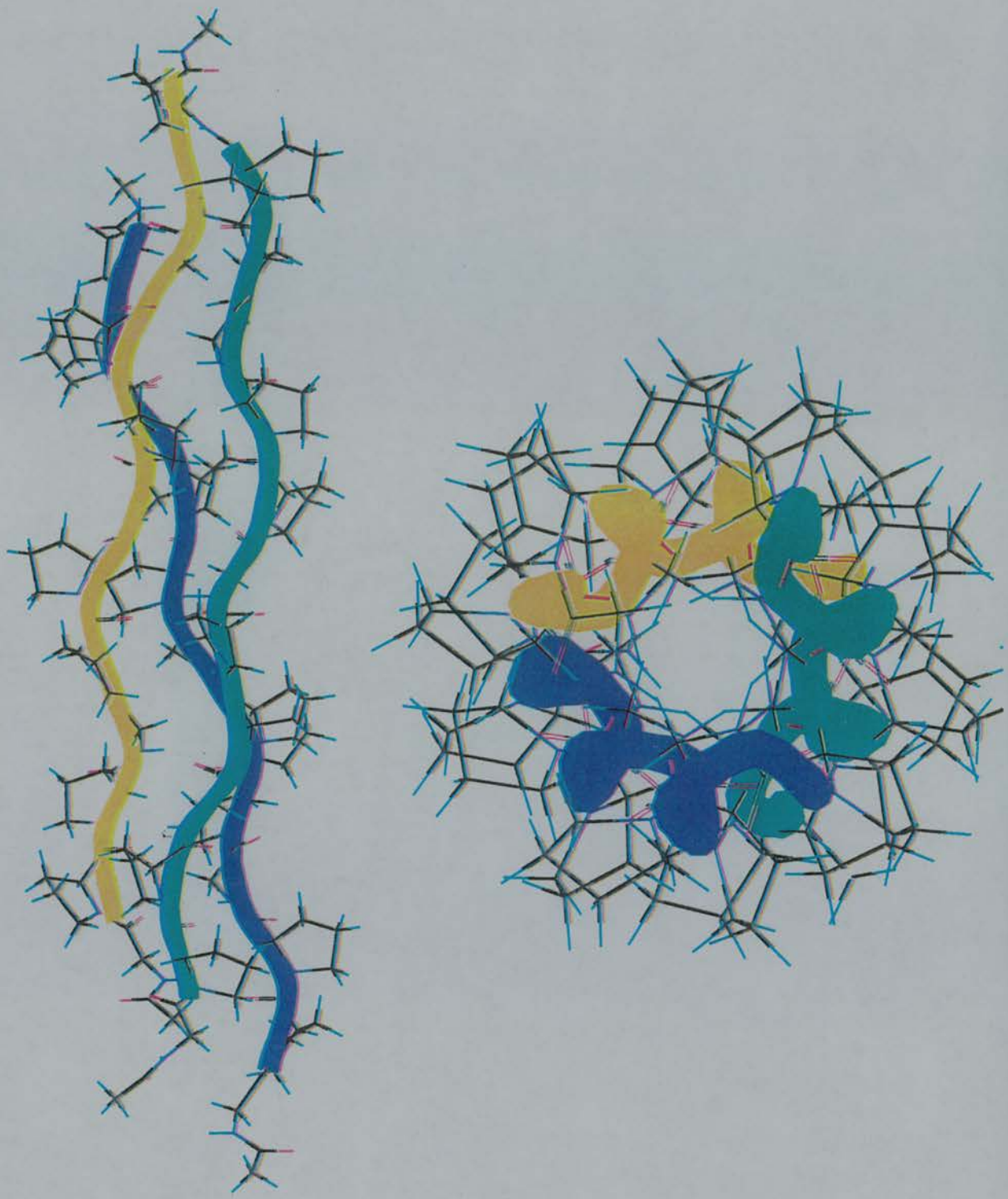

Figure 1.1 Schematic representation of collagen based on a repeating Glycine-Proline-4-Hydroxyproline. (a) Three α chains folded into a superhelix with glycine residues at the centre of the molecule; (b) end-on view looking down the centre of the long axis of the superhelix. From RasMol Software.

distinct collagen types and to describe the biosynthesis and the post-translational modifications of collagen type I with particular emphasis on the final structure of the collagen and the steps that determine it.

1.1.1 Collagen Family.

All collagens comprise three polypeptide or α chains formed by the repeating Gly-X-Y sequence where X and Y are often proline and hydroxyproline respectively. Other amino acids can be present in X and Y allowing stabilizing interactions between α chains (van der Rest & Garrone, 1991). Each α chain twists in a left-handed helix with three residues per turn and the three chains are wound together in a right-handed triple helix (Figure 1.1) to form a rod-like molecule about 1.4 nm in diameter (Ramachandran & Reddi, 1976). Glycine in every third residue is essential for the folding of the three chains into a triple helix. A left-handed twist is introduced in the peptide backbone by the pyrroline ring of proline placing the glycine residues in each chain into the centre of the of a triple helix.

1.1.2 Collagen Types.

To distinguish one collagen type from another, vertebrate collagens were assigned Roman numerals in order of discovery. Polypeptide chains have been distinguished by being called α1, α2, α3 etc. The collagen family can be divided into sub-groups; fibrillar collagens, fibril associated collagens with interrupted triple helices (FACIT), basement membrane collagens and short chain collagens (Table 1.1). These groupings

Collagen Subgroup	Collagen Type	Composition	Supramolecular Structure	Distribution
Fibrillar	I	α1(I), α2(I)	Large diameter banded fibrils	Skin, bone, tendon, ligament, cornea.
Fibrillar	II	α1(II)	Small diameter banded fibrils	Cartilage, vitreous, annulus fibrosus.
Fibrillar	III	α1(III)	Small diameter banded fibrils	Foetal skin, tendon, aorta, cornea
Fibrillar	V	α1(V), α2(V), α3(V)	Fine banded fibrils	Same as type I
Fibrillar	XI	α1(XI), α2(XI), α3(XI)	Monomers staggered by 67 nm	Cartilage
FACIT	IX	α1(IX), α2(IX) α3(IX)	Covalently crosslinked to surface of type II collagen fibrils	Cartilage.
FACIT	XII	α1(XII)	Probably associates with surface of type I collagen fibrils	Type I containing tissues.
FACIT	XIV	α1(XIV)	-	Type I containing tissues
Basement membrane	IV	α1(IV), α2(IV), α3(IV), α4(IV), α5(IV)	Non-fibrillar network	All basement membranes.
Basement membrane	VII	α1(VII)	Anchoring fibrils	Skin, oral mucosa, cervix.
Short Chain Collagens	VIII	α1(VII), α2(VII)	-	Descemet's membrane, embryonic heart, placental capillaries.
Short Chain Collagens	X	α1(X)	-	Hypertrophic cartilage.
VI	VI	α1(VI), α2(VI), α3(VI)	3-5 nm, beaded microfibrils with 100 nm periodicity	Skin, cornea, tendon, ligament, cartilage.

Table1.1 Genetically distinct collagen types (Ayad *et al.*, 1994).

are based on each collagen's function and genetic similarity. This introduction to collagen will focus on the fibrillar collagen type I.

1.1.2.1 Fibrillar Collagens.

Fibrillar collagens are defined as those which have an uninterrupted triple helical region as the major part of the molecule and which form characteristic D banded fibrils. This group includes collagen types I, II, III, V and XI, which form the bulk, extracellular fabric of the major connective tissues such as skin, bone, tendon, ligaments and cartilage.

1.1.3 Biosynthesis of Collagen Type I

The biosynthesis of fibril forming type I collagen as soluble precursor procollagens is a two stage process, intracellular and extracellular (reviewed by Kadler, 1994).

The first, intracellular steps involve the synthesis of nascent ∝ chains which undergo various post-translational modifications on transport to the rough endoplasmic reticulum. As a result of these modifications and several bound molecular chaperones, the chains are folded into a triple helical, soluble procollagen molecule. This is then secreted from the cell via transport to the Golgi apparatus and vesicles, again regulated by chaperone proteins and directed to the plasma membrane by the N-terminal propeptide (Lee *et al.*, 1992).

The second, extracellular steps involve the proteolytic cleavage of the C- and N-propeptides of procollagen, using secreted enzymes, to form collagen molecules which begin to self assemble into fibrils. The action of lysyl oxidase on the growing fibrils promotes crosslinking within the fibrils which provides stabilization.

1.1.3.1 Intracellular Steps

A. Transcription and Translation

Collagen type I and other fibrillar collagens are related in that they all have a similar gene structure (reviewed by Chu & Prockop, 1993). For collagen type I the proα1(I) gene contains 51 exons and the proα2(I) gene 52 exons. The exons coding for the triple helical sequences are all multiples of 9 base pairs corresponding to a Gly-Xaa-Yaa triplet; most common are 45, 54 and 108 base pairs. The exons coding for the N and C non-helical domains are larger and unrelated. This highly conserved sequence suggests that the fibrillar collagen genes have evolved from an ancestral multi-exon gene coding for collagen triplets (Vuorio & de Crombrugghe, 1990). On transcription the large primary transcripts that contain copies of both the exons and introns, are poly-adenylated and the introns are removed before being exported to the cytoplasm for translation.

Translation of pre-procollagen mRNA occurs on free ribosomes. The signal peptides interact with an intermediate cytoplasmic signal recognition particle (SRP) to produce a SRP-polypeptide complex able to associate with the endoplasmic reticulum. Once in the endoplasmic reticulum, signal peptidase releases the procollagen chains. These nascent chains now undergo a number of modifications.

B. Post-Translational Modifications

Prolyl 4-hydroxylase, prolyl 3-hydroxylase and lysyl hydroxylase catalyse the conversion of peptidyl proline to 4-hydroxyproline, peptidyl proline to peptidyl 3-hydroxyproline and peptidyl lysine to hydroxylysine, respectively (reviewed by Kivirikko *et al.*, 1989). These enzymes have similar mechanisms of action and require

a non-triple-helical substrate; formation of a triple helix stops the activity of the enzymes.

Proline 4-hydroxylase hydroxylates the peptidyl proline when it is in the sequence -X-Pro-Gly. Studies have shown that the affinity of the enzyme increases with the number of repeats of this sequence as signified by a decrease in Km (Pihlajaniemi *et al.*, 1991). This suggests that there are either multiple binding sites on the enzyme or that with an increasing number of repeats the protein becomes more structurally like collagen. A two step model for prolyl 4-hydroxylase activity has been suggested (de Waal & de Jong, 1988; de Jong, *et al.*, 1991). In this scheme, there is thought to be a weak association between the prolyl 4-hydroxylase molecule and a random coil proα-chain. The second step was perceived as a "one dimensional" search whereby the enzyme seeks out permissive X-Pro-Gly sequences for subsequent hydroxylation of proline. With hydroxylation, a conformational change occurs in the nascent collagen backbone that promotes triple helix formation (Bruckner, *et al.*, 1978).

As well as 4-hydroxyproline, a small number of 3-hydroxyproline residues are formed but only at the X position and only when 4-hydroxyproline occurs at the Y position of the Gly-X-Y repeating structure of collagen. Although it is known that 4-hydroxyproline is needed for the stabilisation of the triple helix, little is known about the function of 3-hydroxyproline in collagen.

The hydroxylation of peptidyl lysine by lysyl hydroxylase requires the lysine to be in the sequence X-Lys-Gly and the mechanism of action is similar to that of prolyl 4-hydroxylase. The hydroxyl groups of the hydroxylysine serve important functions in providing attachment sites for glycosyl residues and in the formation of interchain covalent crosslinks.

Other enzymatic modifications also occur at this stage. Glycosylation of the hydroxylysine residues takes place although the extent of glycosylation varies between collagen types, between the same collagen type in different tissues and in diseases caused by mutations in collagen genes. The functions of the carbohydrate groups are unknown but it has been hypothesized that they play a part in the regulation of collagen fibril diameter (Batge *et al.*, 1997). Glycosylation of asparagine residues in the propeptides of procollagen also occurs. The functions of the asparagine-linked carbohydrate units of procollagen are unknown although these groups are mannose-rich and some functions may be mediated through interactions with mannose receptors. This certainly applies to their clearance by liver endothelial cells (Smedsrod *et al.*, 1990).

After the enzymatic post-translational modifications, assembly of the proα-chains into procollagen occurs by nucleation and propagation processes (Kuivaniemi *et al.*, 1991). The hydroxylation of the proline residues at the C-propeptides in individual chains bring about the formation of a nucleus, by hydrophobic and electrostatic interactions. These hydroxyproline residues are thought to bring the three chains into correct dihedral angles so proper hydrogen bonds can form (Bulleid *et al.*, 1997). Non-specific folding of ∝-chains is prevented by bound heat shock protein 47, which is one of the several chaperone proteins that play a role in collagen folding (Nagata & Hosokawa, 1996). Interchain disulphide bonds form between these C propeptides to stabilise the folding (Byers, *et al.*, 1975). Protein-disulphide isomerase is a catalyst for the formation of the disulphide bonds. This is another of the chaperone proteins present during collagen folding. It has been shown that it plays a role as a subunit of prolyl 4-hydroxylase and in coordinating the assembly of the procollagen molecule (Wilson *et*

al., 1998). When the chains are in register the folding of the triple helix occurs, said to be "zipper-like" folding, proceeding in a C to N direction to form procollagen (Engel & Prockop, 1991). The cis to trans isomerization of the peptide bonds of the imino acids is a rate-limiting step (Davis *et al.*, 1989) Type I procollagen has propeptides at both ends of its three polypeptide chains. The N-terminal propeptides are composed of three structural regions: a globular N-terminal portion, a central triple helical region and a short C-terminal noncollagenous sequence. In the proα2 (I) chain, the N-terminal propeptide of several species lacks the N-terminal globular domain. The C-terminal propeptides of type I procollagen do not contain a triple helical domain. Procollagen is transported through the Golgi apparatus, controlled by heat shock protein 47 (Nagata, 1998) and then in vesicles from the Golgi apparatus to the extracellular matrix.

1.1.3.2 Extracellular Steps

A. Fibril Self-Assembly

The procollagen molecules become aligned in a nonstaggered array (Marchi & Leblond, 1983) in the vesicles until reaching the extracellular space. Here the pro-peptide regions are cleaved from the procollagen, by the enzymes N-peptidase and procollagen C-peptidase, resulting in a collagen molecule of 300 nm long (Figure 1.2). This removal of the pro-peptides initiates fibril self-assembly.

Spontaneous fibril self-assembly does not need enzymes or other factors and will occur easily in collagen solutions *in vitro*. Many studies on fibril formation *in vitro* have been carried out. Two main systems have been used; reconstitution of fibrils from acid extracted collagen and a cell free system where procollagen is sequentially

cleaved to collagen by the procollagen metalloproteinases. These fibrils formed in both *in vitro* systems are indistinguishable from those formed *in vivo* with respect to the growing tips and linear axial mass distribution. The exception is that they tend to be narrow in diameter and lack the tightly structured appearance of fibrils seen in tissues (Miyahara *et al.*, 1982). This is assumed to be under cell mediated control. The cell free system was developed because there was evidence that the cleavage of N- and C-propeptides of collagen play a role in diameter regulation. The level of C-proteinase has a major effect on the shapes of the fibrils in this system (Holmes *et al.*, 1996). It is not known to what extent the *in vitro* results can be applied *in vivo*. Although fibril assembly is a self assembly process, it is under considerable cellular control which is not all accounted for in the *in vitro* systems. Table 1.2 shows a summary of comparisons of fibrils from *in vitro* and *in vivo* models.

Fibril Assembly Characteristics	**Developing Tendon (*in vivo*)**	**Acid-soluble type I collagen (*in vitro*)**	**Type I pCcollagen plus C-proteinase (*in vitro*)**
Linear AMD's of fibril tips	+	+	+
Tip shape set at early stage	?	+	+
Limiting diameter at early stage	+	+	-
Unipolar fibrils	+	+	-
Bipolar fibrils	+	-	+

Table 1.2. shows a summary of the growth characteristics of early collagen fibrils in 2 *in vitro* and 1 *in vivo* system. AMD is axial mass distribution. (Kadler *et al.*, 1996)

Growth of the fibrils is largely directed by repeated clusters of hydrophobic and hydrophilic residues that divide the collagen molecule into 4.4 x D-units and cause the molecule to associate so that each is staggered by one D-unit or multiple of D-units relative to its nearest neighbours (Hulmes *et al.*, 1973; Doyle *et al.*, 1974). Short telopeptide sequences at the N-and C- termini of the triple-helical domains are important in stabilizing these initial aggregates (Brennan & Davison, 1980). From experiments performed *in vitro* it was

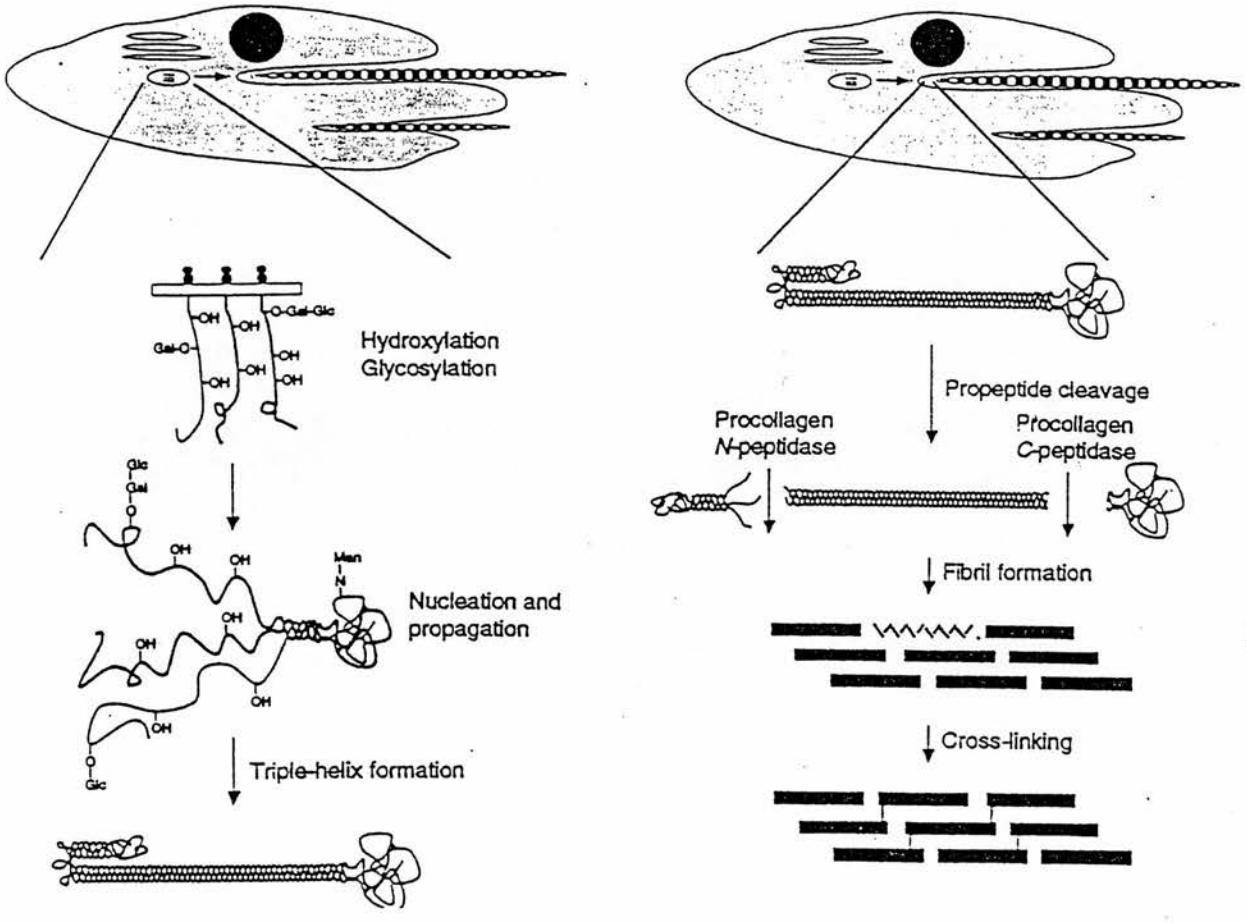

Figure 1.2 The structure of the procollagen molecule and its processing to collagen (Kadler, 1994).

seen that newly formed fibrils had a blunt end and a pointed end or tip (Kadler *et al.*, 1990).

Initial growth of the fibrils is exclusively from the pointed end or α tip. Later β tips appear on the blunt end; then the fibrils grow simultaneously in both directions from the α tips and the β tips. This end-to-end accretion of collagen molecules into long, thin filaments occurs before the side-to-side aggregation of such filaments into broader fibrils. Regulation of the fibril diameter and length are as yet not well understood. This regulation is evident in the growth of collagen fibrils *in vivo*, but this regulation is lost when the collagen is extracted or when fibrils are generated from pure solutions. Other types of collagen and proteoglycans may have a role in exerting control over lateral growth of fibrils. Collagen types III and V have been found predominantly in type I containing fibrils in tendon, ligament, bone and skin and they also copolymerize with type I *in vitro* which has led to the suggestion that they may play a role in the regulation of fibril growth. The glycosaminoglycan side chain of what appears to be decorin has been immunolocalized to the surface of collagen fibrils in several tissues. Decorin is known to inhibit collagen fibrillogenesis and to alter the morphology of the fibrils formed *in vitro* which again suggests a role for proteoglycans in the control of fibril growth (Doane *et al.*, 1992). The structure of the fibrils will be discussed in detail in a later section. With the assembly of fibrils comes the formation of inter- and intramolecular covalent crosslinks.

1.1.4 Collagen Crosslinking.

Collagen crosslinks are vital for the strength and normal function of the collagen fibrils. They are based on aldehyde formation and condensation involving specific lysine and hydroxylysine residues. This process is catalysed by a single enzyme, lysyl oxidase.

1.1.4.1 Lysyl Oxidase

Lysyl oxidase catalyses the oxidation of telopeptide lysine and hydroxylysine residues to their respective aldehydes, allysine and hydroxyallysine. Although this is the only enzyme involved in the formation of crosslinks, the activity of lysyl hydroxylase after translation of the collagen is vital in determining the type of crosslink formed, thus playing a major part in the characteristics of a particular tissue.

Lysyl oxidase is a copper ion-dependent enzyme and needs molecular oxygen and an aromatic carbonyl compound. This compound was originally thought to be pyridoxal 5'-phosphate or pyrrolinoquinoline quinone (reviewed by Seigal, 1979 and Kagan & Trackman, 1991) but is now known to be lysyl tyrosyl quinone formed by internal crosslinking within the active site of lysyl oxidase (Wang *et al.*, 1996). The mechanism of action for lysyl oxidases is complex. The amine substrate is initially oxidized to the aldehyde by passage of two electrons derived from the α-carbon of the substrate into the enzyme-linked, carbonyl cofactor. The reduced enzyme species can then be reoxidized to the initial, catalytically competent form upon the binding of oxygen to which two electrons are passed to form and release hydrogen peroxide. Copper is thought to be involved in this step. The activity of lysyl oxidase is

dependent on a fibrillar substrate (Yamauchi *et al.*, 1988b) and it appears that it binds to the triple helical portion of the collagen molecules. The fact that crosslinks are located throughout a fibril suggests that the enzyme acts on growing fibrils as opposed to fully formed fibrils, otherwise the crosslinks would only be located on the surface of the fibril.

In the fibrillar collagens, the crosslinking aldehydes on the telopeptides are located in nearly identical sites (Eyre & Glimcher, 1973; Robins & Duncan, 1983, 1987), three in the N-terminal portion of the molecule (one in each chain) and two in the C-terminal portion (one in each $\alpha 1$ chain). Bifunctional crosslinks are formed when a telopeptide aldehyde reacts with lysine or hydroxylysine in a conserved sequence in the helical region (-Gly-X-Hyl-Gly-His-Arg-), which occurs symmetrically at about 230 amino acid residues from each end (Fietzek *et al.*, 1977).

Intramolecular crosslinks are formed when an aldol condensation occurs between two aldehydes in adjacent chains and intermolecular crosslinks are formed when telopeptide aldehydes and the ε amino group of either lysine or hydroxylysine from the helical region on another α chain react forming a Schiff base. As physiological ageing of the tissue occurs there is a steady loss of these bifunctional crosslinks and mature crosslinks are formed. The bifunctional crosslinks condense with a further amino acid to produce these chemically different crosslinks.

Since crosslinks can be formed from lysyl derived and hydroxylysyl derived residues, two pathways have been described (Figure 1.3). The allysine pathway, involving intermediates formed from lysyl residues, predominates in skin, cornea and other soft tissues. The hydroxyallysine route of crosslinking seems to predominate in weight bearing and mineralized tissues.

1.1.4.2 The Allysine Crosslinking Pathway

A bifunctional crosslink is formed between telopeptide allysine and helical hydroxylysine called dehydro-hydroxylysinonorleucine (dehydro-HLNL). This aldimine crosslink was first isolated from rat tail tendon after reduction of the tissue with NaB^3H_4 to stabilise the Schiff base (Bailey & Peach, 1968). Unlike hydroxyallysine derived crosslinks, the aldimine does not undergo re-arrangement to form the ketoamine form (see hydroxyallysine crosslinking pathway section).

The maturation of reducible crosslinks involving histidine has led to many proposed crosslinks. Aldol-histidine and histidino-hydroxymerodesmosine (HHMD) were two such reducible crosslinks that were isolated from bovine skin by reduction with NaB^3H_4 (Tanzer *et al.*, 1973). It was proposed that a Michael addition to the α-β aldol unsaturated bonds of aldol condensation product to form aldol-histidine was followed by the formation of a Schiff base between the remaining carbonyl group on the aldol condensation product to form dehydro-HHMD. There is much contention as to whether these crosslinks exist (Bernstein & Mechanic, 1980), or whether they are an artefact of the reduction procedure (Robins & Bailey, 1973a).

Another histidine based, non-reducible crosslink has been isolated from skin called histidino-hydroxylysinonorleucine (HHL). This is a trifunctional crosslink formed from the condensation of hydroxyallysine, allysine and histidine. The formation of HHL has been linked to the disappearance of dehydro-HLNL with ageing of the tissue (Yamauchi *et al.*, 1988a).

1.1.4.3. The Hydroxyallysine Crosslinking Pathway.

Two bifunctional, reducible crosslinks are formed between telopeptide hydroxyallysine and either helical lysine or hydroxylysine to form dehydro-hydroxylysinonorleucine (HLNL) and dehydro-dihydroxylysinonorleucine (DHLNL), respectively. As with telopeptide allysine and helical hydroxylysine from the allysine pathway, these bifunctional crosslinks also form a Schiff base, but the presence of the hydroxyl group on the aldehyde in this case allows the Schiff base to re-arrange from an aldimine to a more stable ketoamine, hydroxylysino-5-oxo-norleucine via a practically irreversible Amadori re-arrangement (Robins & Bailey, 1973b, 1975).

As physiological ageing occurs, there is a decrease in the concentration of reducible crosslinks in many different tissues from a number of species, a process that is mimicked during "ageing" *in vitro*. These reducible crosslinks are converted into non-reducible, more stable mature crosslinks. The trifunctional, non-reducible, naturally fluorescing compounds, pyridinoline (Pyd) and deoxy-pyridinoline (Dpd) represent one form of the mature crosslinks. Pyd was first isolated and characterised from an acid hydrolysate of bovine Achilles tendon (Fujimoto, 1977). Dpd was first isolated from Pyd in hydrolysates of bovine femur and was found at levels approximately one fifth that of Pyd. (Ogawa *et al.*, 1982). Based on the relationship between the loss of bifunctional crosslinks and the appearance of trifunctional crosslinks two mechanisms for the formation of these crosslinks have been proposed. One mechanism suggested that two bifunctional ketoamine crosslinks condense to form one trifunctional crosslink and hydroxylysine (Eyre & Oguchi, 1980). The evidence supporting this mechanism was the stoichiometry of the loss of the bifunctional crosslinks to form the

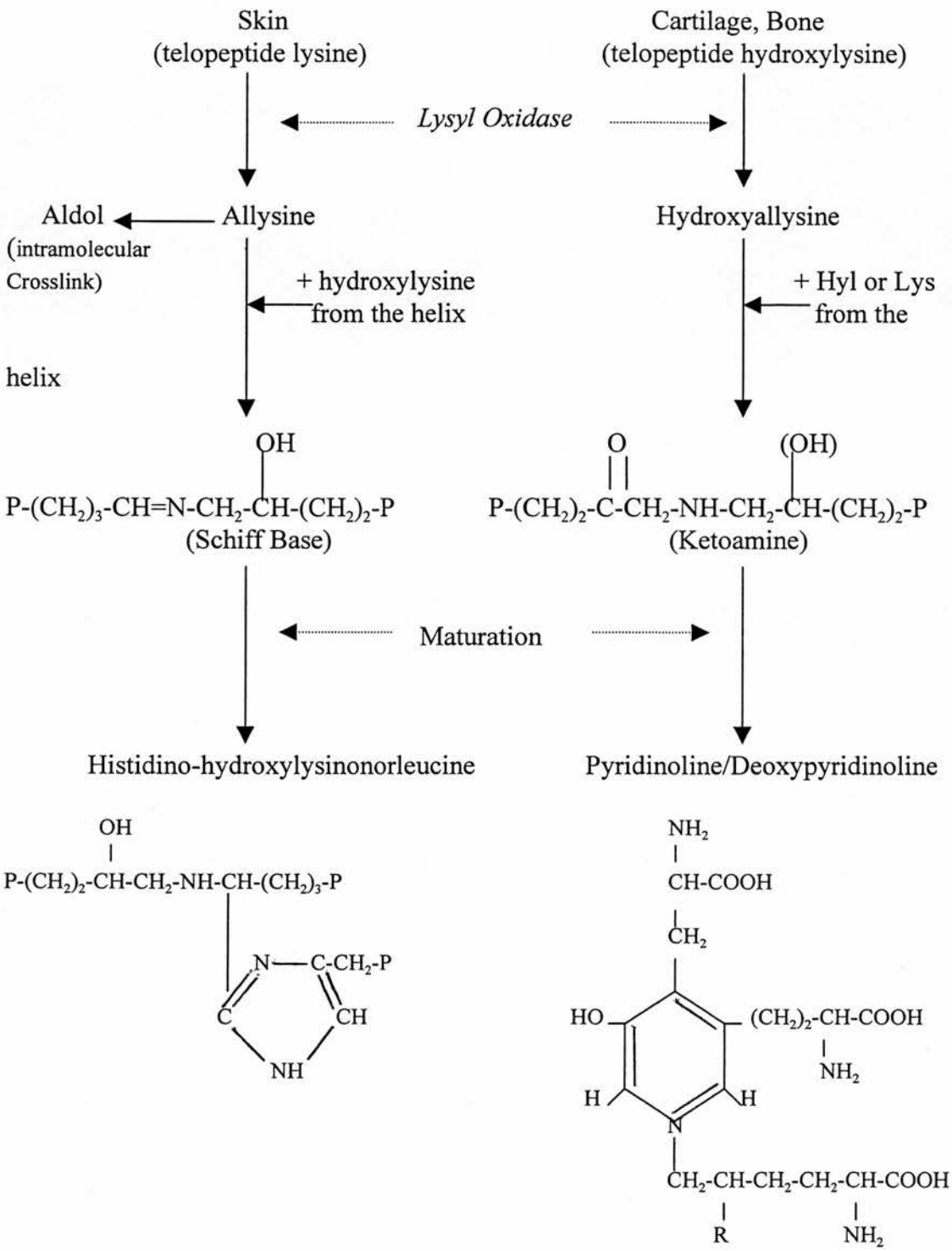

R = OH for Pyridinoline and H for Deoxypyridinoline, the latter involving lysine from the helix

Figure 1.3 Schematic diagram showing the (a) Allysine crosslinking pathway and (b) Hydroxyallysine crosslinking pathway.

trifunctional crosslink in an *in vitro* study (1.9 bifunctional crosslinks lost in forming a trifunctional crosslink). An alternative mechanism proposed that hydroxyallysine reacts through an aldol condensation with a bifunctional ketoamine crosslink to produce the mature crosslink (Robins & Duncan, 1983). It was argued that this mechanism was more sterically favourable than the previous one.

1.2 The Structure of Collagen Type I Fibrils.

Collagen type I forms fibrils of a variety of sizes, 500 nm diameter homotypic fibrils in tendon and the 50-100 nm diameter heterotypic fibrils in skin. These fibrils provide a dual function in tissues. First, they provide tensile strength in connective tissues and second they provide a scaffold for the attachment of molecules and cells.

1.2.1 The Molecular Packing of Collagen.

1.2.1.1 Axial Arrangement of the Molecules.

X-ray diffraction and electron microscopy have been the principal techniques used to probe the three dimensional structure of fibrils. Collagen exhibits a characteristic banded appearance in the electron microscope. When negatively contrasted with heavy-metal stains, the electron opaque stain penetrates into gaps in the fibril structure. The first observation of the D periodicity in collagen fibrils using X-ray diffraction was in hydrated rat tail tendon (Bear, 1942, 1944). It is widely acknowledged that in the axial direction there is considerable long range order of the fibrils (Figure 1.4). Neighbouring molecules are staggered by integral multiples of D (i.e., nD, n=1,2,3,4, where D ~ 67 nm, depending on the tissue source) (Hodge & Petruska, 1963). The D-periodicity of collagen type I fibrils is known to an accuracy of one residue. Using a value of 234 residues for the 64 nm D period length (Hulmes *et al.*, 1973; Meek *et al.*, 1979), the residue spacing, h, computes to 0.286 nm and is in good agreement with diffraction measurements of the axial translation of Gly-X-Y repeat units (Kadler, 1994).

Because of the non integral ratio of type I collagen molecular length (4.4 x D) /D, regions of gap and overlap are produced within the fibril. The overlap is approximately 0.4 D and the gap region is approximately 0.6 D (Hayashi & Nagai, 1974). The gap-overlap explains the negative staining pattern and is sometimes referred to as the "two dimensional structure" of the fibril.

X-ray diffraction studies carried out have suggested that the portions of the collagen molecules in the gap region are more mobile than those that comprise the overlap region (Fraser *et al.*, 1983). It was concluded that the factors contributing to the increased mobility in the gap region as compared with the overlap region were a

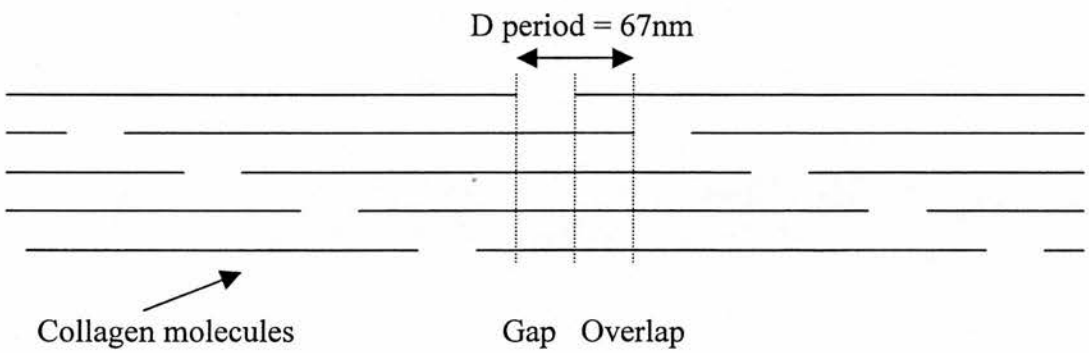

Figure 1.4 The Hodge & Petruska axial packing arrangement of collagen molecules in the fibril.

reduced packing density, a lower content of triplets containing two imino acid residues known to stabilise the collagen helix, a lower content of hydroxyproline residues and a lower content of aromatic residues, known to confer rigidity in globular proteins (Fraser *et al.*, 1987).

1.2.1.2 Lateral Arrangement of the Molecules

There have been many attempts to incorporate the one dimensional structure of the fibril into a three dimensional packing arrangement. Analysis of X-ray diffraction data led to a number of conflicting models, many of these based on discrete, rope-like microfibrillar sub-structures within the fibrils. A five-stranded microfibril, where five molecules are adjacently staggered and rolled into a hollow cylinder whose diameter has satisfied the 3.8 nm equatorial reflection was proposed (Smith, 1968). Two stranded (Woodhead Galloway *et al.*, 1975), four stranded (Veis & Yuan, 1975), other five stranded (Miller & Parry, 1973) and eight stranded microfibril models (Hosemann *et al.*, 1974) were also proposed.

Re-interpretation of X-ray diffraction data led to a new model for the crystalline regions of the fibril, based on quasi-hexagonal molecular packing (Hulmes & Miller, 1979). This concluded that the collagen molecules within the fibril are tilted to the fibril axis and packed on a quasi-hexagonal lattice that is both laterally and axially sheared. This model does not support or discredit the existence of microfibril structures although the unit cell does contain five molecules (Figure 1.5 a). Compressed microfibril models have also been proposed and these more closely satisfy the restrictions imposed by crosslinking (Bailey *et al.*, 1980; Piez & Trus,

1981). This model has the same unit cell, the difference being the assignment of molecular segments within the unit cell.

Subsequent studies performed on tendon collagen stained with phosphotungstic determined the unit cell to be triclinic and the quasi hexagonal packing of the molecules to be appropriate but that it could be defined more precisely in three dimensions and refined (Fraser *et al.*, 1983, 1987).

Another model was proposed that differs significantly from the triclinic unit cell model. Collagen molecules with no axial stagger are associated into 300 nm bunches. Bunches are aligned head to tail and penetrate into each other by 30 nm to form microfibrils which are axially staggered by 67 nm with respect to each other (Kajava, 1991).

The validity of both of these models was deliberated using diffraction data optimised by removing the diffuse scatter from the images. This work concluded that the packing of molecules is on a triclinic lattice and that the model proposed by Kajava was inappropriate due to the limited agreement between the calculated positions of intensities and those observed (Wess *et al.*, 1995). A subsequent study was carried out using indexing of Bragg peak intensity on the row-lines of the triclinic unit cell to test possible sheet and microfibril packing. It was found that the sheet-type conformations can not account for the observed low-angle off-meridional Bragg peak intensity distribution. A superior fit was obtained with D-staggered, left-handed microfibril structures (Wess *et al*, 1998).

Although in some connective tissues, X-ray diffraction reveals three dimensional crystallinity in the molecular packing within fibrils, the continued presence of diffuse scatter indicates significant underlying disorder. A model was proposed that could

account for both the short range (liquid-like) and long range (crystalline) order (Hulmes, *et al.*, 1995). The investigators studied evidence from electron microscopy for a concentric organisation in collagen fibrils that was observed (Katsura *et al.*, 1991; Parry & Craig, 1984). This led to a number of concentric and spiral packing arrangements being considered. The model is based on the classic axial packing, where adjacent molecules are staggered by D. In cross section, a sheet of thickness 3.8 nm can be formed by a repeating pattern of five molecules with equivalent segments separated by 2.7 nm. The fibril consists of a number (n) of these sheets wrapped around the fibril axis, to form an n start equiangular spiral (Figure 1.5 c).

a)

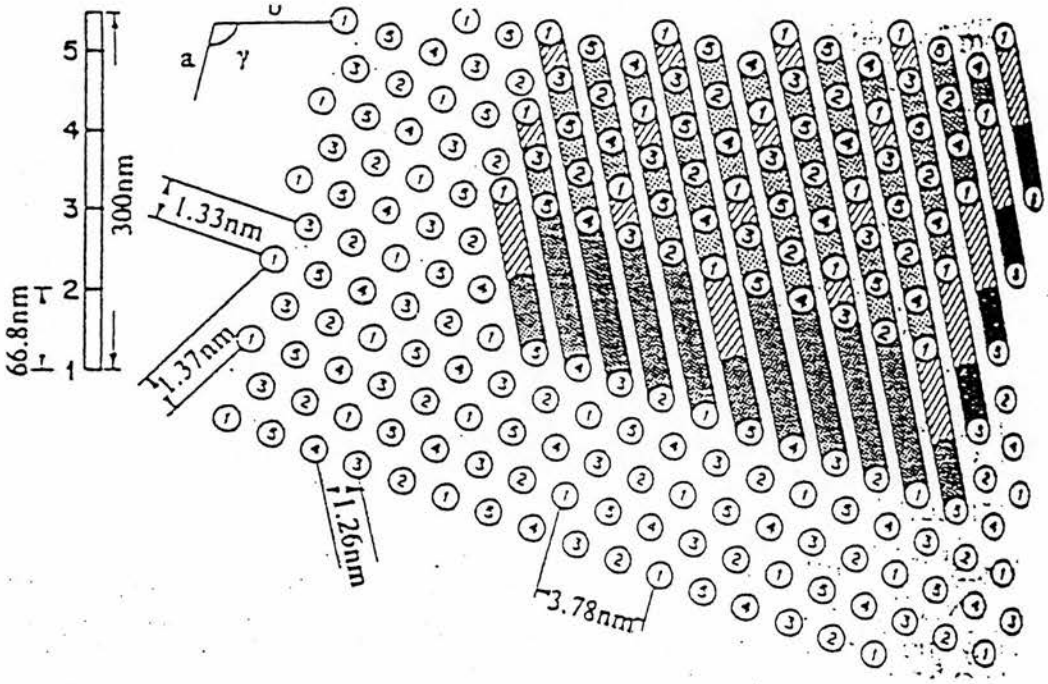

Figure 1.5 a) shows the molecular packing model proposed by Hulmes & Miller, 1979 based on a quasi-hexagonal arrangement. This diagram shows the molecular segments (as designated by the numbers) in one D (67 nm) thick transverse section. The numbers at the top end of the thick, shaded lines show the segments in the upper surface and the numbers at the bottom of these lines show the lower surface. The thick, shaded lines themselves demonstrate the molecular tilt and connectivity between the upper and lower surfaces. The half shaded line shows the gap region. The distances 1.26 nm, 1.37 nm and 1.33 nm correspond to the spacings of the three Bragg planes. The same unit cell dimensions could arise by the regular combinations of two 1D (&4D) staggers and one 2D (&3D) stagger in the 3 principal directions as well as more irregular patterns of intermolecular n x D staggers.

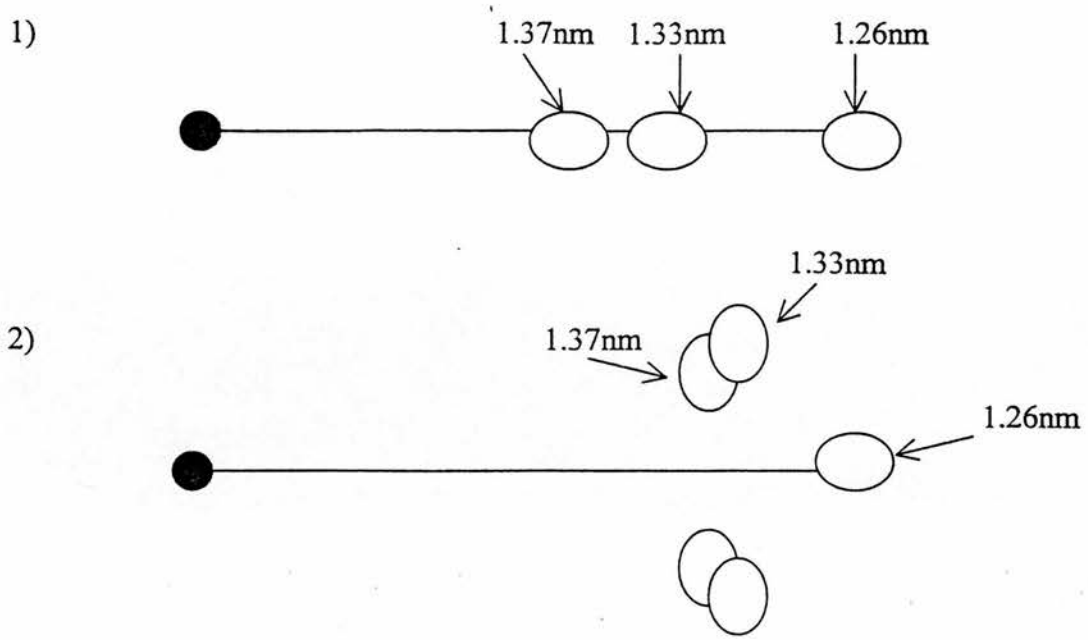

Figure 1.5 b) shows a schematic diagram of the positions of the Bragg reflections 1) if there were no molecular tilt and 2) as they are observed.

c)

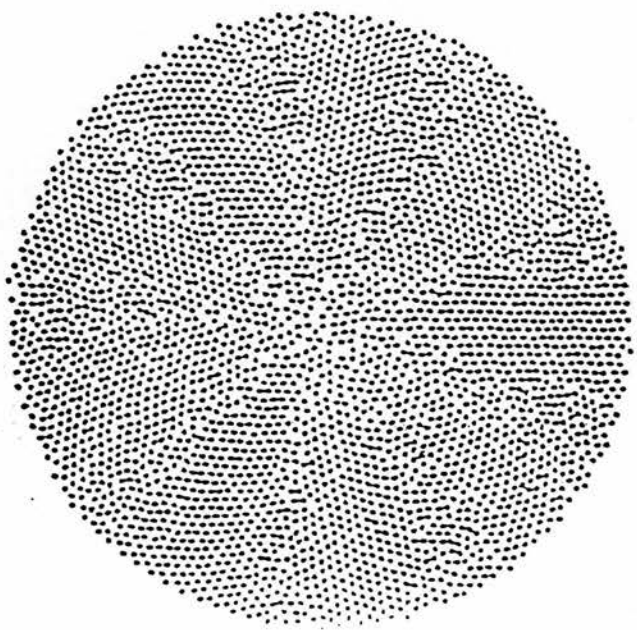

Figure 1.5. c) shows the concentric packing arrangement of collagen molecules as proposed subsequently by Hulmes *et al.*, 1995. The quasi hexagonal packing model in a) assumes an ordered array of collagen molecules but observed X-ray diffraction data shows the presence of diffuse scatter indicating regions of disorder. This radial packing model attempts to reconcile the regions of order and disorder observed with the electron microscope data showing concentric organisation of the fibrils.

1.3 Mineralization

One of the major functions of the vertebrate skeleton is to provide mechanical strength for support and protection of tissues and organs. The precise underlying biomechanical and biological basis for skeletal strength remains poorly understood. It involves a complex series of events which culminates in mineralization; the deposition of the calcium phosphate salt, hydroxyapatite in the organic extracellular matrix consisting mainly of collagen.

Mineralization occurs in a variety of vertebrate tissues. Bone, mineralizing turkey leg tendon, dentin, cementum and enamel all mineralize. At the molecular level bone, dentin and mineralized turkey leg tendon all have similar structures but bone and dentin both have more complex ultrastructure than tendon, which contains an orderly arrangement of parallel type I collagen fibrils. Many investigators have used turkey leg tendon as a model system for mineralization in bone. As well as having an ordered arrangement of collagen molecules that facilitate structural studies, nonmineralized, actively mineralizing and fully mineralized environments can be studied in the same tissue. For this reason, this review will primarily concentrate on the mineralization of bone and mineralizing turkey leg tendon.

Controversy still exists in almost all aspects of mineralization, from site of nucleation, nucleating agent, size and shape of the crystal to location and growth of the mineral. The aim of this introduction to mineralization is to review work that has been carried out in this field and present its findings.

1.3.1 The Nature of the Mineral

Bone mineral is a microcrystalline, non-stoichiometric, structurally imperfect analogue of hydroxyapatite (Posner, 1987). Investigations have been conducted to determine whether hydroxyapatite is the only observed mineral phase or whether a non-apatitic calcium phosphate precursor can be detected. Electron diffraction studies revealed that in developing fish fin (Landis *et al.*, 1981) and embryonic chick bone (Landis & Glimcher, 1978) the earliest mineral deposited was a non-crystalline (amorphous) phase. X-ray diffraction of increasing density separated fractions of ground embryonic chick bone suggested the precursor of bone apatite to be brushite (Roufosse *et al.*, 1979). It was suggested that the presence of brushite in this investigation was an artefact of specimen preparation or an occurrence not related to bone formation (Betts *et al.*, 1979). In all these cases the only phase seen in developing bone, as opposed to embryonic bone, is apatite mineral.

Much more recent studies have indicated that a non-apatitic environment is present in young mineral in mineralizing turkey leg tendons. Fourier transform infrared microscopy of the youngest mineral in mineralized turkey leg tendon, i.e., the mineral which has been deposited last, has indicated the presence of a non-apatitic and/or acid phosphate environment, whereas older mineral has been shown to have the characteristic of poorly crystalline hydroxyapatite (Gadaleta *et al.,* 1996).

Attempts have been made to define the molecular formula for bone apatite although the exact stoichiometry is dependent on the age of the bone. It was found that the earliest bone apatite deposited is calcium deficient, as in the case of chemically precipitated hydroxyapatites. With maturation, the bone crystal becomes less calcium

deficient, though never reaching the stoichiometry of perfect hydroxyapatite (Posner, 1985). It seems sufficient to describe bone mineral as a calcium and hydroxyl deficient (Rey *et al.*, 1995; Holden *et al.*, 1995), hydrogen and carbonate containing analogue of hydroxyapatite characterised by structural imperfection and a high surface area.

1.3.2 Nucleation of the Mineral Phase

There have been many mechanisms proposed for the nucleation of mineral in bone and related tissues. It is now generally accepted that it occurs by some heterogeneous nucleation of hydroxyapatite out of a solution containing calcium and phosphate ions. Nucleation due to removal of biological inhibitors, interaction with calcium binding molecules, or precipitation out of locally supersaturated calcium phosphate solutions have all been considered as possible mechanisms (Glimcher, 1984). The first two proposed mechanisms suggest possible roles for the noncollagenous proteins present in mineralizing tissues. Each of the major noncollagenous proteins will be reviewed in a later section and their conceivable role in the mineralization process discussed.

1.3.2.1 The Site of Nucleation

There are conflicting views as to the initial site for mineral deposition. Using X-ray diffraction, the gap region has been implicated as being the location of the first mineral deposition in turkey leg tendon (White *et al.*, 1977). Further study suggested that the site of nucleation is located towards the N-terminus of the gap region (Berthet-Colominas *et al.*, 1979). These authors put forward the notion that there may be a specific three dimensional arrangement of amino acids that form a nucleating site in the non-helical, telopeptides of the collagen molecule itself or on a noncollagenous

protein, covalently linked to the collagen molecule. A different site of nucleation, though still in the gap region, was implicated using electron microscopy. The first crystals of uranyl acetate stained turkey leg tendons were observed at the e band in the gap region and at the surface of the fibrils (Traub *et al.*, 1992a). The e band extends over approximately 8 nm of the fibril and lies near the middle of the collagen gap region which is contrary to the earlier proposed site of nucleation being near the N-terminus of the gap region. In electron micrographs of ultrathin sections of rat incisors and of 10 month old human femoral cortex, the first observed mineral deposits were dotlike structures or islands that were found in the gap regions but were also found, to a lesser extent, in the overlap regions (Hohling *et al.*, 1971).

Small angle X-ray scattering has also been a useful tool in the investigation of mineral nucleation. Studies of long bones from mice and rat calvariae also suggest the first observable deposition of mineral is in the gap regions of the fibrils; however, no distinct nucleation site was observed. The mineral was laid down in monolayers of calcium phosphate (Fratzl *et al.*, 1991). From these investigations, it seems a universal finding that the first observable mineral in bone and turkey leg tendon is located within the gap regions of fibrils, but analyses using various electron microscopy methods have led investigators to another possible site.

A two dimensional microscopy study of turkey leg tendons revealed the first mineral detected is associated with small vesicular structures located between collagen fibrils (Landis, 1985, 1986). It was reported that after growth of the mineral in vesicles, nucleation of mineral particles follows, within or on the surface of the collagen fibrils. Once this nucleation has occurred, additional sites in the extracellular matrix are observed in which vesicles are absent and calcium phosphate particles associate

exclusively with collagen. It was interesting to note that in this investigation when the initial mineral deposition occurs within or on the surface of the collagen fibrils, no disruption of the vesicles could be detected and they appear to maintain their structural integrity. Further investigations, however, using three dimensional imaging reported that once the mineral phase is deposited, the membranes of extracellular vesicles cannot be distinguished microscopically. This suggests that they are disrupted by the mineral or a physicochemical event or that they are being obscured by the increasing electron density of the inorganic mass (Landis & Song, 1991). It was hypothesised that both vesicles and collagen mineralize by spatially independent means even when these structures are in close proximity (Christoffersen & Landis, 1991).

It has also been proposed that vesicular mineral propagates into extravesicular spaces and then into the neighbouring collagen. The evidence behind this is that all the collagen-associated mineral in turkey leg tendon studies can be ultimately linked to mineral laden vesicles. It was hypothesised that there is a temporal sequence of mineralization beginning in matrix vesicles and proceeding to adjacent collagen fibrils (Arsenault *et al.*, 1991; Kohler *et al.*, 1994).

The argument contesting this notion is that regardless of whether mineral crystals are also deposited within matrix vesicles, they cannot, in the solid state, directly cause new crystals to be initiated in collagen fibrils spatially separated from the vesicles (Glimcher, 1989). The proposed nucleating agent must be at the site of mineralization. Even within a single collagen fibril, new crystals forming in different gap regions separated spatially, either laterally or axially along the fibril, represent independent nucleation sites within a single fibril.

1.3.2.2 Nucleating Agents

Although much work has been carried out investigating nucleating agents on *in vitro* mineralization models, this aspect remains unclear. Various noncollagenous proteins and the collagen itself have all been implicated as playing a role in nucleation either as nucleators or growth inhibitors.

A Proteoglycans.

There are two major proteoglycans present in bone which are structurally, chemically and immunologically distinct from one another (Fisher *et al.*, 1983a). Histochemical data suggests they may be responsible for orientation of collagen fibrils, filling the gap region in nonmineralized, but not in mineralized tissues (Scott & Haigh, 1985). Both these proteoglycans have been suggested as having roles in inhibiting and nucleating mineralization.

Results from studies carried out on the effects of proteoglycans on hydroxyapatite formation and growth in metastable calcium phosphate solutions suggested that proteoglycans inhibit mineralization (Chen & Boskey, 1985, 1986). However, it was argued that these studies had been performed under non-physiological conditions of limited calcium availability (Hunter, 1991). This was deemed important as the chondroitin sulphate chains of proteoglycans can bind calcium ions and this binding has been correlated with the ability of chondroitin sulphate to inhibit hydroxyapatite formation (Hunter *et al.*, 1985). *In vivo*, binding of calcium to proteoglycan would not reduce the free calcium concentration, in other words, physiological conditions are steady state, whereas *in vitro* conditions are non-steady state.

The effects of proteoglycans on hydroxyapatite formation under non-steady-state and pseudo-steady-state conditions were observed and the findings suggested that the inhibition of hydroxyapatite by proteoglycans is largely due to calcium binding (Hunter & Szigety, 1992). It was suggested further that proteoglycan may act as a promoter and not an inhibitor of mineralization. In fact, earlier reports stated that when proteoglycans are immobilised on insoluble substrates they induce mineral from metastable solutions that do not spontaneously mineralize (Lussi *et al.*, 1988). Results from a proteoglycan isolated from bovine bone suggested that the proteoglycan is closely associated with both the mineral and the collagen matrix and it was hypothesised that such a molecule might facilitate the structural network for the induction of mineralization in bone (Hashimoto *et al.*, 1995).

B Phosphoproteins

This group of proteins in bone comprise primarily of a phosphorylated glycoprotein called osteonectin, two sialoproteins (osteopontin and bone sialoprotein) and a group of proteins rich in phosphoserine and phosphothreonine. In general, the phosphoproteins, with the possible exception of osteonectin, have comparable properties despite their lack of structural homology. Highly anionic, the phosphoproteins tend to be localised in the mineralized matrix, to bind to both calcium and hydroxyapatite with high affinity and to either inhibit or promote hydroxyapatite mineral deposition.

In vitro, phosphoproteins have a wide range of functions. Experiments subjecting demineralized chick bone collagen to variable amounts of bone phosphoproteins caused hydroxyapatite formation in a dose dependent manner from metastable calcium

phosphate solutions (Endo, 1987). These data suggested that these proteins could serve as nucleators.

Osteonectin was first suggested as being a promoter of mineralization as studies carried out demonstrated that osteonectin could bind to collagen (denatured type I) (Termine *et al.*, 1981a) and mineral ions (Termine *et al.*, 1981b). However, subsequent *in vitro* work showed that osteonectin at 0.15μM was a potent inhibitor of hydroxyapatite seeded growth in metastable calcium phosphate solutions (Romberg *et al.*, 1986). This led to the hypothesis that osteonectin may function to prevent the initial mineralization of newly synthesized, not yet mature osteoid. Monoclonal antibody experiments determined that the maximum cellular production of osteonectin was detected in immature bone cells supporting this view (Bianco *et al.*, 1988) and subsequent studies using polyclonal antibodies showed a similar labelling (Romanowski *et al.*, 1990).

The major phosphoproteins of bone are bone sialoprotein (BSP) and osteopontin (Fisher *et al.*, 1983b; Prince *et al.*, 1987). BSP is quite specific to bone whereas osteopontin is expressed in a variety of tissues, but at higher levels in bone than elsewhere. Studies carried out in an *in vitro* double diffusion agar gel model suggested that BSP induces the formation of hydroxyapatite, whereas osteopontin has no effect at calcium and phosphate concentration products below the threshold for spontaneous precipitation (Hunter & Goldberg, 1993). A similar system was also used to study osteopontin alone except agar was used instead of gelatin. This showed that higher concentrations of osteopontin inhibit both *de novo* hydroxyapatite formation and growth (Boskey *et al.*, 1993). Further investigations, using metastable calcium phosphate solutions at constant pH found that as little as 0.1 μg/ml osteopontin

significantly inhibited apatite formation (Hunter *et al.*, 1994). Based on EM appearances of hydroxyapatite growth in the presence of 0-100μg/ml osteopontin, it appears that this protein blocks crystal elongation, rather than secondary nucleation, implying that osteopontin binds with high affinity to one or more crystal faces (Boskey *et al.*, 1993). The studies in the gelatin system that propose that BSP is a hydroxyapatite promoter have been duplicated in the agar system (Boskey, 1994) demonstrating that the results are not system specific. Further investigations using an agarose gel system demonstrated that chemical modifications of BSP carboxylate groups eliminates the nucleation activity of BSP, but enzymic dephosphorylation has no effect (Hunter & Goldberg, 1994). The investigators suggested that polycarboxylate sequences represent a general site for growth-modulating interactions between proteins and biological crystals.

C. Gamma-carboxyglutamic Acid Containing Proteins

This group of proteins consists of bone Gla-protein or osteocalcin and matrix Gla-protein. Osteocalcin is found in bone and in dentin and matrix Gla-protein is found in cartilage as well as bone. Osteocalcin, *in vitro*, has a high affinity for calcium (Romberg *et al.*, 1986) and has been shown to inhibit hydroxyapatite formation in supersaturated solutions (van der Loo *et al.*, 1987) and from seeded hydroxyapatite systems (Boskey *et al.*, 1985; Romberg *et al.*, 1986). However, it was demonstrated that it does not alter mineral deposition initiated by Ca^{2+}-phospholipid-PO_4 (Boskey *et al.*, 1985).

It has been hypothesized that it is the unique structural features of osteocalcin (Figure 1.6) that dictate the association with calcium ions and mineral surfaces and perhaps

confers upon this protein the ability to modulate the mineral dynamics of bone. Osteocalcin could inhibit or stimulate nucleation, precipitation or metamorphosis of Ca^{2+}-phosphate mineral phases or it could mobilise calcium ions from crystal surfaces (Hauschka & Wians, 1989). However, it is improbable that osteocalcin is involved in the stimulation of nucleation of mineralization as osteocalcin gene "knockout" studies carried out indicate that the transgenic mice have no impairment of mineralization (Ducy *et al.*, 1996). This does not mean, however, that osteocalcin plays no role in mineralization. An increase in bone formation was observed in these experiments indicating a possible role for osteocalcin in the regulation of mineralization.

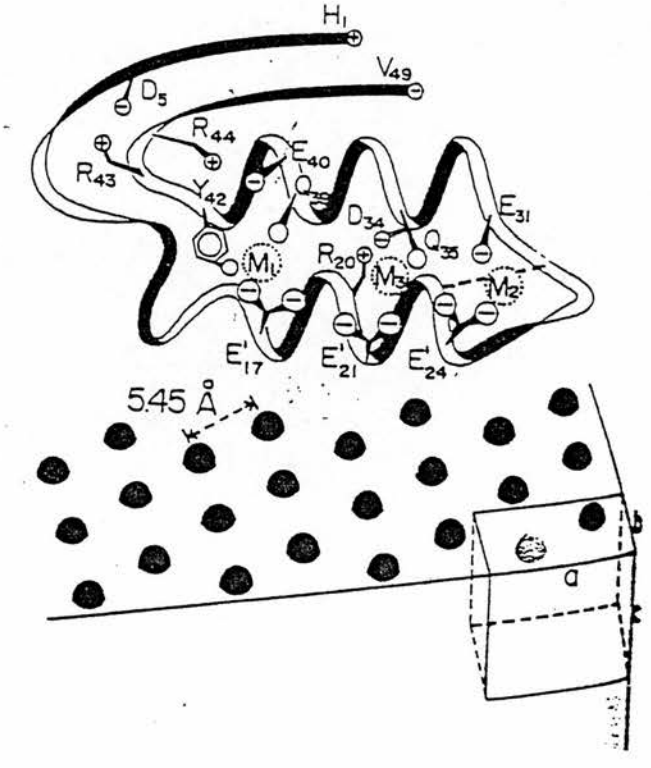

Figure 1.6 Model for the calcium induced structure of osteocalcin showing its probable mode of interaction with Ca^{2+} in the hydroxyapatite crystal lattice (Hauschka & Wians, 1989).

1.3.3 Mineral Growth

This section is intended to deal with the growth of the mineral crystal after nucleation and the size and shape of these mature crystals. There is as much contention over the size, shape and growth of the mineral as there is over its nucleation. These conflicting theories will be reviewed in this section.

1.3.3.1 The Shape of Mineral Crystals

There are two schools of thought over the shape of bone and turkey leg tendon mineral crystals: plate-like and needle-like.

An early study using the transmission electron microscope (TEM) to study dispersed human bone crystals concluded that the crystals were all plate-like in shape (Robinson, 1952). However, subsequent studies using embedded thin sections of mature bone concluded that they are all needle-like in shape (Fernandez-Moran & Engstrom, 1957; Speckman & Norris, 1957). Ensuing studies showed that whenever care was taken to observe these needle-shaped crystals at different tilt angles, they were shown to be edge on views of plate shaped crystals (Johansen & Parks, 1960; Steve-Bocciarelli, 1970; Landis *et al.*, 1977).

Both electron microscopy and X-ray diffraction techniques have been used to study turkey leg tendon mineral crystals. Selected area dark field electron microscopy was used to study newly mineralizing turkey leg tendon (14-week-old turkeys). This method enabled the direct visualisation of apatite and the specific determination of the crystallographic axes (a, b-axes or c-axis). It was concluded from this study that needle shaped crystals are present at early stages of mineralization (Arsenault, 1988). TEM

studies carried out on isolated leg tendon fibrils from turkeys aged 13, 14 and 15 weeks, again showed needle-shaped crystals present (Traub *et al.*, 1992b). Previous studies, however, carried out by the same investigators using electron microscopy of isolated fibrils showed that in 21-week-old turkey leg tendons platelet-shaped crystals were present (Traub *et al.*, 1989). It was hypothesized from the collected data therefore, that in turkey leg tendon the earliest crystals present are needle-like which develop into plate-like crystals with age. This was supported by earlier work done on dentin. Series of tilted electron micrographs of developing dentin showed that in the youngest tissue only needles were present but in more mature tissue, the tilting views showed plates (Hohling *et al.*, 1974). This was repeated on other hard tissues. It was suggested that nanometer-sized apatitic islands, rapidly coalesce to needles and afterwards to platelets (Hohling *et al.*, 1997).

Studies using topographic imaging found that isolated mineral crystals from the leg tendons of 15-week and 21-week-old turkeys were all plate-like crystal for both ages of tendon (Landis *et al.*, 1991). Isolated crystals from many other sources of tissues have also been examined. Single crystals from fish, chicken, mouse and bovine bone have been studied using TEM which reported that only plate-like shaped crystals were present in any of these tissues also (Kim *et al.*, 1995). No needle shaped crystals have ever been isolated from any sources and only plate-like crystals have been obtained. There has been a tentative suggestion that perhaps needle-like crystals are not stable outside the collagen matrix.

High voltage electron microscopic tomography studies done on sections of tibiae from normal 17-day-old embryonic chicks also found plate-like crystals present (Landis *et al.*, 1996), although it must be noted that this study is not of the turkey leg tendon.

All of the investigators mentioned above have used electron microscopy techniques to study the shape of the mineral in various tissues. Small angle X-ray scattering (SAXS) has also been used, which rules out artefacts due to sample preparation necessary for electron microscope studies. Investigations into the shape of the mineral crystals in mineralized turkey leg tendon and in bone (calvaria, femur and iliac crest) from 1-year-old mouse, 2-year-old rat and 3-year-old dog were carried out using SAXS. It was found that the crystals present in 14-week-old turkey leg tendon were in fact plate-like, but the predominant crystal shape in all the bone samples tested was needle-like (Fratzl *et al.*, 1992). Further SAXS studies on adult human bone found plate-like crystals present as with mineralizing turkey leg tendon. It was noted from these collected data that the crystals seemed to be needle-like in bone from animals growing continuously (like mice and rats), but more plate-like in the case of bone with comparatively low turnover (like adult humans or turkey leg tendon). It was hypothesized that mineral crystals nucleate as needles, which then grow to become platelets (Fratzl *et al.*, 1995). Statistical models of both plate-like mineral crystals and plate-like crystals in a collagen matrix were calculated to test the SAXS results. The plate-like mineral model was in excellent agreement with the data collected of turkey leg tendon and the needle-like mineral model for bones of mice and rats. It was found that with increasing mineral density, the individual needles merge into plates to give a mineral structure with high interconnectivity (Fratzl, 1994).

From all the studies carried out on turkey leg tendon, both needle and plate shaped crystals have been detected, using different methods, in early and later stages of mineralization. At the same time as the SAXS studies were published, it was reported that using atomic force microscopy and electron microscopy to study turkey leg

tendons, both needles and plates are present in the tendon at the same time. It appeared that needle-like crystals fill the extrafibrillar volume and plate-like crystals are found within the fibrils (Lees *et al.*, 1994). The age of the birds used was not taken into consideration in this investigation. As the legs were "obtained from the meat market", there was possibly a wide variation in age, which has proved an important factor in previous investigations.

1.3.3.2 The Size and Location of the Crystals

Not only does the size calculated for mineral crystal depends upon the shape calculated but also upon the location of the growing mineral in relation to collagen. Both of these factors will be discussed in the following section.

Various electron microscopy techniques have been used to calculate the sizes for mineral crystals. It was reported, using TEM, that the average lengths and widths of dispersed human bone crystals, found to be plate-like, are 50 x 25 nm (Robinson, 1952). These dimensions were confirmed by similar studies carried out on crystals of several different animals (Weiner & Price, 1986). TEM studies of embedded thin sections of bone reported that the average lengths of the crystals are 40 nm with widths only slightly less (Robinson & Watson, 1952). However, in contrast, the same technique employed by other investigators, who had reported the presence of needle-like crystals, found the diameter to be 3-6 nm and the length to be 20 nm (Fernandez-Moran & Engstrom, 1957). Again, different dimensions for needle-like crystals were reported for dog and human bone. This study found the length of the crystals to be 60-70 nm (Speckman & Norris, 1957), which was comparable to the length recounted for the plate-like crystals found in ox bone (Steve-Bocciarelli, 1970). Other investigations

were of 6 day old rat calvariae, which were reported as having crystal lengths ranging from 10 to 80 nm (Nakahara & Kakei, 1984) and from human bone and rat bone, studied by TEM in the selected dark field diffraction mode, which obtained values of 32.4 ± 16.3 nm for human bone crystals and 17 ± 5 nm for rat bone crystals (Arsenault, 1989).

Small angle X-ray scattering techniques found the thickness of the crystals for bone (calvaria, femur and iliac crest) from mouse, rat and dog ranged from 3-4 nm and were remarkably constant for different bones of a given animal. The mean thickness of mineral crystals in turkey leg tendon as also calculated and found to be in the order of 2 nm (Fratzl *et al.*, 1992). The lengths of all these crystals have been reported to be at least 30 nm (Matsushima *et al.*, 1982).

The electron microscopic techniques used to measure turkey leg tendon crystals have given varying results. Using TEM in the selected dark field diffraction mode, the crystals of turkey leg tendon were investigated. This study found the crystals to be needle-like with lengths of 5-20 nm (Arsenault, 1988). High voltage electron microscopic tomography, however, showed plate-like crystals to be present, as reported earlier, with variable crystal length up to 170 nm, variable crystal widths of 30-45 nm and uniform thickness of 4-6 nm (Landis *et al.*, 1993). The approach using atomic force microscopy in conjunction with electron microscopy, referred to in the earlier section, showed plate-like crystals present having an average dimension of 58 nm and the needle-like crystals also present with an average thickness of 7 nm and a length of at least 90 nm (Lees *et al.*, 1994).

The varying results between electron microscopy and SAXS investigations led to a comparative study between TEM and X-ray diffraction methods on dispersed bone

crystals. TEM was considered the most reliable method for estimating bone crystal size in this instance, although the inherent drawbacks of preparing the samples in this manner was noted by the authors and it was concluded that the study may be biased towards smaller values than the larger *in vivo* ones (Ziv & Weiner, 1994).

Mineral was first located in the gap region between the collagen molecules of turkey leg tendon studied by X-ray diffraction and neutron diffraction (White *et al.*, 1977). It was deemed by these investigators, that the gap region was the only place where the mineral could occupy without disrupting its fibrillar structure. The subsequent nucleation studies, that have already been mentioned in a previous section, corroborated this evidence as the majority of the studies demonstrated that nucleation of the mineral crystals was within the gap region. This implies that as the crystals grow they must fill the gap region, but do they grow further to form crystals of sizes that must be accommodated not only in the gap region but elsewhere? From much of the evidence above it can be seen that although the thickness of the crystal appears to be limited, the sizes calculated for the length and width of the mineral appear to vary enormously. Both are far greater than the dimensions of the gap region within the collagen fibrils. Many different hypotheses have been proposed for the growth of the mineral crystals and how the collagen accommodates these growing crystals to the sizes observed.

TEM studies carried out on mineralizing turkey leg tendon confirmed that crystals are located within the gap region of the collagen fibril. It was also observed that although the crystal lengths and thicknesses calculated in this study were consistent with their being in the gap region, their widths are almost an order of magnitude larger than an individual gap diameter. Models of collagen fibril organisation (Katz & Li, 1973;

Hulmes *et al.*, 1985) predict that the adjacent gaps are in contact with one another at the same "height" in the fibril (Figure 1.7). The consequence of such a structure is that extended grooves are formed whose lengths and thicknesses are the same as individual gaps but whose widths are much larger. It was suggested that the crystals form in these grooves (Weiner & Traub, 1986).

Further observations from selected-area dark field electron microscopy studies showed that, at the early stages of mineralization in turkey leg tendons, the mineral crystals are clearly located within the gap regions of the collagen but that at later stages they are also observed to be in the overlap regions. Again from the width measurements it was proposed that the quarter staggered arrangement of collagen molecules allows for the lateral alignment of adjacent gap regions, thereby creating gaps large enough for the placement of apatite crystals (Arsenault, 1988).

Topographic imaging of mineralizing leg tendons of 15-week-male and female turkeys also revealed that the initial deposition of mineral is in the gap region. In addition, crystals were found in the overlap region (Landis *et al.*, 1991). This research and subsequent, more detailed studies using tomography showed that smaller and larger crystals seem to fuse in coplanar alignment to form larger mineral platelets. The width of these crystals is of the order of 45 nm, well beyond that of single collagen gap regions, estimated at 1-3 nm, again implying that the mineral is accommodated in grooves formed by adjacent gap regions as illustrated in Figure 1.8 (Landis *et al.*, 1993). A scenario was proposed for the growth of mineral crystals in turkey leg tendon based mainly on the relative sizes of the crystals. Initial growth of needle-like crystals is within the gap regions until they are of equal length. At this point further crystal growth along the length of the fibril is presumably temporarily inhibited by the

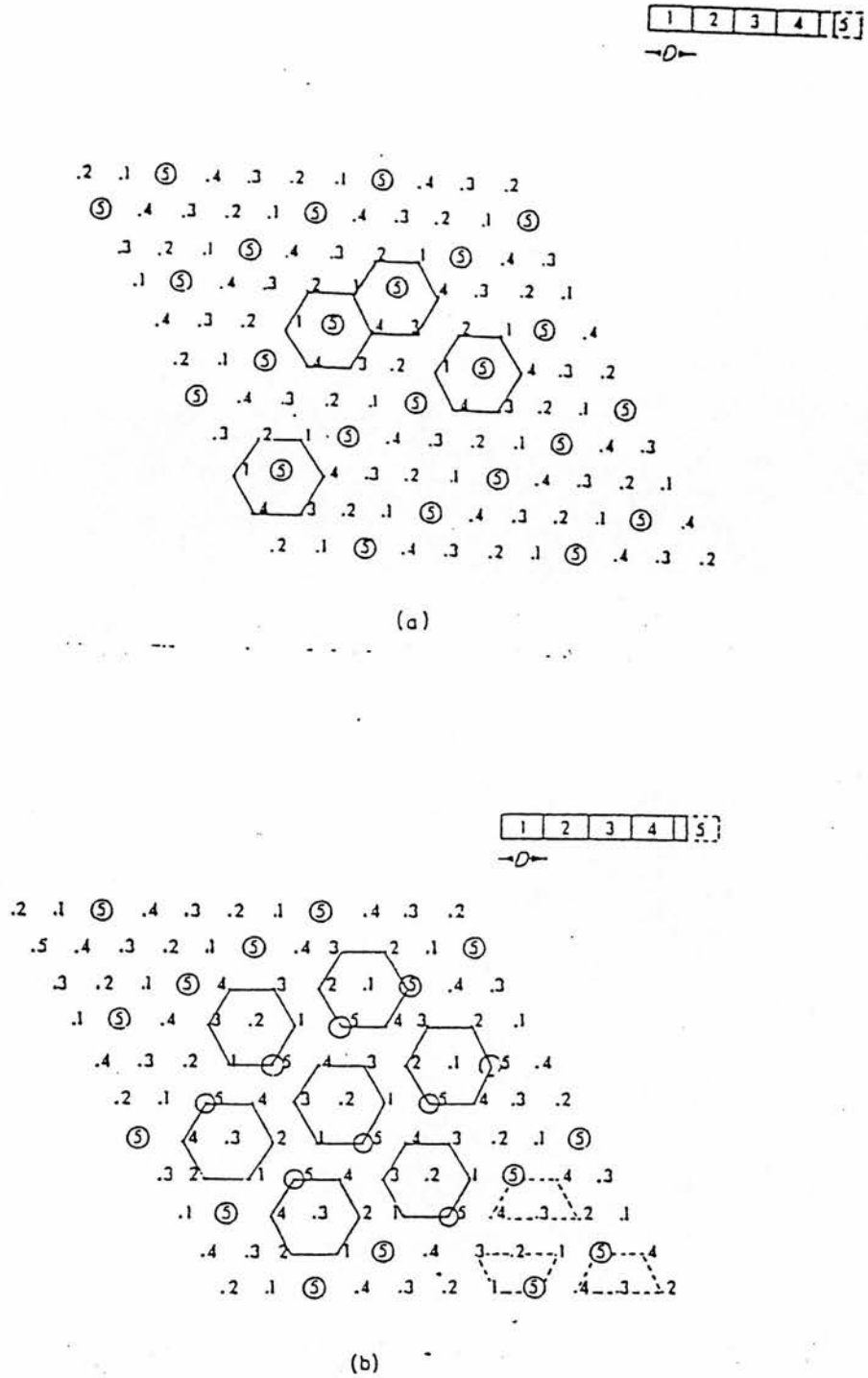

Figure 1.7. This diagram shows the packing model proposed by Katz & Li, 1973.

a) Their theoretical model is based on a near hexagonal packing of collagen molecules (this was prior to the Hulmes & Miller, 1979 quasi-hexagonal collagen packing model as shown in Figure 1.5 a). The molecules are staggered with respect to one another by D or some multiple of D. This staggering is such that holes are produced by gap regions being arranged in a linear array.

b) The same molecular packing is shown with possible groupings of molecules into microfibrils. Many authors have proposed the existence of collagen molecules being grouped together in microfibrillar arrays, five stranded microfibrils being the most popular. This figure shows that the proposed model for lateral packing does not exclude the possibility of microfibrillar arrangements. Hexagonal array of heptamers are indicated by a solid line and pentamer microfibrils are indicated by dashed lines.

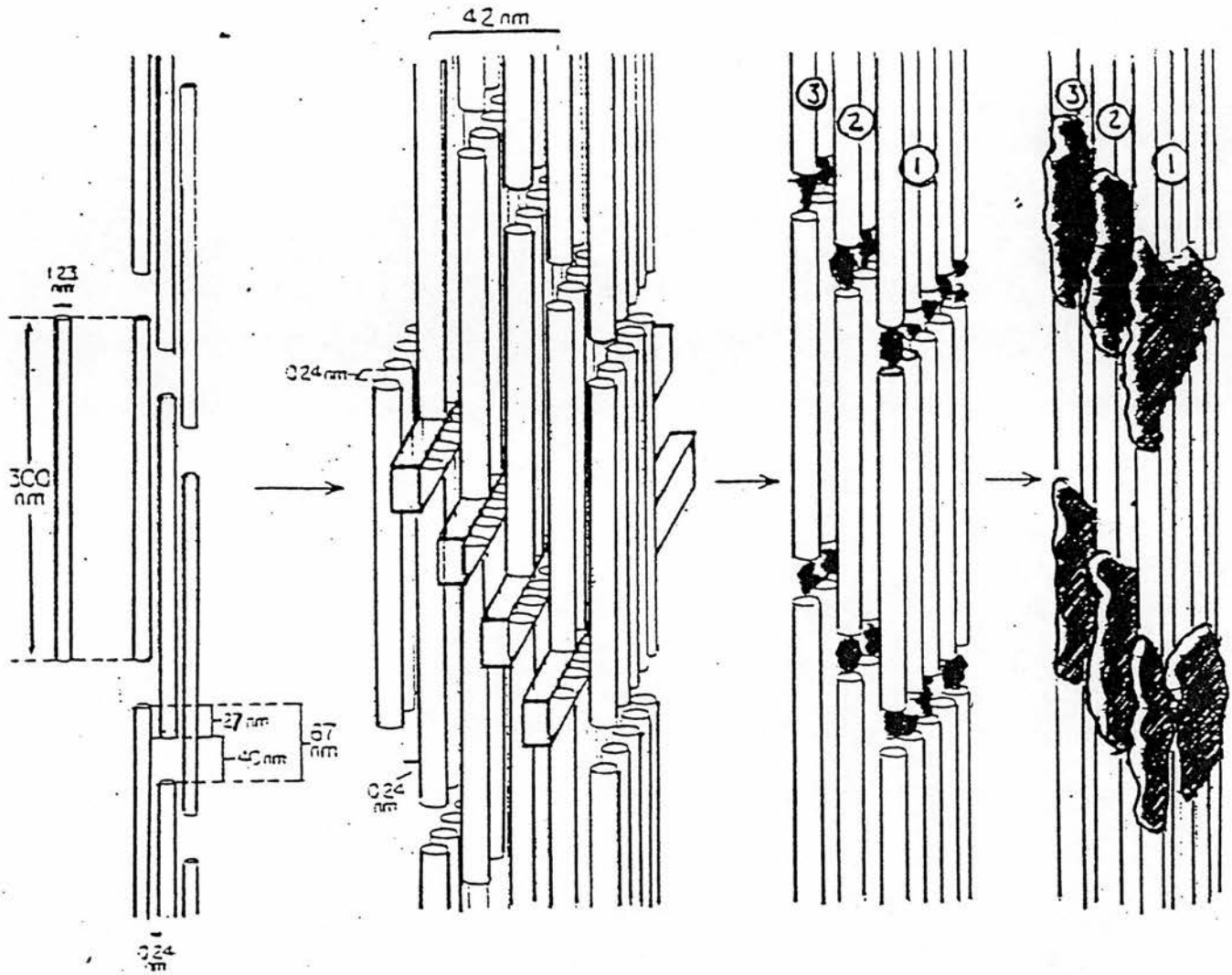

Figure 1.8. shows a schematic diagram of the model proposed by Landis *et al.*, 1993, to account for the presence of large, irregularly shaped mineral plates within the gap regions of a fibril. This diagram outlines the steps of progressive mineralization of a 3D array of collagen molecules. The molecules are arranged in the quarter-staggered pattern axially and so that the gap and overlap regions are aligned in register laterally. A cylinder represents a single collagen molecule of 300 nm in length and 1.23 nm diameter. The gap region is shown as being 40 nm and the adjacent overlap as 27 nm. Together they constitute the typical 67 nm periodicity characterising collagen assembly. The space between each molecule is 0.24 nm. The rectangular block represents the channels through the aligned gap regions that are formed by this collagen packing arrangement.
The second right figure illustrates early deposition of mineral crystals (black bodies) that are accommodated in the gap regions between the collagen molecules.
The figure on the far right illustrates the conceptual length and width of mineral being accommodated by this packing model. The irregularly shaped large and small mineral deposits may occupy the overlap regions to a certain extent and widthwise their growth is not limited to a single gap region but it may proceed into and beyond unoccupied gap regions in adjacent molecules. These can fuse together to create larger crystals.

confines of the collagen overlap regions. The crystals continue growing as belts or ribbons along the grooves of the fibril from the surface inwards and eventually across the other side of the fibril. Further crystal growth requires some distortion of the collagen fibril structure, but most of the crystals do eventually grow, at least to some extent, out of the grooves into the overlap regions (Traub *et al.*, 1992). Further tomography studies of embryonic chick bone suggested that these mineral crystals are also arranged in this fashion to accommodate larger crystals (Landis *et al.*, 1993).

From the above evidence it seems that a lot of the investigators using electron microscopy techniques are in agreement, although other investigators using TEM on dentin and bone observed a different location for the mineral. Needle-like crystals lying in dense strips between collagen fibrils were observed with practically no crystals within the fibril (Lees & Prostak, 1988). The needle-like crystals were noticed to be bunched in phase with the collagen banding and with the same spatial periodicity. This was said to account for the X-ray diffraction patterns which show the mineral to be associated with the gap regions (White *et al.*, 1977).

SAXS was also used to investigate the location of the growing mineral crystals. Studies carried out on bone samples from mice and rats suggested that the mineral is located within the gap region of the fibril with virtually none outside the fibril, although this could not be discounted (Fratzl *et al.*, 1991). It was also revealed from this work that the model proposed for the crystals growing along grooves created by adjacent gap regions in register (Traub *et al.*, 1991) does not agree with SAXS data. An interference maximum that should be induced by this arrangement was not observed.

Further SAXS work carried out on mineralizing turkey leg tendon studied the lateral and axial packing of the collagen molecules. Two questions were addressed by this investigation. Firstly, whether the crystals lie inside the overlap region, as had been previously proposed as the Bragg-spacing of collagen strongly decreases with increasing mineral content. This had led to the previous conclusion that the crystals must lie between the collagen fibrils and not inside (as far as the overlap region is concerned). Secondly, how crystals with average thicknesses of 3-4nm in bone and of 2nm in turkey leg tendon could be present in the gap region ~1.5nm. Both these questions were answered and the following model was proposed; in the first stages of mineralization, the mineral is predominantly deposited within the gap region of the collagen and therefore the overlap region is almost mineral free at this time. As mineralization progresses, more and more crystals are formed within the overlap zone pushing away the molecules (Fratzl *et al.*, 1993).

From the majority of this evidence it seems as though there is mineral located within the gap regions of collagen fibrils and it does extend into the overlap regions in time with progressive mineralization. However, not all the studies agree that the mineral extends through adjacent gap regions and the existence of extrafibrillar mineral cannot be ruled out, although it seems unlikely that there is no mineral located within the fibrils. In fact, further work carried out by the same authors using the atomic force microscope and electron microscopy on fully mineralized turkey leg tendons found not only needle-like crystals in the extrafibrillar volume but also plate-like crystals within the fibrils (Lees *et al.*, 1994).

1.4 Collagen Packing in Mineralized Tissues

As has been implied in the previous section on mineralization, the packing arrangement of collagen in nonmineralized tissues differs to that in mineralized tissues. Four perturbations of the collagen structure can be detected: (1) the X-ray diffraction and neutron diffraction fibre parameters, (2) the fibril shape, (3) the pattern of intermolecular crosslinking and (4) the segmental motion of the collagen fibril (Volpi & Katz, 1991). These changes will be reviewed in this section.

1.4.1 The X-ray Diffraction and Neutron Diffraction Parameters

Many structural studies have been carried out using X-ray diffraction and neutron diffraction to detect changes in the packing of collagen molecules within a fibril with mineralization. One of the first studies was conducted on mineralized turkey leg tendon using X-ray diffraction. The principal finding of this study was that the first equatorial reflection of collagen in freshly excised mineralized tendon had a d-spacing of 1.33nm which was intermediate between the values for dried collagen, both mineralized and nonmineralized, 1.2nm and fresh nonmineralized collagen, 1.4nm. This is a measure of the decrease in lateral separation between collagen molecules. It was hypothesized that, since this spacing is a sensitive monitor of moisture levels in collagen, mineralization reduces the amount of water that can associate *in vivo* with the collagen component in tissue (Eanes *et al.*, 1970). It was also concluded that the mineral crystallites infiltrate the fibrils yet lie externally to the intermolecular space, that the crystallites seen within the fibrils are actually situated between "microfibrils"

and that the crystals compress the "microfibrils" squeezing the collagen molecules closer together.

Neutron diffraction also determined the equatorial diffraction spacing of the collagen in fully mineralized tissues to vary inversely with the wet tissue density (Lees *et al.*, 1984). Dried tissue spacing was essentially the same for all tissues (1.1nm), whether mineralized or not.

It is not just in turkey leg tendon where mineralization brings about the compression of collagen molecules within fibrils. X-ray diffraction of mineralized and demineralized cortical bone from cow tibia showed the d spacings to be 1.23nm and 1.52nm, respectively (Lees & Hukins, 1992). These reported equatorial d-spacings for wet nonmineralized, wet mineralized and both dried nonmineralized and mineralized tissues have been consistent with other reported values both previously and since. Although the data that has been collected has been consistent in all these studies, the interpretation of these data has varied dramatically.

From the previous section on location of the mineral, it was reported that Lees and co-workers believed that the majority of the mineral within mineralized tissues is located extrafibrillarly and only small crystallites are located within the gap regions between the collagen molecules (Lees & Prostak, 1988; Lees & Page, 1992; Lees *et al.*, 1994). Part of the evidence for this conclusion was the changes of the equatorial spacing between collagen molecules of mineralized and nonmineralized tissues. It was hypothesized that if there were crystallites between adjacent collagen molecules, the equatorial diffraction spacing could not be the same in dried mineralized and nonmineralized tissues. It was assumed that the fibrils are isotropically compressed by extrafibrillar mineral. Subsequent studies carried out on the effects of sodium chloride

solutions on mineralized and nonmineralized tendon concluded that the extrafibrillar material was different from the intrafibrillar; and therefore the extrafibrillar material is a different kind of composite. It was assumed that the extrafibrillar material does not change dimensions significantly so the collagen molecules in the fibrils can be mobile within a dimensionally stable cage-like structure (Lees *et al.*, 1997).

An alternative model for the structure of mineralized collagen was proposed which features a predominantly intrafibrillar locale for mineral (Katz *et al.*, 1989). This model provided an alternative interpretation for neutron diffraction findings and took into account crosslink data. The alternative interpretation of the neutron diffraction data took into account the complications that arise from neutron diffraction of a multicomponent system. It was suggested that due to contrast effects, the d-spacing is not a monotonic measure of collagen packing density. The model proposed states that, in early mineralization a collagen fibril can accommodate mineral internally, without any change in structure (Figure 1.9). The disposition and size of the mineral reflects the underlying symmetry and geometry of the collagen superlattice. The mineral crystals have their c-axes approximately parallel to the helical axes of collagen molecules, their long lateral axes parallel to the lateral persistence direction of the intermolecular crosslinks and are stacked in parallel with a separation of about 9.0nm. They are about 40nm in length and about 2.0-2.5nm in width. Upon further crystal growth, a redistribution of space within the fibrils occurs by means of anisotropic compression of those molecular segments that are not in any way constrained by intermolecular crosslinks. These are the segments that are arranged normally to the vector describing the direction of the crosslinks (Figure 1.10). They can be compressed

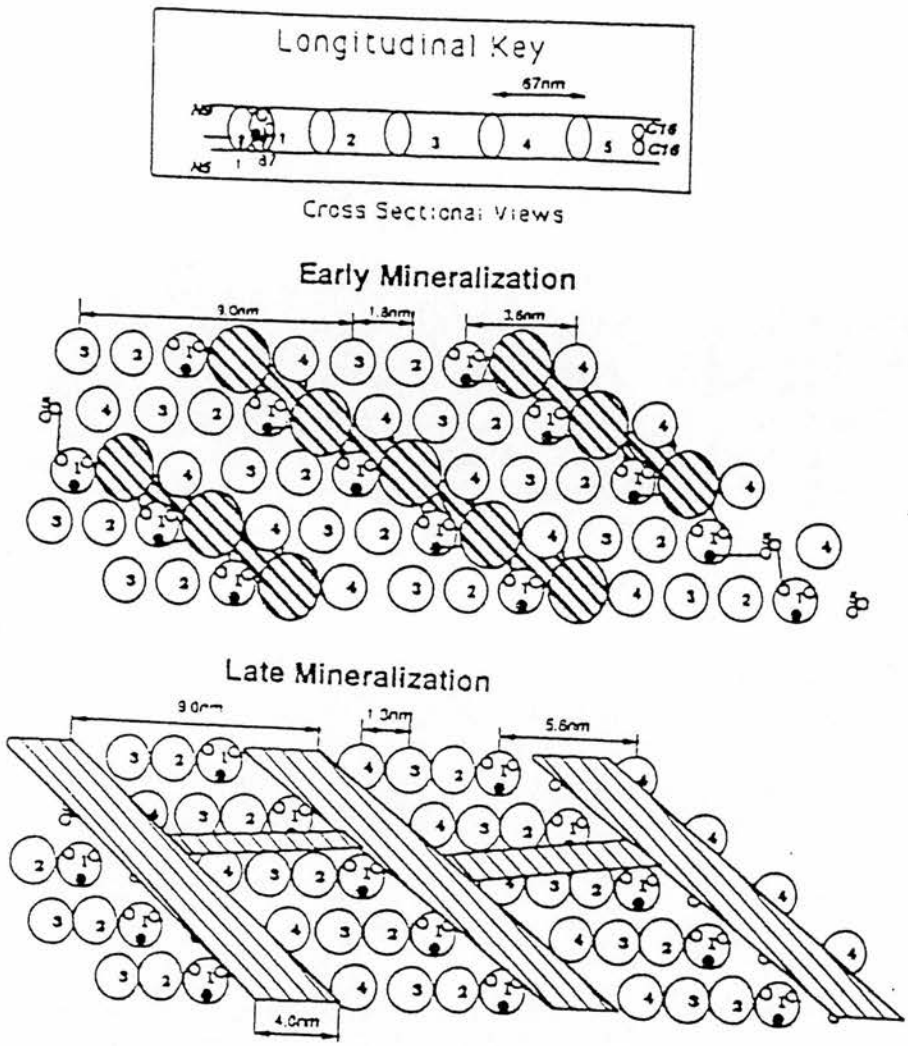

Figure 1.9. shows a cross sectional view of mineralizing collagen fibres in the model proposed by Katz *et al.*, 1989, to accommodate mineral within the fibril and to account for the observed compression of the molecules within the fibril.
The longitudinal key shows the cross section of a collagen molecule. Segments 1-4 are 67 nm long each and segment 5 is approximately 30 nm long. In segment 1 the open circles containing 2 smaller open circles and a solid filled circle represent residue 87 crosslinking site on $\alpha 1$ and $\alpha 2$ chains respectively. The open circles in segment 5 represent the C terminal telopeptide crosslink sites on $\alpha 1$ chains only. Lines between segments 1 and 5 denote crosslinks. The mineral is represented by shading.
In early mineralization, the mineral is accommodated within the gap regions between molecules and overlapping into adjacent gap regions without compressing the collagen molecules. With further growth, there is a redistribution of space within the fibrils as a result of an anisotropic compression of the molecular segments that are not constrained by intermolecular crosslinks, as shown in late mineralization. In yet later stages of mineralization the crystals extend into the overlap regions axially and fuse with one another, laterally by means of dendritic process.

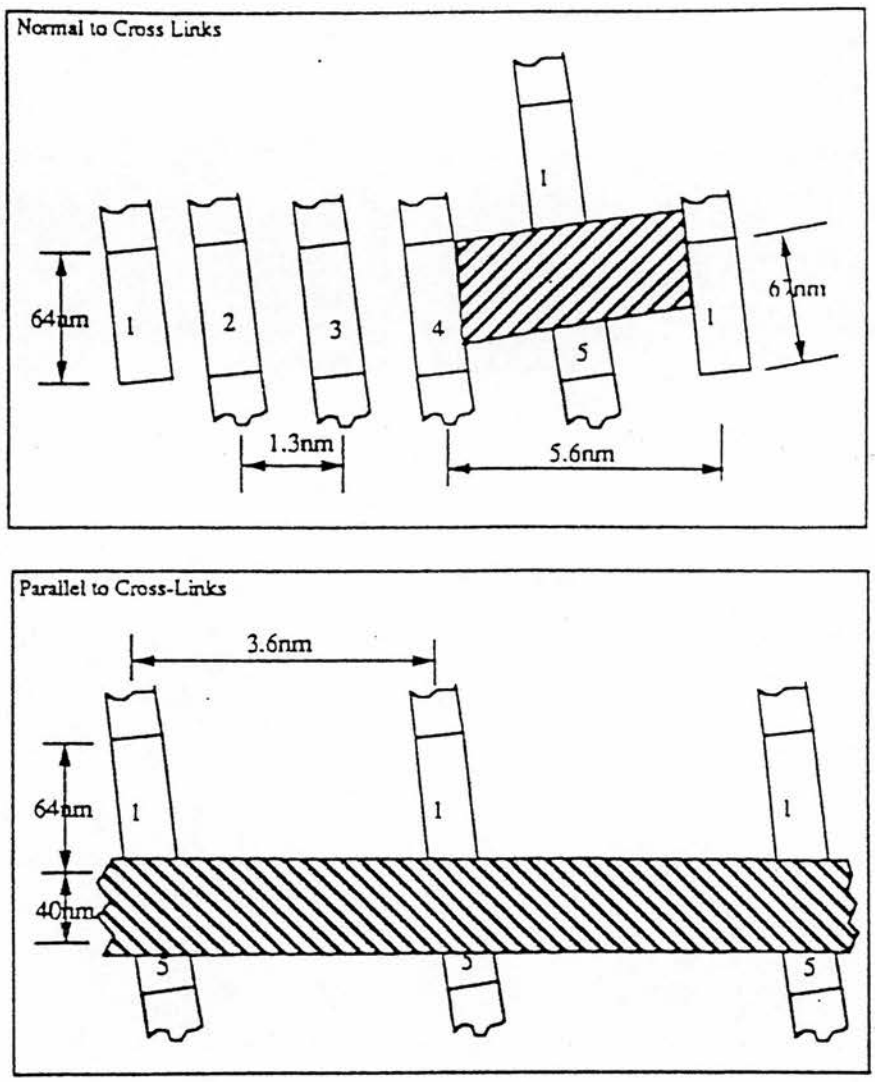

Figure 1.10. This figure shows the model proposed by Katz *et al.*, 1989 and shown in cross section in Figure 1.9 in a longitudinal view for the late mineralization. The numbers represent the D length segments through the collagen molecule. The top diagram is normal to the crosslinks and the bottom diagram is parallel to the crosslinks. All the segments are shown to tilt away from the fibre axis increasing the lateral dimensions of the gap to 4 nm. They are also tilted in the direction parallel to the fibre axis becase the compressive strain is part of an axially periodic twisting deformation throughout the fibril. The mineralization is also shown to extend into the overlap region.

up to their interaxis distance of close-packing, about 1.3nm. Because such deformations tend to follow the symmetry of the structure, the collagen molecules flex away from the fibril axis in an axially periodic way. This reduces the axial repeat of a mineralized fibril to about 64nm. In yet later stages of mineralization, the crystals extend into the overlap regions, axially, and fuse with one another laterally, by means of dendritic processes.

Small angle X-ray scattering carried out by Fratzl and co-workers, discussed in the previous section with regards to location of the mineral, also investigated the collagen packing with mineralization. It was noted in this investigation that the various proposed models for the equatorial arrangement of collagen molecules assumed a regular crystalline arrangement for the molecules, obtained from structure refinements using mainly the X-ray scattering from rat tail tendon. For wet turkey leg tendon or demineralized bone, however, it was well known that the X-ray scattering patterns do not consist of sharp Bragg reflections (as expected for a crystalline arrangement) but rather of broad diffuse maxima indicating a much lower degree of order. Other investigators (Woodhead-Galloway & Machin, 1976) showed that the X-ray scattering, due to the lateral arrangement of the collagen molecules in turkey tendon, is better described assuming a two-dimensional liquid structure rather than a periodic arrangement. Small angle scattering was used to investigate wet, dry and mineralized turkey leg tendon and computer simulation to compare quantitatively the measured X-ray spectra to a model which assumes a fluid-like lateral arrangement of molecules in collagen fibrils. It was found that, as with other investigations, the d-spacing of fresh tissue was greater than dry tissue; also it found that the width of the peak changes. For dry samples the peak was reasonably sharp but for wet samples the peak becomes

broad so that a regular arrangement of the molecules is unlikely. Therefore the investigators assumed the liquid like arrangement. Figure 1.11 shows a) the observed equatorial X-ray scattering, b) the computer model of the lateral packing of collagen molecules and c) the calculated equatorial scattering for the computer models. From the liquid-like arrangement of the molecules in the equatorial plane, the authors discovered a very natural model for the equatorial structure of mineralized collagen is obtained. With the use of computer simulation it was shown that, just by replacing progressively the water inside the fibril by mineral, it is possible to nucleate reasonably large crystals even inside the overlap region. In some regions of the mineralized tissue, the collagen molecules have then a much smaller spacing than in the wet tissue, which explains the common observation that the Bragg-spacing of the molecules decreases with the mineral content of the tissue (Fratzl *et al.*, 1993).

The axial packing of the collagen molecules in mineralized tissues, unlike the equatorial packing, is not under dispute. The axial spacing found for dried, nonmineralized turkey leg tendon was 64±0.3nm and for wet, native tendon and wet or dry mineralized tendon was 67±0.3nm (Bigi *et al.*, 1988). Further work carried out by these authors on decalcified tendon showed that the deposition of mineral in the relatively disordered gap regions increases the structural order and results in better alignment of the collagen fibrils along the tendon axis (Bigi *et al.*, 1991).

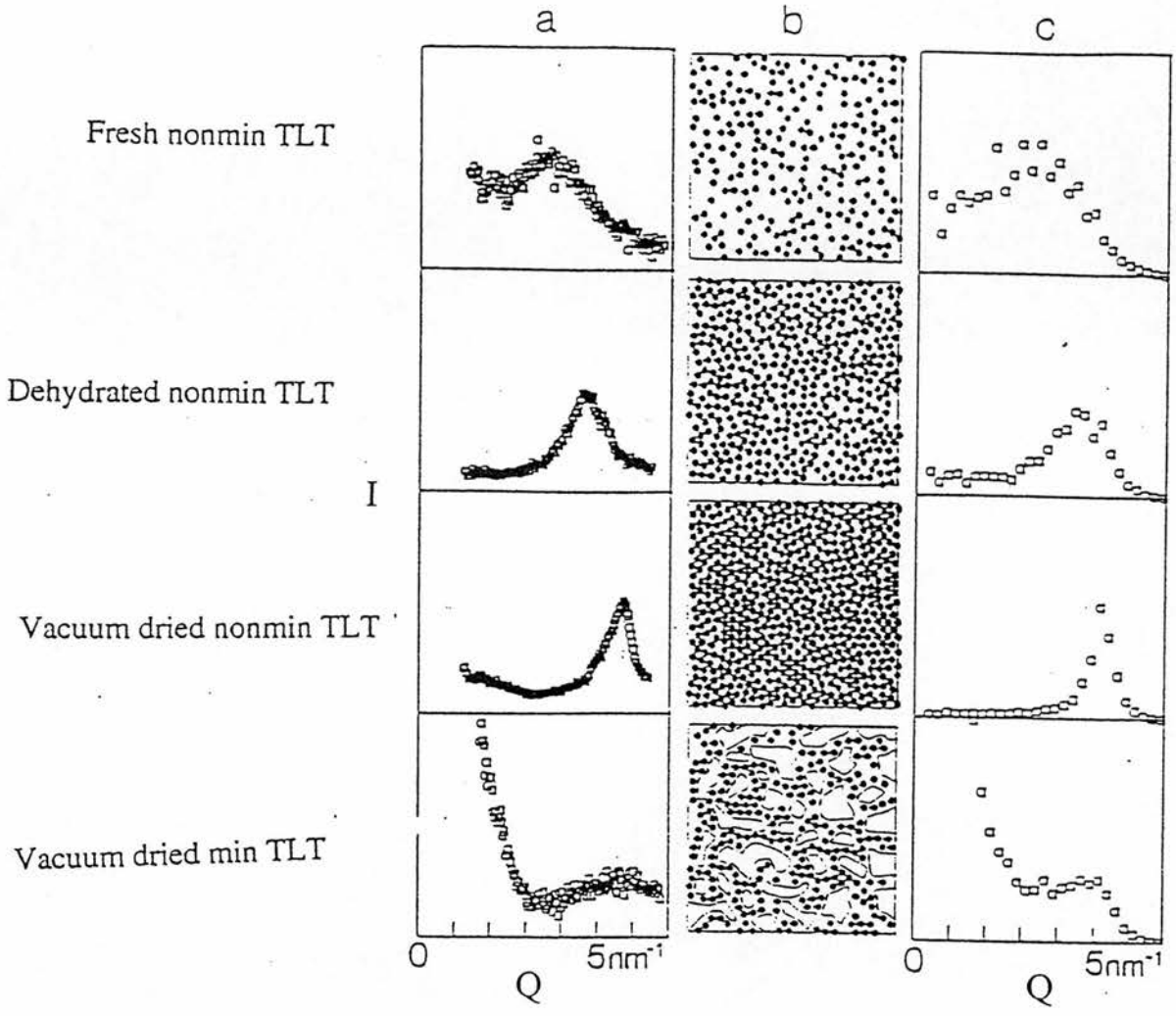

Figure 1.11. demonstrates the models proposed by Fratzl *et al.*, 1993 where collagen molecules are packed laterally as for a hard disc fluid. A hard disc fluid assumes that there is no attraction of the molecules when the distance between them is greater than the sum of their radii but infinite repulsion if the distance is less than the sum of their radii. This means that the molecules can occupy anywhere in the fibril with no attractive forces between them, the only restriction being they cannot overlap, laterally. The panels in a) are the integrated equatorial intensity from the observed X-ray diffraction patterns. The panels in b) show computer models of possible configurations of the hard disc fluid. The black dots represent collagen molecules and the larger bodies in the bottom panel represent the mineral. The packing function is 0.3 for native, nonmineralized collagen, 0.56 for slightly dried unmineralized collagen and 0.7 for vacuum dried unmineralized collagen. For the mineralized tendon, the model shows the same number of molecules as for the native tendon but they are rearranged to make place for mineralized crystals. The panels in c) are the calculated integrated equatorial intensity for the computer models in b). The computer models appear to give the good agreement between calculated and observed equatorial intensity.

1.4.2.Fibril Shape

An investigation using high voltage electron microscopy and stereomicroscopy into the spatial relationship between the inorganic crystals of calcium phosphate and the collagen fibrils of pickerel and herring bone was carried out. One of the observations made in this study was that by using three-dimensional computer reconstruction of serial transverse and longitudinal sections it could be seen that there are periodic swellings along the collagen fibrils corresponding to the gap regions as mineralization proceeds. Bulging of fibrils was observed only in the more heavily mineralized regions of the tissue. This result suggested that structural changes of the collagen fibrils may occur to accommodate additional mineral mass during the progressive increase in the deposition of a solid phase of calcium phosphate within the fibrils (Lee & Glimcher, 1991).

An alteration of the collagen fibril diameter was also seen in cementum. Calcifying collagen fibrils were seen, using transmission electron microscopy, to expand while decreasing interfibrillar space, with the deposition of mineral crystals (Kim *et al.*, 1995).

1.4.3 The Pattern of Intermolecular Crosslinking

Many studies have been carried out on the crosslink profiles in nonmineralized and mineralized tissues. Comparisons between the two different crosslink profiles have been made and hypotheses proposed to account for these changes.

The molecular distributions of intermolecular crosslinks in foetal bovine bone collagen fibrils (Yamauchi *et al.*, 1989) have been compared to those recorded in a previous study for periodontal ligament (Yamauchi *et al.*, 1986). The results showed that the

COOH-terminal telopeptide portions of bovine bone collagen molecule shared a very similar crosslinking system as periodontal ligament. The hydroxylysine and lysine in this telopeptide of the α1 chains were quantitatively converted into aldehydes which stoichiometrically crosslink to hydroxylysine-87 on both α1 and α2 chains of neighbouring molecules. The ratio of crosslinked α1 to α2 chains in the fibrils was 3 to 1. Since a 2:1 ratio of α1 to α2 derived crosslinks on a hexagonal array is associated with randomised angular (azimuthal) orientation of collagen molecules, the ratio of 3:1 strongly indicates that collagen molecules in these tissues are packed into fibrils with a fixed azimuthal orientation (Figure 1.12). Although these authors found similar crosslinking patterns for both tissues in the COOH-terminal, the NH_2-terminal telopeptide was quite different. In periodontal ligament the NH_2 telopeptide was found to be utilised for a dehydro-HHMD and dehydro-HLNL crosslink formation. Few aldehyde derived crosslinks were found in this telopeptide of the bone collagen. It was suggested that the relative paucity of crosslinks in this region in the bone collagen may favour mineralization.

The crosslinking in the COOH-terminus was further investigated. The 16^C residue of the α1 chains of bone collagen from foetal (4-6 month embryo) and mature (2-3 year old) bovine animals was studied. It was found that the COOH-terminal crosslinking changed with maturation. It was hypothesized that at first, each 16^C residue in each of the two α1 chains of the collagen molecule is incorporated into a sheet-like pattern of intermolecular iminium crosslinks which stabilises the young, nonmineralized fibril as a whole. In time some of these labile crosslinks mature into pyridinoline while others dissociate back to their precursor form. The latter is likely due to changes in the molecular packing brought about by the mineralization of the collagen fibrils. The

resultant reduction in crosslinking connectivity, it was hypothesized, may provide a mechanism for enhancing certain mechanical characteristics of the skeleton of a mature animal (Otsubo *et al.*, 1992).

Crosslinking at the NH_2-terminal was also investigated, although the tissue used for this study was bovine dentin collagen. Studies of this tissue provided evidence that pyridinoline is also located in the NH_2-terminal telopeptides (α1-chain 9^N or α2-chain 5^N) and α1 chain 930 (Kuboki *et al.*, 1993). Although this evidence is contrary to the crosslink profile in the NH_2-terminal telopeptide in bone, it can be assumed that the paucity of crosslinks in this region, as reported for bone, cannot be a mechanism used in every mineralized tissue.

From these results it was assumed that the nascent mineral crystals are deforming collagen either by mechanical forces or osmotic forces. However research on turkey leg tendon brought this assumption into dispute. The crosslinks in mineralized, nonmineralized and transitionally mineralized (portion of the tendon at the edge of mineralization) portions of 1-year-old, fully mineralized tendon, were measured. It was discovered that, in the nonmineralized portion of the tendon, the predominant mature crosslink present is pyridinoline, whereas in mineralized portions there are appreciable levels of deoxy-pyridinoline present. The molecular loci of pyridinoline in nonmineralized collagen and deoxypyridinoline in the mineralized collagen were found to be identical. As the precursors of both these crosslinks are different, the authors tentatively concluded that the post-translational chemistry and molecular environments of the fibrils are different in these two portions of turkey leg tendon (Yamauchi & Katz, 1993). This result implies that perhaps there is resorption of

existing collagen with mineralization and a newly synthesized collagen with a different lysine hydroxylation state produced.

1.4.4 Segmental Motion

Nuclear magnetic resonance (NMR) spectroscopy was used to compare the molecular dynamics of the collagen backbone in three types of collagen fibres: in reconstituted fibres of chick calvaria collagen that are not crosslinked and not mineralized; in intact rat tail tendon collagen fibres that are crosslinked but not mineralized; and in intact rat

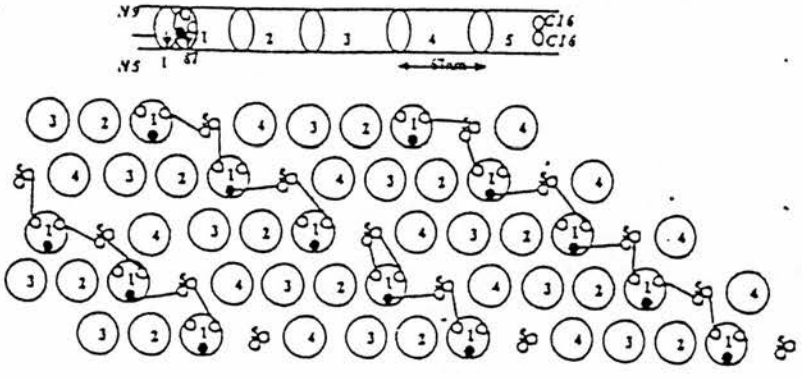

Figure 1.12. shows a molecular packing model for skeletal tissues as derived from crosslink data by Yamauchi *et al.*, 1989. The longitudinal key shows the cross section of a collagen molecule. Segments 1-4 are 67 nm long each and segment 5 is approximately 30 nm long. In segment 1, N9 and N5 represent the N-terminal telopeptide crosslink sites on the α1 and α2 chains respectively. The open circle containing 2 smaller open circles and a solid filled circle in this segment represent residue 87 crosslinkage site on α1 and α2 chains respectively. The open circles in segment 5 represent the C-terminal telopeptide crosslink sites at residue 16 of the C telopeptide (C16) on α1 chains only. The lines connecting these represent crosslinks. The molecules in this model are based on a hexagonal lattice 4 x 1D staggered molecules and 2 x 2D staggered molecules. All the molecules have the same angular orientation which results in a 3:1 ratio of α1 to α2 chain intermolecular crosslinks. This crosslinking forms sheet-like structures rather than microfibrillar.

calvaria collagen fibres that are crosslinked and mineralized. These studies showed that the rms amplitude of the anisotropic backbone motion that occurs in reconstituted collagen fibers is slightly reduced by crosslinks, whereas the amplitude of this motion is significantly reduced by mineral (Torchia & Szabo, 1985).

The effects of mineral upon the dynamics of several types of amino acid side chains in collagen were also investigated. In contrast with the results obtained for the backbone motions, the side chain motions were only marginally more hindered in mineralized samples as compared with nonmineralized samples (Sarkar *et al.*, 1987).

1.5. Aim

From the foregoing evidence it is clear that very few aspects of mineralization are understood. The aim of the present research has been to determine how the structure of collagen influences mineralization and whether changes in the packing of the collagen observed with mineralization are a consequence of mineralization itself or whether these changes occur prior to mineralization and perhaps play a role in the mineralization process.

Two model systems have been used, an *in vivo* system, turkey leg tendon and an *in vitro* system, foetal bovine bone cell culture. Turkey leg tendon has been used as a model for mineralization many times; its parallel, highly organised fibrils and both nonmineralized and mineralized portions make it an excellent model. Figure 1.13 shows X-ray pictures of a turkey leg from 8 to 20 weeks of age. The tendons can be seen to mineralize during this time. The foetal bovine bone cell culture system was used because the model is capable of producing sheets of bone as opposed to the discrete nodules of mineral common to other osteoblast cell culture systems.

Both biochemical and structural studies were performed on samples. Crosslink analysis and X-ray diffraction have been used to investigate the structures of mineralizing tissue with a view to determining any changes with mineralization.

a)

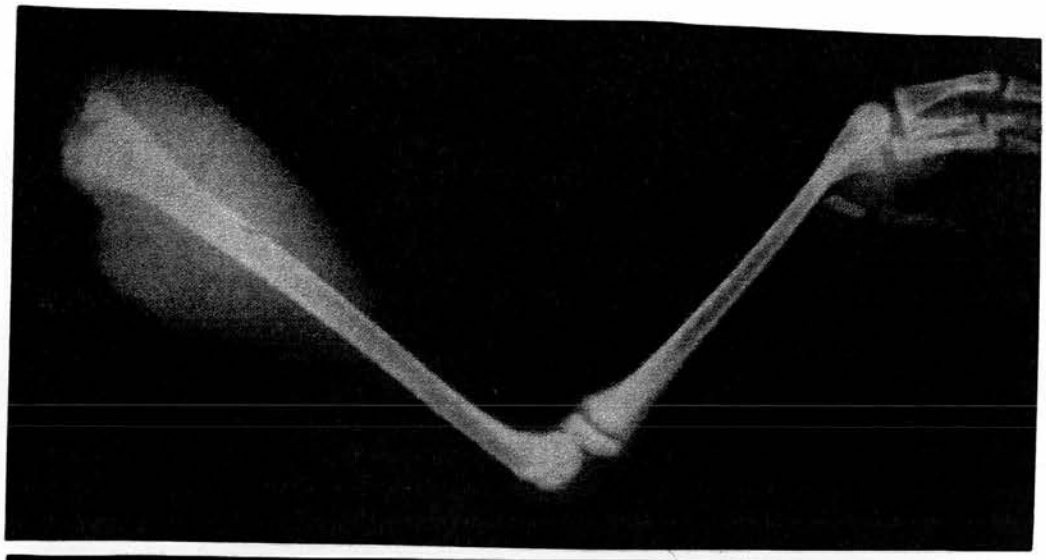

b)

c)

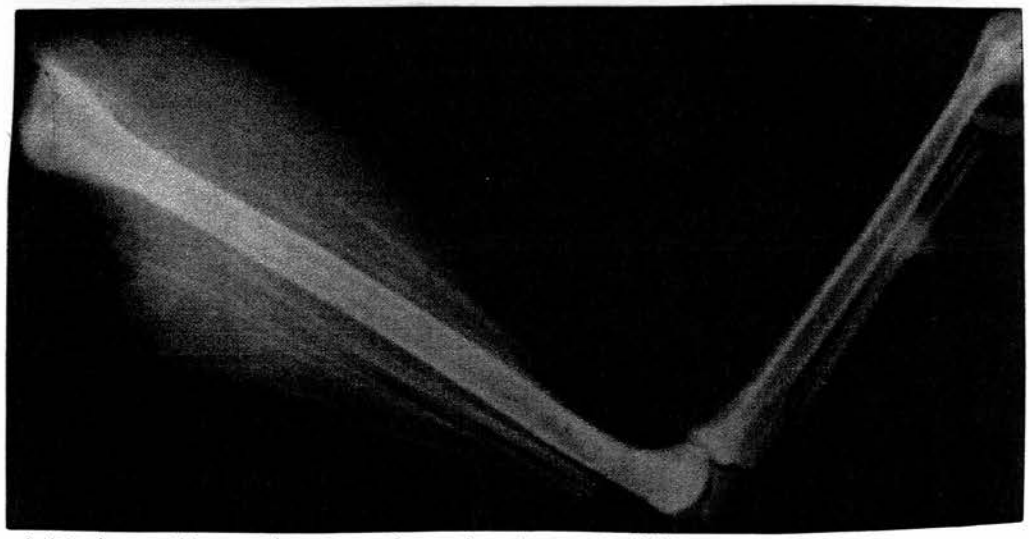

Figure 1.13 shows X-ray pictures of a turkey leg at 3 different ages.

a) 8 weeks of age. No mineralization of the tendons can be seen.
b) 12 weeks of age. The start of mineralization can just been seen on the bottom of the muscle side, closest to the joint.
c) 20 weeks of age. Mineralization of the tendons can clearly be seen in the muscle side and towards the bones of the foot. Note that no mineralization of the tendons occur over the joint.

Chapter 2

Materials and Methods

2. Materials and Methods

2.1 Crosslink Analysis of Turkey Leg Tendons

2.1.1 Materials

Sodium boro(^{3}H)hydride was supplied by Amersham International, Amersham, U.K. *o*-phthaldialdehyde (OPA) was provided by Sigma Chemical Company, Poole, U.K. P11 phosphocellulose was supplied by Whatman Biosystems, Maidstone, U.K. The scintillation fluid, N.E. 265, was obtained from N.E. Technology Ltd, Edinburgh, U.K. All other chemicals used were analytical grade.

2.1.2 Methods

2.1.2.1 Preparation of Tissue, Reduction and Hydrolysis.

The leg tendons were excised from both male and female turkeys sacrificed at different ages. After surrounding tissue had been removed, the tendons were equilibrated in phosphate buffered saline (50mM phosphate, 150mM NaCl, pH7.6; PBS). The tendon was reduced as described previously (Robins *et al*, 1973) with sodium boro(^{3}H)hydride (final activity, 0.1mCi/ml and 7.3Ci/mmol NaB^3H_4). After 5 minutes, unlabelled $NaBH_4$ (1mg) was added and the mixture stirred for 30 minutes. The reduced tendons were washed copiously with water and then sectioned as desired, weighed and hydrolysed in 6M HCl for 16h in sealed hydrolysis vessels.

The reduced, hydrolysed samples were dried under vacuum, washed with water and dried again, and finally redissolved in 1.0ml of water.

2.1.2.2 Hydroxyproline Analysis.

To determine the free hydroxyproline from hydrolysates, the "direct acid" method as described by Firschein and Shill (1966) was used with the exception that isopropanol was substituted with 2-methyl cellosolve.

2.1.2.3 Determination of Pyridinoline and Deoxypyridinoline.

The method used to determine pyridinoline and deoxypyridinoline was the Gilson ASPEC HPLC system described previously (Pratt *et al*, 1992).

2.1.2.4 Determination of Dihydroxylysinonorleucine (DHLNL) and Hydroxylysinonorleucine (HLNL).

An HPLC method was used in the separation of DHLNL and HLNL that involved post-column derivatization of samples with OPA. Before this rapid, quantitative analysis could be performed a cleanup of the hydrolysates was necessary.

A. Sample Preparation

Phosphocellulose P11 was used for the cleaning step, a method that was developed from that used by Fujimoto for isolating pyridinium crosslinks (Fujimoto, 1980).
A slurry was prepared by washing the P11 sequentially in 0.5M NaOH, 0.5M HCl and water according to the manufacturers instructions. Mini-columns (2ml) were prepared with this slurry and washed with several column volumes of 0.1M HCl. An aliquot of

hydrolysate was added to 0.1M HCl (3ml) and applied to the column. This was washed three times with 0.1M HCl (6ml) and the crosslinks eluted with 0.5M HCl (10ml).

A percentage recovery of the reducible crosslinks was calculated by running ^{3}H-labelled crosslink standard on one of the P11 mini-columns. Scintillation fluid (2.5ml) was added to two 200µl aliquots of the eluate, one with 1µl sodium boro(^{3}H)hydride added, a 20µl aliquot of the original ^{3}H-labelled crosslink standard and a 1µl aliquot of sodium boro(^{3}H)hydride. The radioactivity of all these samples was then measured using a Tricarb Series 4000 Minaxi Scintillation Counter for 2 minutes each.

A quenching correction was then applied and a percentage recovery of the crosslinks was calculated. Each eluate was then dried under vacuum.

B. Separation

The column used to separate DHLNL and HLNL was a 25cm x 0.4cm i.d. stainless steel column, packed under gravity with a slurry of Locarte cation-exchange resin (5.5-6.5µm). It was equilibrated with 0.068M tri-sodium citrate-HCl buffer, pH 4.0 at 1ml min^{-1} at 70°C using a column oven (Anachem Ltd, Beds, U.K.). The crosslinks were applied to the column in 0.068M tri-sodium citrate buffer-HCl, pH 2.2 (2ml) and were separated using a pH gradient, from 50% A (0.068M tri-sodium citrate-HCl, filtered and degassed, pH4.0) to 100% B (pH 5.0) over 50 minutes at a flow rate of 1ml min^{-1} (Gilson 305 and 306 HPLC pumps, Gilson Instruments, France) at 70°C. The retention time for DHLNL was 26 minutes and for HLNL was 32-34 minutes. One minute fractions were collected, 750µl aliquots of each 1ml fraction was taken for quantification with OPA, leaving 250µl for scintillation counting.

C. Measurement of Specific Radioactivity

The radioactivities of the eluted fractions were measured using a TriCarb Series 4000 Minaxi Scintillation Counter. The 250µl aliquots had scintillation fluid (2.5ml) added and were counted for 2 minutes each or longer if the levels of radioactivity were low. The crosslink containing fractions were identified and the corresponding 750µl aliquots were pooled and dried ready for analysis with OPA.

D. Quantification

Post-column derivatization with an alkaline solution of OPA in the presence of a strong reducing agent (Roth, 1971) allows the detection of amino acids in the nanomole range.

OPA (100mg) was dissolved in ethanol (1.25ml) and 2-mercaptoethanol (0.5ml) and added to borate buffer (250ml, 0.4M boric acid, 0.39M potassium hydroxide, filtered and degassed) and was pumped at 1ml min^{-1}. The dried down fractions were re-run on the column with the eluate being pumped through a T-piece in order to mix with the OPA solution. A fluorimeter (Shimadzu RF 535, Dyson Instruments Ltd, Tyne and Wear, U.K.) was used in the detection of the derivatized crosslinks with excitation at 355nm, emission at 450nm and the data processed by a Shimadzu R-3A Integrator (Dyson Instruments).

2.2. Experiment to Measure Collagen Turnover in Turkey Leg Tendons

2.2.1 Materials

L-[5-^{3}H] Proline was supplied by Amersham International, Amersham, U.K. Standard grade Dowex 50W-X8 (H^+ Form, particle size 0.15-0.3mm, 50-100μm mesh) and Dowex 50W-X8 (H^+ form, particle size 0.04-0.075mm, 200-400μm mesh) were supplied by BDH Merck, Leics, U.K. All other chemicals used were analytical grade.

2.2.2. Methods

2.2.2.1 Purification of L-[5-^{3}H] Proline.

In order to eliminate any naturally occurring radiolabelled contaminants in the L-[5-^{3}H] proline, that might interfere with the quantification of the labelled material incorporated into protein, purification of the starting material, using ion-exchange chromatography was necessary.

A. Ion-exchange Chromatography

L-[5-^{3}H] Proline (4mCi, 1mCi/ml) was acidified with 0.1M HCl to pH 2.2 and applied to a Locarte column (cation resin 5.5-6.5μm, 0.9cm^2 x 15cm). The proline was eluted with tri-sodium citrate-HCl (filtered and degassed, pH 3.0) at 0.6ml min^{-1} at 55°C. The proline eluted at 57-63 minutes.

B. Desalting

A slurry of Dowex 50W-X8 (H^+ form, 50-100μm mesh) cation exchange resin was prepared by equilibrating firstly in 2M NaOH for 30 minutes at 60 °C and, after washing with water, with 2M HCl before washing again with water. The fractions containing proline were pooled and applied to a Dowex column (2ml) and washed with water (40ml). The desalted L-[5-^{3}H] proline was eluted with 10% v/v ammonia (10ml) and dried under vacuum. The recovery of the purified L-[5-^{3}H] proline was 2.5mCi.

2.2.2.2 Labelling *In Vivo*

The dried proline was redissolved in PBS (5ml) and filtered twice through sterile 0.2μm syringe filters (GelmanSciences, Northampton, U.K.). L-[5-^{3}H] proline (2mCi) was injected intravenously into a 12 week old, female turkey. Twelve days after injection the bird was sacrificed and the legs were removed and stored at -20°C.

2.2.2.3 Analysis of the Tissue

The tendon was prepared as described in earlier sections except that it was reduced using KBH_4. Hydroxyproline was measured using the colorimetric assay as described previously.

A. Separation of Proline and Hydroxyproline

Proline and hydroxyproline had to be separated using a system that would enable a large amount of both to be applied to a column in order to obtain sufficient radioactivity to quantify adequately the small amounts of ^{3}H labelled material present.

Trials using a Locarte ion exchange column to separate proline and hydroxyproline proved unsuccessful as only 500 nmoles could be applied to the column. A method adapted from a previously published abstract (Partridge and Elsden, 1961) was developed.

A slurry of Dowex 50W-X8 (H^+ form, 200-400μm mesh) was prepared as previously described. The resin was then allowed to equilibrate in tri-sodium citrate-HCl (0.068M, pH 2). An aliquot of hydrolysate (4μMoles hydroxyproline) in tri-sodium citrate-HCl (0.068M, pH 1.5, 1.5ml) was applied to a Dowex column (2ml). Hydroxyproline and proline were eluted in tri-sodium citrate-HCl (0.068M, pH 2) flowing under gravity. Hydroxyproline standard eluted at 21-24ml and proline standard eluted at 33-39ml. An aliquot of 250μl from each 3ml fraction was mixed with scintillation fluid (2.5ml) and kept at 4°C for at least 30 minutes to minimise chemiluminescence artefacts. Each fraction was counted for 5 minutes.

B. Quenching Correction

L-[5-^{3}H] proline (1μl) was added to aliquots (250μl) of each fraction from a nonmineralized tendon sample and a mineralized tendon sample. Scintillation fluid was added (2.5ml) and each was counted for 5 minutes after 30 minutes at 4°C.

2.3 Foetal Bovine Bone Cell Culture to Determine Any Changes in Crosslinking with Mineralization.

2.3.1 Materials

Dulbeccos Modified Eagles Medium (DMEM) and Dispase were supplied by GibcoBRL, Life Technologies, Paisley, U.K. Insulin, transferrin and selenium (ITS), Collagenase, Penicillin/Streptomycin solution and Trypsin-EDTA were obtained from Sigma Chemical Company, Poole, U.K. Heat inactivated Foetal Calf Serum (FCS) was supplied by GlobePharm, Surrey, U.K. L-[U-^{14}C]Lysine monohydrochloride was supplied by Amersham International, Amersham, U.K. All the other chemicals used were analytical grade.

2.3.2 Methods

2.3.2.1 Foetal Bovine Bone Cell Culture.

The model used for these experiments was described previously (Whitson *et al*, 1992). The femurs of midterm foetal calves were obtained from freshly slaughtered animals. All the skin, muscle and periosteum were stripped from the bones and the cartilaginous ends removed. Longitudinal strips of the outer cortex were excised and washed in sterile PBS at 37°C to remove any blood and tissue left. These strips of cortex were then added to 20ml initial digestion media (DMEM, 0.5mg/ml collagenase, 3mg/ml dispase and 10,000U penicillin, 10mg streptomycin/ml) and incubated at 37°C for 3h. After this time the tubes were shaken vigorously for 2

minutes to release the cells. This cell suspension was removed to 50ml centrifuge tubes whilst the bone strips were rinsed in 10ml rinse media (DMEM and 15% FCS) to stop digestion. This stop media and the cell suspension were combined and filtered through a 45μm screen filter (Millipore, Herts, U.K.). The remaining bone strips were placed in fresh tubes and after adding 20ml final digestion media (DMEM, 3mg/ml dispase and 5% FCS), were incubated at 37°C overnight. The filtered 3h cell suspension and stop media were centrifuged for 5 minutes and the pellets washed in 5ml rinse media. These were then centrifuged again, before being resuspended in 6ml of growth media (DMEM, 1mM pyruvate, 15% FCS, 5μg/ml ascorbic acid and 10,000U penicillin, 10mg streptomycin/ml). This cell suspension was then plated out in two 35mm culture dishes (3ml of cell suspension in each). The cultures were incubated at 37°C in a humid environment of 95% air and 5% carbon dioxide. The same procedure of taking the cell suspension and washing the bone strips before filtering, centrifuging and plating out was performed on the overnight digest. The culture medium was changed on the first day after seeding and every 48h thereafter until the cells were almost confluent, ready for passage.

When ready for passage, the cells were washed thoroughly with sterile PBS before 5ml of trypsin-EDTA was added for 10 minutes. After this time, the cells had two washes with 10ml of rinse media, before being centrifuged and resuspended in 5ml growth media. The cells were then counted and evenly seeded at 300 cells mm^{-2} in 24 well plates with 2ml of growth media in each well. The medium was changed the day after this second seeding and every 48h after that until the cells had reached confluence and partial multilayering.

At this time, the growth medium was substituted for mineralizing media (DMEM, 1mM pyruvate, 15% FCS, 50μg/ml ascorbic acid, 10mM β-glycerol phosphate, 15mM HEPES buffer, 5μg insulin, 5μg transferrin, 5ng selenium/ml and 10,000U penicillin, 10mg streptomycin/ml). This medium was changed every 24h for the rest of the experiments.

2.3.2.2 Crosslink Changes in Existing Collagen with Mineralization.

L-[U-^{14}C]Lysine monohydrochloride was added to four cultures (final activity 1μCi/ml) for 48h in growth medium. After this time each culture was washed three times with sterile PBS (2ml). Growth medium was added to two of these labelled cultures after washing and mineralizing medium was added to the other two. The respective media were changed every 48h (Figure 2.2 a).

2.3.2.3 Crosslink Changes in Newly Synthesized Collagen with Mineralization.

L-[U-^{14}C]Lysine monohydrochloride was added to two cultures (final activity 1μCi/ml) for 48h in growth medium. After this time each culture was washed three times with sterile PBS (2ml). Growth medium was again added to the labelled cultures. At the same time, six other, unlabelled cultures were transferred to mineralizing medium L-[U-^{14}C]Lysine monohydrochloride was added (final activity 1μCi/ml) and left for 48h. Again, after the labelling, each culture was washed three times with sterile PBS (2ml) and mineralizing medium was added. All respective media were changed every 48h (Figure 2.2 b).

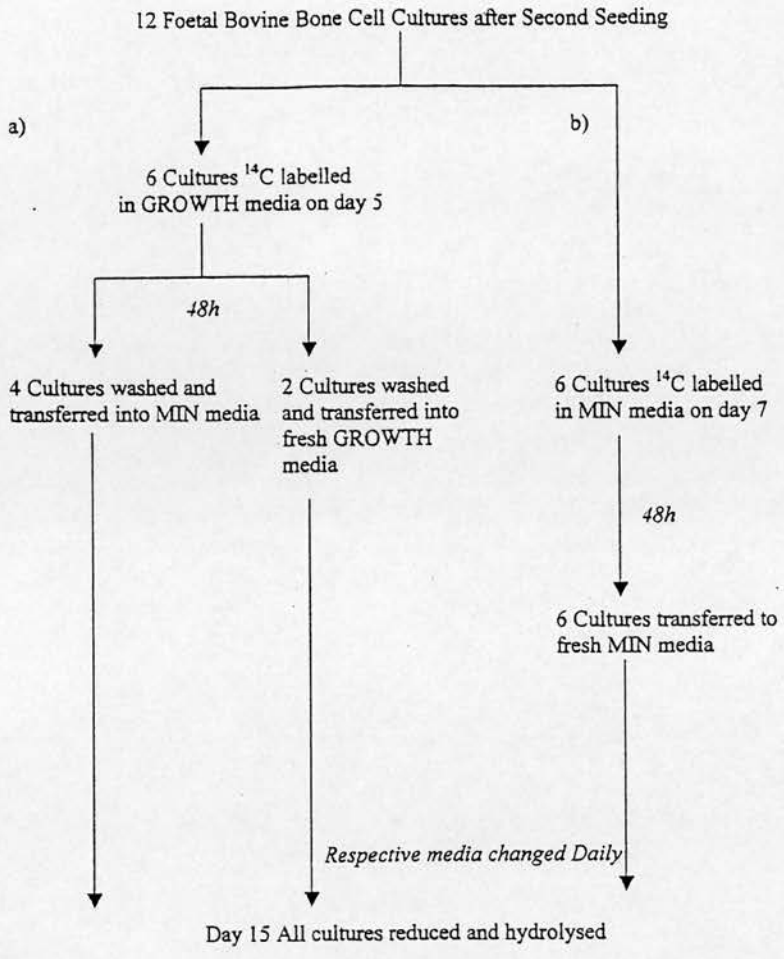

Figure 2.2. Experimental protocols to investigate changes in lysine hydroxylation state in existing and newly synthesized collagen after mineralization using ^{14}C-Lysine pulse chase labelling. a) shows the experimental protocol for investigating changes in existing collagen while in b) the scheme to show changes in newly synthesized collagen is delineated. In both schemes 300 cells mm^{-2} were seeded into 2ml of Growth medium (DMEM, 1mM pyruvate, 15% FCS, 5μg/ml ascorbic acid and 10,000U penicillin, 10mg streptomycin/ml) in the wells of a 24 well plate. After the indicated number of days (5 for a) and 7 for b)) the cells were washed and 2ml of medium containing 2μCi/ml ^{14}C Lysine was added. To follow lysine hydroxylation change in a) exisiting collagen, 4 cultures were incubated in labelled Growth medium for 48h, after which they were washed and grown in unlabelled Mineralizing medium (DMEM, 1mM pyruvate, 15% FCS, 50μg/ml ascorbic acid, 10mM β-glycerol phosphate, 15mM HEPES buffer, 5μg insulin, 5μg transferrin, 5ng selenium/ml and 10,000U penicillin, 10mg streptomycin/ml) and changed every day for a further 8 days. For comparison a control was repeated but grown in unlabelled Growth medium after labelling. b) To follow changes in newly synthesized collagen, labelling was carried out in Mineralizing medium on day 7. After 2 days the cultures were transferred to cold mineralizing medium, again changed every day for a further 8 days. In each of the experiments, all cultures were reduced and hydrolysed before the labelled components were separated.

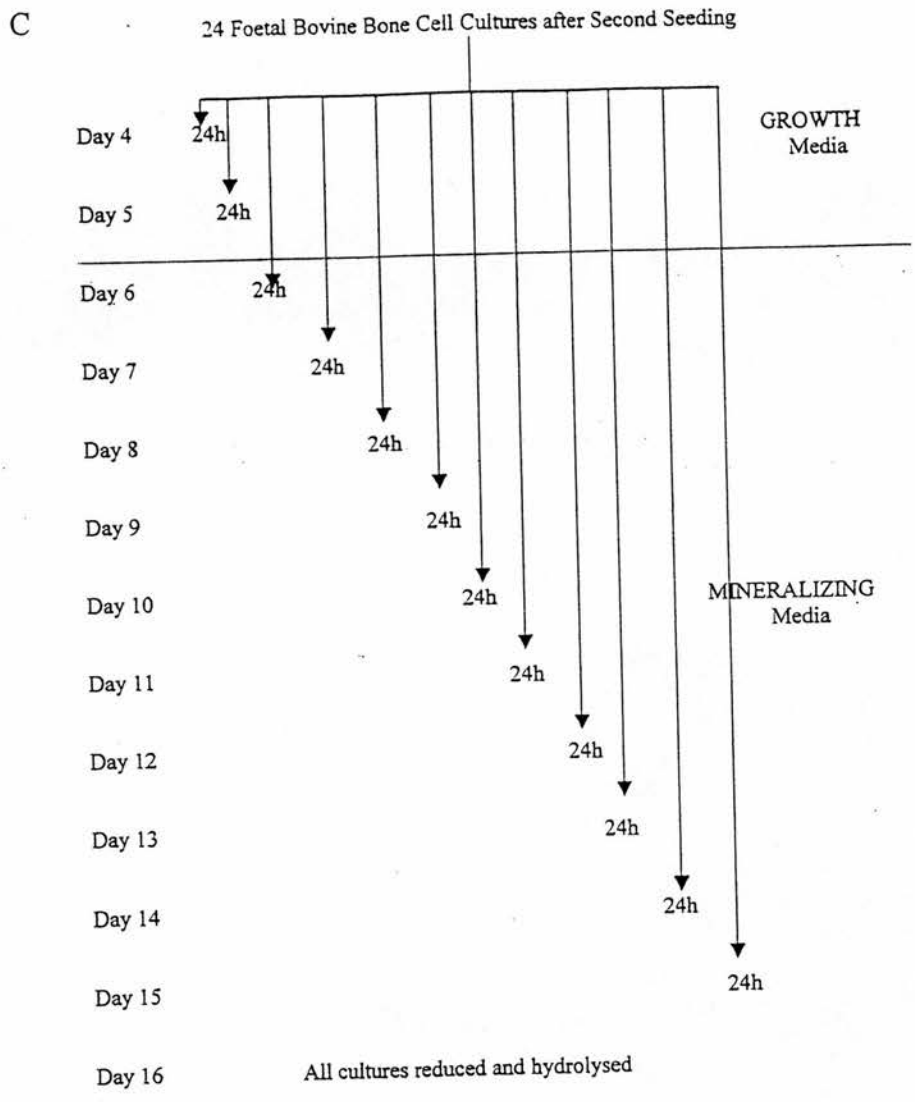

Figure 2.2. c) describes the experimental protocols used to investigate when changes in lysine hydroxylation state occur using ^{14}C-Lysine pulse chase labelling. The cells were seeded as described for a) and b). On day 4 after the second seeding, 2 cultures were labelled as for a) and b) but only for 24h before being washed and transferred to unlabelled medium. Each day after this 2 fresh cultures were labelled for 24h for a further 11 days. The medium used to chase the label is indicated in the figure. All cultures were transferred from Growth medium to Mineralizing medium on day 6. On day 16 all cultures were reduced and hydrolysed before the labelled components were separated.

2.3.2.4 Time Course to Determine When any Changes in Crosslinking Occur.

Twenty four cultures were used for this experiment. Two cultures were labelled with L-[U-^{14}C]Lysine monohydrochloride (final activity 1μCi/ml) for 24h each day. For the first 3 days all the cultures were in growth medium; on the fourth day all the cultures were transferred to mineralizing media for the remaining time. After the 24h labelling the usual washing procedures were carried out (Figure 2.2 c).

2.3.2.5 Reduction and Hydrolysis of Cell Cultures.

At fourteen days after the initial transfer of the cultures into mineralization media all the cultures were washed with sterile PBS (2ml) for 10 minutes. 18.5 mM KBH_4 (1ml) was added to each culture for 20 minutes. They were then washed copiously in water and 6M HCl (1ml) was added to each. Each culture was transferred to sealed hydrolysis vessels and hydrolysed for 16h.

The reduced, hydrolysed samples were dried under vacuum, washed several times with water and finally redissolved in 1ml of water.

2.4 Analysis of Crosslinks

2.4.1 Materials

Dansyl Chloride was obtained from BDH Merck, Leics, U.K and 9-fluorenylmethyl chloroformate (FMOC-Cl) was obtained from Sigma Chemical Company, Poole, U.K. All other reagents were standard grade.

2.4.2 Methods

2.4.2.1 Hydroxyproline Determination

Measurement of hydroxyproline in each cell culture was carried out using a reversed phase HPLC method as described previously (Einarsson *et al.*, 1983 and Einarsson, 1985) to minimise the amount of material needed. This method involved a pre-column fluorescent derivatization of the hydrolysate with (OPA)-mercaptoethanol and then with 9-fluorenylmethyl chloroformate (FMOC-Cl). Hydroxyproline was separated using an acetonitrile gradient. A standard preparation of hydroxyproline was run before and after samples and all samples had 3,4 dehydroproline added as an internal standard.

2.4.2.2 Determination of ^{14}C Labelled Crosslinks.

Ion-exchange chromatography was used to separate the crosslinks and the specific radioactivities of the fractions were determined.

A. Sample Preparation

The samples were prepared as previously described for DHLNL and HLNL determination in an earlier section, using phosphocellulose P11 mini-columns.

B. Separation

Each dried sample from P11 mini-columns was redissolved in tri-sodium citrate-HCl (0.068M, pH 2.2, filtered and degassed, 2ml) and applied to a Locarte column (cation resin 5.5-6.5 μm, 0.9cm^2 x 15cm). The crosslinks were eluted with tri-sodium citrate-

HCl (0.068M, pH 4.6, filtered and degassed) at 0.6ml min^{-1} at 55 °C. Pyd and Dpd standards eluted at 45-55 minutes, DHLNL standard eluted at 90-100 minutes and HLNL standard eluted at 155-165 minutes.

C. Measurement of Specific Radioactivities

The radioactivities of each fraction were measured using CA 1900 Scintillation Counter. An aliquot (500µl) was taken from each fraction and mixed with scintillation fluid (2.5ml). These aliquots were then kept at 4°C for at least 30 minutes to minimise chemiluminescence. Each fraction was counted for 5 minutes.

D. Separation of Pyridinoline and Deoxypyridinoline

The fractions containing Pyd and Dpd were pooled and acidified with 0.1M HCl to pH 2.2 and re-applied to the ion exchange column. These were eluted with tri-sodium citrate-HCl, pH 4.25 (filtered and degassed) at 0.6 ml min^{-1} at 55 °C. The retention times for Pyd and Dpd standard were 85 minutes and 125 minutes respectively.

2.4.2.3 Verification of the Presence of Pyridinoline and Deoxypyridinoline.

To verify that the radioactive fractions eluting at the same time as the pyridinium crosslink standards were in fact Pyd and Dpd they firstly had to be desalted and then applied to the Gilson ASPEC HPLC system as previously described in an earlier section. Pyridinium crosslinks are strongly adsorbed to ion-exchange columns at room temperature and therefore the system used to desalt reducible crosslinks cannot be used.

The radioactive fractions eluting at the same time as Pyd and Dpd standards were pooled and dried under vacuum and then redissolved in acetic acid (0.4M). These were then applied to a Sephadex G10 column (1.7 x 140cm) and eluted with acetic acid (0.4M) at 0.3ml min^{-1}. The retention time for Pyd and Dpd standards was 370-400 minutes.

2.4.2.4 Verification of the Presence of DHLNL and HLNL.

The fractions containing radioactivity that were eluting at the same time as DHLNL and HLNL were verified using rpHPLC. The fractions were desalted and aliquots were dansylated and compared to standards of hydroxylysine, lysine, HLNL and DHLNL. Other aliquots were subjected to periodate cleavage (Robins & Bailey, 1975) before being dansylated and run on rpHPLC. These were compared to dansylated proline and hydroxynorvaline.

A. Desalting of DHLNL and HLNL

The radioactive fractions of interest were acidified to pH 4 with 0.1M HCl and applied to Dowex 50W-X8 (H^+ form, 50-100μm mesh) columns (2ml) as previously described in an earlier section. Each column was washed with water (40ml) before crosslinks were eluted with 10% v/v ammonia (10ml). The desalted samples were dried under vacuum.

B. Periodate Cleavage

Periodate cleavage of reducible crosslinks results in proline and hydroxynorvaline(Robins & Bailey, 1975). A dried, desalted sample was redissolved

in 500µl of water. A 500µl aliquot of 20mM acetic acid/20mM sodium periodate solution was added to this to give a solution of 10mM acetic acid and periodate respectively. This solution was left for 5 minutes at room temperature. After this time the pH was raised to pH 8 with 0.5M phosphate buffer. Potassium borohydride (5mg) was added and the solution left at 30minutes. After this time the pH was dropped to pH 2 with 2M glacial acetic acid and the solution desalted again using a Dowex H^+ (50-100µm) mini columns as previously described and the eluate dried. These dried, periodate cleaved samples were then dansylated as described in the following section.

C. Dansylation

The preparation of samples and the HPLC conditions were adapted from a method for dansylating sugars (Mopper and Johnson, 1983). Post column derivatization of reducible crosslinks with OPA as used in earlier sections, was not used for this validation, as this method requires nanomole quantities of crosslink whereas picomoles of dansylated amino acids can be detected.

The dried, desalted sample was redissolved in water (300µl). Sodium carbonate (0.3M, pH 9, 50µl) was added to a 50µl aliquot of sample and then mixed before 100µl of dansyl chloride solution (10mg/ml acetone) was added. This was then mixed thoroughly before being incubated in a water bath at 60°C for 30 minutes. After cooling 10µl of HCl (0.2M) and 790µl sodium acetate (0.05M) was added. 100µl of this solution was then applied to a Microsorb C18 reverse phase column (25cm x 4.4mm). The dansylated derivatives were eluted using the gradient in Table 2.1 at 1ml min^{-1}, where Buffer A was 83% sodium acetate-HCl (0.05M, pH 6.5), 12.5%

acetonitrile and 5% isopropanol and Buffer B was 19% sodium acetate-HCl (0.05M, pH 6.5), 80% acetonitrile and 1% isopropanol, both filtered and degassed.

Time (minutes)	**Buffer A %**	**Buffer B%**
0	90	10
10	90	10
40	20	80
50	20	80
51	90	10
60	90	10

Table 2.1 The gradient used for eluting dansylated fractions.

2.5 X-Ray Diffraction Theory and Instrumentation.

This section is intended to explain the fundamental principles of X-ray diffraction with particular reference to collagen, thus setting in context the later parts of this thesis. Similarly the instrumentation used is also covered.

2.5.1. Principles of X-ray Diffraction

When X-rays interact with matter these electromagnetic waves are scattered by the electrons within the matter. Figure 2.3 shows a monochromatic beam of X-rays incident on the surface of a crystal at an angle θ. P, Q and R represent the edges of a family of planes distance d apart. Plane P reflects AX in XD. Similarly plane Q reflects BY in YE at the same angle θ. Although the beam penetrates many more planes only the top two need to be considered.

Since Q is lower than P, the beam path BYE is longer than AXD by the amount GY + YH. This is called the path difference.

Since angle GXA = 90° and angle AXP = θ, then angle PXG = 90°

Since angle PXY = 90°, then angle GXY = θ

Similarly it can be shown that angle YXH = θ

From Δ GXY, $\sin\theta = \frac{GY}{d}$ therefore, $GY = d\sin\theta$

From Δ YXH, $\sin\theta = \frac{YH}{d}$ therefore, $YH = d\sin\theta$

Therefore, the Path Difference $(GY + YH) = 2d\sin\theta$

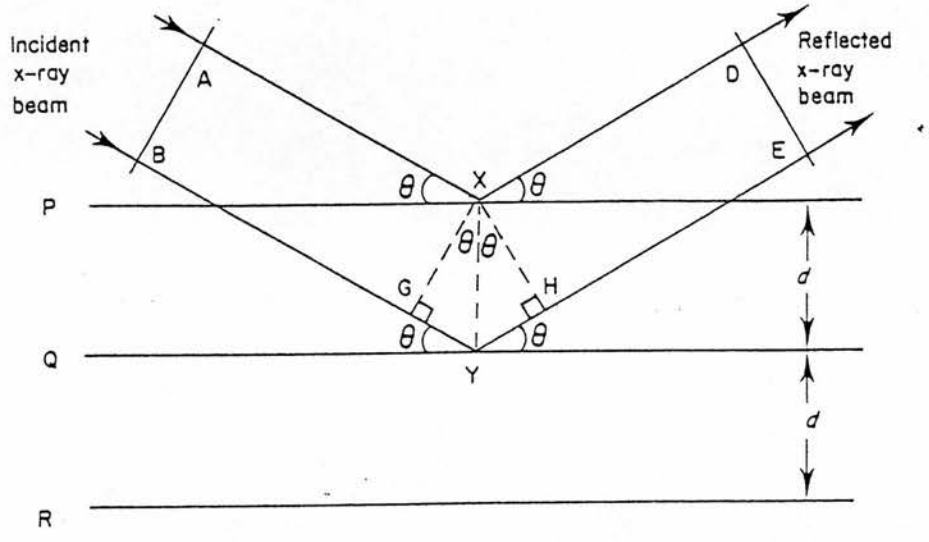

Figure 2.3. Diagram showing a monochromatic beam of X-rays incident on the surface of a crystal at an angle θ.

Now the two reflected rays, XD and YE, will constructively interfere when the path difference is equal to the wavelength (λ) or a multiple of it. Thus the condition for X-ray diffraction is:

$$2d\sin\theta = n\lambda \qquad \text{Bragg's Equation}$$

where n is an integer (1,2,3, etc) called the order of reflection. Figure 2.4. shows the Bragg condition when n = 1, ie when the path difference equals one wavelength,

$$GY + YH = \frac{\lambda}{2} + \frac{\lambda}{2}$$

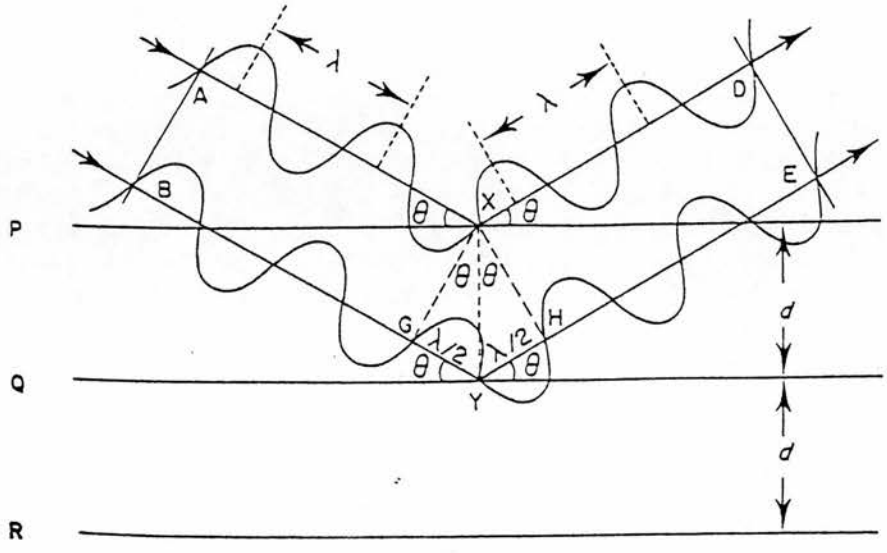

Figure 2.4. A diagram showing the Bragg Condition

The scattering due to one molecule is weak and impossible to detect therefore the effect must be amplified. This is achieved if a large number of identical molecules are arranged in a regular array as are the collagen molecules within a sample. The diffraction effect results in the continuous scattering due to one molecule being resolved into a series of discrete peaks. There is a reciprocal relationship between the sample in real space and the diffraction pattern. This is the Fourier transform of the samples electron density. The Fourier transform of an electron density itself can undergo a Fourier transform to give the electron density again. Two components are needed for this, the amplitude of the wave of electron density and the phase of the waves. The amplitude can be measured from the intensities of the discrete peaks of scatter but the phase cannot be recorded.

2.5.2 Instrumentation

All the X-ray diffraction data collected for this thesis was collected using Synchrotron Radiation. This is the electromagnetic radiation produced when electrons or positrons move at relativistic energies in a circular path. Synchrotron radiation is highly collimated, linearly polarised in the orbit plane and is generally much more brilliant (photons per second per unit area per unit solid angle) than conventional laboratory light sources. This enables the scatter of weakly diffracting samples to be viewed in minutes preventing a loss in hydration that would occur using conventional X-ray sources. Actual beam damage to the tissue is also minimized using synchrotron radiation as beam damage is directly proportional to the time spent exposed to X-rays as well as the flux passing through a sample (Mandelkow *et al*, 1981). Data was collected at the C.L.R.C., Synchrotron Radiation Source (SRS) at Daresbury, England, U.K. and The European Synchrotron Radiation Facility (ESRF), Grenoble, France.

2.5.2.1. S.R.S., Daresbury

S.R.S Daresbury is a three-stage machine for accelerating electrons, comprising a linear accelerator (an "electron gun"), a booster synchrotron and a storage ring. Electrons are fired from the linear accelerator into the booster synchrotron, where they are accelerated to almost the speed of light before being injected into a storage ring. Here the electrons travel in a vacuum inside a tube around the 96m circumference of the ring and remain stored in orbit producing radiation for 10-20h at a time. Synchrotron radiation is produced at each of the 16 bending magnets in the storage ring and released down beamlines. Radiation of different wavelength is then

channelled to individual experimental stations. A number of beamlines at Daresbury are devoted to selecting a narrow range of radiation in the wavelength region corresponding to the CuKα peak of conventional X-ray sources (0.154nm).
Due to the nature of the axial periodicity of collagen, in order to collect the first order of diffraction a camera of sufficient length must be used to separate the first order from the main beam. The minimum length of the camera necessary for this at Daresbury is 1.5m. It is impossible to obtain all of the required reflections from wavelength of X-rays and therefore two separate beamlines are used. Station 7.2 is used for high angle diffraction and station 16.1 has been used for small angle scattering.

A. Station 7.2

Station 7.2 provides a monochromatic X-ray beam of wavelength 1.488**Å** for both protein crystallography and fibre diffraction. A range of collimators were used in collection of data from this station from 300μm to 50μm slits. The camera used to collect the high angle scatter was an aluminium tube sealed at either end by X-ray transparent mylar. The whole camera was flushed through with helium before use to eliminate unwanted scattering from air. The backstop used was a transparent backstop to enable the beam centre to be found but still absorbed the main beam. Data was collected using both Molecular Dynamics Image Plates and an 18cm Marr image plate system.

B. Station 16.1

This station is a high intensity diffraction station at a fixed wavelength of 1.488Å. The station has been optimised for low angle scattering studies. The camera used at this station was a 2.5m length and the beam size 500 x 500μm. Data was collected on a fast multi-wire linear detector.

2.5.2.2. European Synchrotron Radiation Facility (ESRF)

ESRF is the first fully operational 3rd generation synchrotron radiation facility in the world. The synchrotron X-rays are about a trillion times brighter (10^{12}) than conventional X-ray sources used in laboratories.

A. Beamline 1, ID13

This beamline at ESRF is a microfocus beamline. A 2D focusing small angle X-ray scattering camera based on a circular Bragg-Fresnel lens (Snigirev *et al.*, 1993) was used. The focused beam size at the sample point was of about 1.5x2.0μm^2.

2.6 X-ray Diffraction

2.6.1 Preparation of the Tissue to Investigate the Edge of Mineralization using X-ray Diffraction and Crosslink Analysis on Turkey Leg Tendons.

Lengths (~20mm) of whole, cleaned, turkey leg tendons of different ages were sectioned longitudinally to 30μm using a cryostat. Alternate sections were put on ~10μm thick sections of mica (Agar Scientific, Essex, U.K.) and the other sections were placed on microscope slides. All the sections were kept hydrated. A thin ring of

silicon grease was applied around the edge of the samples placed on the mica, and then a drop of 100% ethylene glycol was administered to the sample. The glycol is known to replace the water in the samples (Landis *et al*, 1977) and is less volatile than water, slowing the drying process and producing similar X-ray spectra to native tendon (Fratzl, 1993). Another ~10μm thick section of mica was then placed on top of the sample. Each edge of the sections of mica were dipped in superglue (Loctite 3) and allowed to dry. These sections were then used for X-ray diffraction. The alternate sections collected on microscope slides for crosslink analysis were wrapped in aluminium foil and stored at -20°C.

2.6.2. Preparation of Whole or Thick Sections of Turkey Leg Tendons for Analysis.

Frozen tendons were thawed and placed in PBS. Whilst in PBS rat tail tendon was tied to either end of nonmineralized turkey leg tendon. The rat tail tendon was used to tension the nonmineralized turkey leg tendon in the sample cell (Figure 2.5). Mineralized tendon samples were simply placed on the mica windows of the sample cell. Pieces of tissue soaked in PBS were also placed in the sample cell to keep the tendon hydrated. The sample cell was sealed and positioned in the sample beam.

2.6.3. Positioning of a Sample

The sample sections "sandwiched" in mica were mounted on a specially made frame and the whole tendon samples were in the sample cell. The sample holders were placed in a goniometer and their position adjusted in the beam. Green X-ray sensitive

paper was put on the back of the samples to ensure the beam is directed to the portion of the sample to be examined.

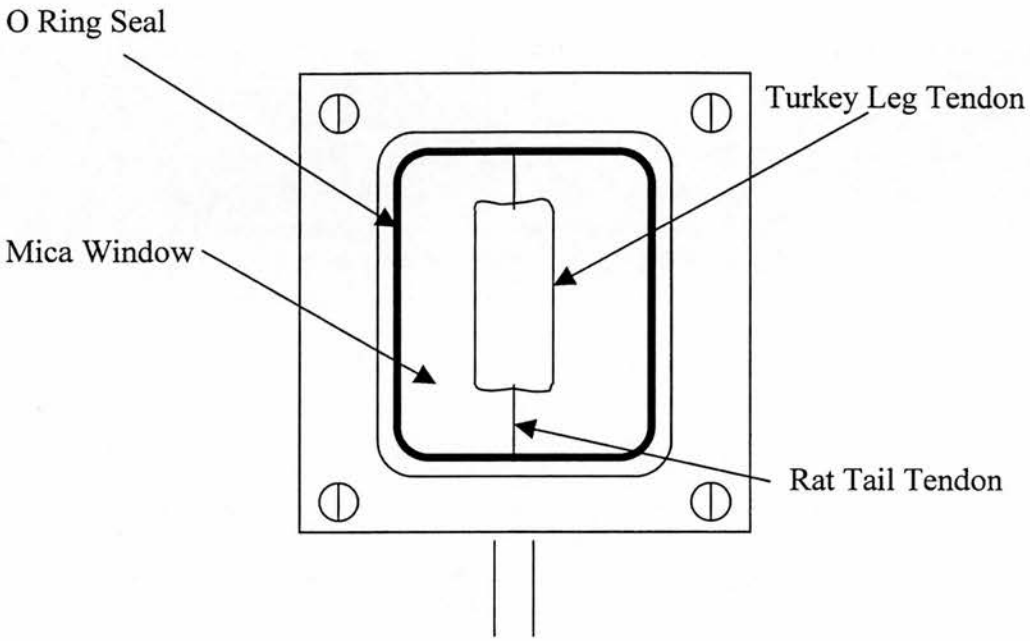

Figure 2.5. A diagram of the sample cell used for whole tendon samples for X-ray diffraction.

2.6.4. X-ray Diffraction of the Samples

2.6.4.1. Data Collection for the Mineral Crystallite Thickness Measurements

All the different ages of tendons were diffracted using beamline 16.1 at SRS, Daresbury. The camera used was 2.5m long. The exposure time was 5 minutes for all of the samples.

2.6.4.2. Data Collection for the Comparison of Mineralized and Nonmineralized Collagen Telopeptides.

All the data collected for these samples were performed using beamline 7.2 at SRS, Daresbury. The X-ray beam was collimated to 200μm. The camera length used was 64cm and the exposure time 300 seconds for all of the samples. The data was collected on a large Marr.

2.6.4.3. Data Collection for the Investigation of the Edge of Mineralization.

The data for this study was collected at beamline 7.2 at SRS and beamline 1, ID13 at SRS, ESRF. At beamline 7.2, the X-ray beam was collimated to 200μm and a camera length of 83cm was used. Each exposure was for 120 seconds. The tissue was moved in the beam using a stepper motor, in 100μm steps.

The data collected at ESRF used a beam size of about $1.5x2\mu m^2$. The sample was stepped in 10μm steps.

Chapter 3

Crosslink Analysis of Turkey Leg Tendon

3. Crosslink Analysis of Turkey Leg Tendon.

In fully mineralized (54 to 56-week-old) turkey leg tendon the mineralized portion has a different crosslinking profile to the areas of tendon that never mineralize (Yamauchi & Katz, 1993). These results implied that a structural change has occurred in the tendon. Whether this change has transpired before mineralization or as a consequence of mineralization remains unclear from the above research. A study into the time course of changes in crosslink patterns was deemed necessary to investigate when the crosslinking profile changes with mineralization to the concentrations previously published in the 54 to 56-week-old tendon.

The results presented in this chapter are of different ages of turkey leg tendon, from before mineralization to actively mineralizing and fully mineralized tendons. It may be useful to re-examine Figure 1.13 showing X-ray pictures of turkey legs at different stages on mineralization before reading this chapter. Different size sections have been analysed with a view to clarifying when the structural changes occur.

3.1 Crosslink Analysis of 34-Week-Old Turkey Leg Tendon.

A fully mineralized tendon of 34 weeks of age was used to verify the previously published results (Yamauchi & Katz, 1993). Figure 3.1 illustrates the sample sections taken from the tendon. Five sections in all were taken over the whole tendon and the crosslinks analysed as described in section 2.1. The results (Table 3.1) confirmed the previously published observations. Nonmineralized tendon had negligible concentrations of Dpd whereas there were appreciable concentrations of Dpd in

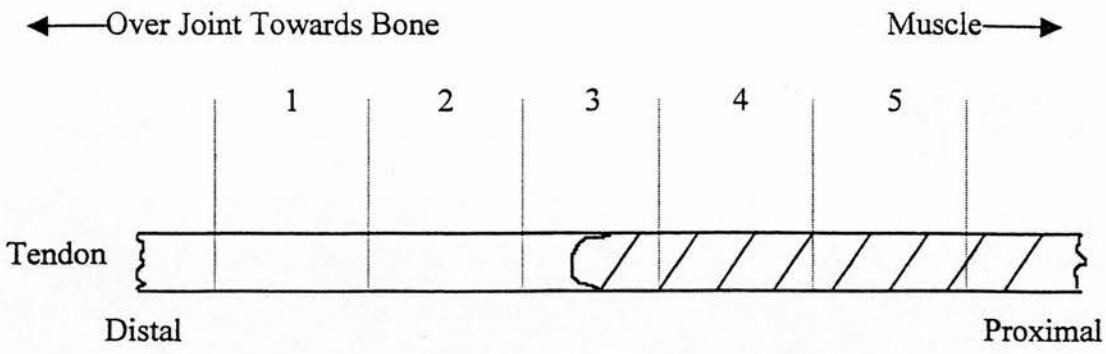

Figure 3.1 a). Illustrates the 1cm sections taken for analysis from a 34-week-old turkey leg tendon. The shaded area denotes mineralization and the open area denotes nonmineralized tendon.

Sample	Collagen (nmol)	Pyd (res/mol)	Dpd (res/mol)	DHLNL (res/mol)	HLNL (res/mol)
1	48.3	0.728	<0.010	0.524	0.351
2	36.3	0.514	<0.010	0.159	0.102
3	33.6	0.690	0.019	0.090	0.071
4	41.0	0.672	0.181	0.076	0.079
5	27.0	0.704	0.289	0.442	0.497

Table 3.1. The results for the crosslink analysis on sections taken from a 34 week old turkey leg tendon. The results for Pyridinoline (Pyd), Deoxypyridinoline (Dpd), Dihydroxylysinonorleucine (DHLNL) and Hydroxylysinonorleucine (HLNL) analysis are shown above and are expressed as residues per mole of collagen.
The numbers of observations on this age of tendon were 4. Although the same trends were seen in all analyses, the respective concentrations of the crosslinks varied. The variance observed in the levels were as great as ± 55%.

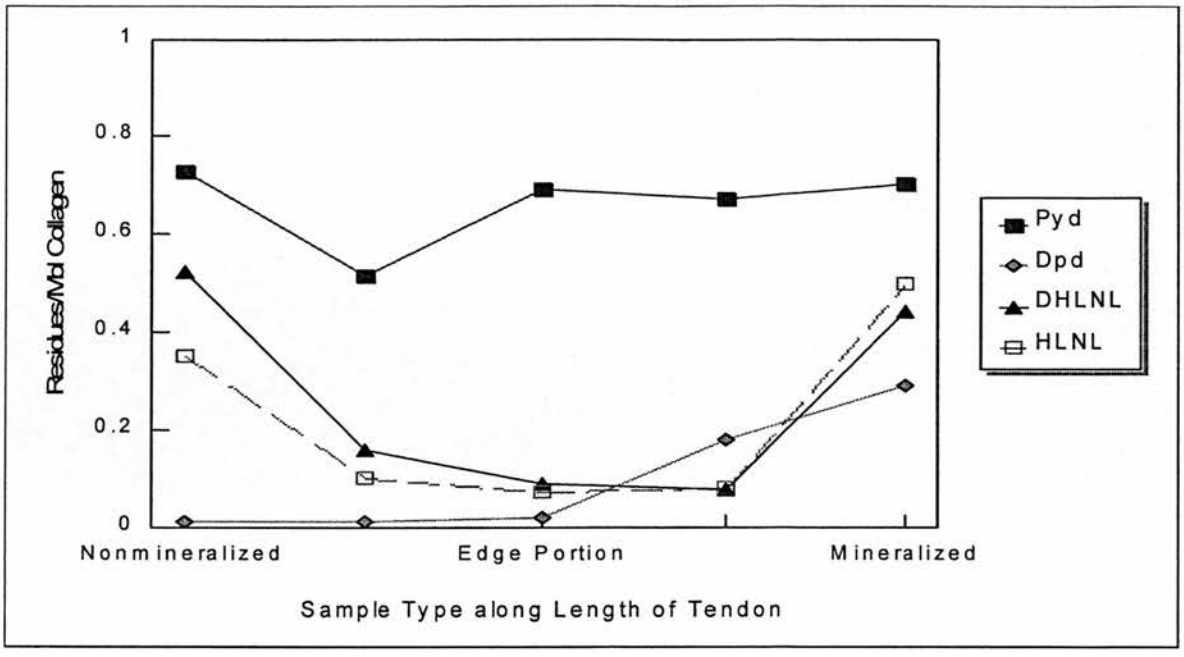

Figure 3.1.b) shows a plot of the data presented in Table 3.1. In this format it can be seen more easily the decrease in the concentrations of reducible crosslinks (DHLNL and HLNL) in the portions close to the edge of mineralization and the increase of Dpd in the mineralized portion of the tendon.

mineralized portions and in the edge region, which included some of the mineralized section. The reducible crosslink concentrations, however, differ from the previously published data. The concentration of HLNL is not significantly greater than the concentration of DHLNL in the mineralized portions and vice versa in the nonmineralized sections (Figure 3.1.b shows this more clearly). In samples 2,3 and 4, (nonmineralized section before the edge, the edge section and the mineralized section after the edge) the level of reducible crosslinks is far less than in the samples taken from the middle of their respective sections (better illustrated in Figure 3.1.b). The 1cm sections taken in the Yamauchi and Katz study were taken in the middle of their respective sections which, in conjunction with these results suggest that there may be a different structure at the edge of mineralization and in the initial portion of both the nonmineralized and mineralized sections. A subsequent study was therefore carried

out taking much smaller portions of a 34-week-old tendon. Twenty 1mm sections were taken from the nonmineralized section through to the mineralized portion as shown in Figure 3.2. The results of this experiment are shown in Table 3.2. The mature crosslinks alone were measured as there was insufficient material for analysis of the reducible crosslinks.

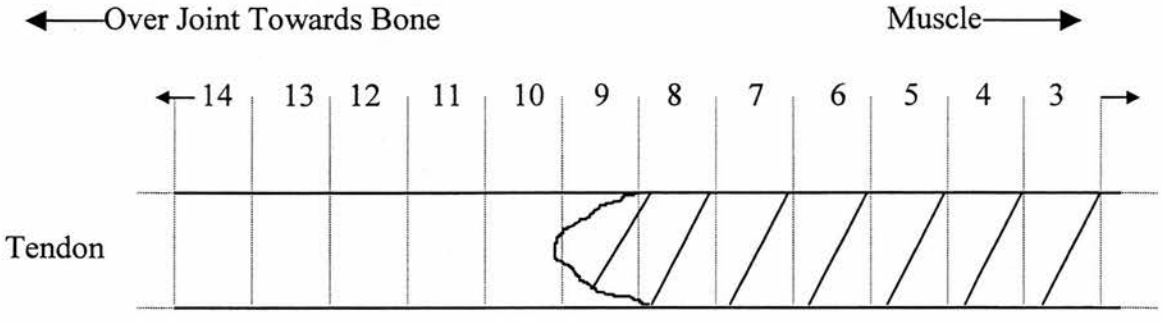

Figure 3.2. illustrates the 1mm sections taken from the mineralized portion (shaded area) through to the nonmineralized portion (open area).

It can be seen that in the mineralized portion the concentration of Pyd and Dpd for each sample is consistent, Pyd being 0.443 ± 0.054 residues/mol collagen and Dpd being 0.380 ± 0.054 residues/mol collagen. The samples which cover the edge region (10 and 11) show differing levels of Pyd and Dpd as would be expected with both mineralized and nonmineralized tissue present. In the nonmineralized portion there is negligible Dpd. The concentration of Pyd in this portion progressively increases for sample sites further from the mineralized portion. From this analysis of fully mineralized tissue, no indication of an intermediate structure at the edge of the mineralizing portion could be found.

Sample	Collagen (nmol)	Pyd (res/mol)	Dpd (res/mol)
1	3.24	0.431	0.393
2	2.24	0.405	0.392
3	2.75	0.426	0.372
4	3.11	0.484	0.434
5	3.30	0.476	0.393
6	4.75	0.389	0.341
7	7.31	0.415	0.382
8	4.15	0.463	0.376
9	3.26	0.497	0.337
10	3.44	0.587	0.229
11	3.23	0.657	0.090
12	8.25	0.622	0.006
13	4.79	0.611	0.007
14	4.00	0.620	0.009
15	3.60	0.669	0.009
16	4.83	0.783	0.010
17	4.61	0.966	0.011
18	2.05	1.102	0.011
19	3.67	1.129	0.011
20	3.74	1.124	0.011

Table 3.2 Results of Pyd and Dpd crosslink analysis on 1mm sections through the mineralized to the nonmineralized portion of a 34-week-old tendon.

3.2 Crosslink Analysis of Actively Mineralizing Tendons.

Crosslink analysis of fully mineralized tendon only indicates the final collagen packing in each region. Therefore, analysis of actively mineralizing tendons was performed to determine whether there were indications of any intermediate packing structures being present before the tissue had fully mineralized.

Tendons from female turkeys aged 8, 12.5, 13, 14 and 16 weeks of age were taken for analysis of mature crosslinks and calcium concentrations. The DHLNL to HLNL ratio was calculated for some of these ages using their specific radioactivity.

Figure 3.3 shows the calcium concentration, mature crosslink concentrations and the DHLNL:HLNL ratios along the length of the tendon of an 8-week-old turkey. There were slightly higher concentrations of calcium at either end of the tendon, but this level is still relatively small which implies this tissue has not started mineralizing. The mature crosslink concentrations are very erratic along the tendon. This is probably due to experimental error. No progressive changes in the crosslink pattern associated with mineralization can be seen.

Figure 3.4 shows these results for a 12.5 week old tendon. At the proximal end of the tendon there were higher concentrations of calcium (up to 105μg/nmol collagen), Dpd concentration had also increased (0.013 residues/mol collagen) although this was still a low concentration of calcium and Dpd. Again, the mature crosslink concentrations were erratic through the rest of the tendon probably due to experimental error. The ratio of DHLNL:HLNL is higher than 1 in the mineralized portions indicating higher levels of DHLNL or lower levels of HLNL.

The results for a 13 week old tendon are shown in Figure 3.5. Again there was a greater concentration of calcium at the proximal end of the tendon (172μg/nmol

collagen) as well as a slightly greater concentration of Dpd (0.01 residues/mol collagen). As with the other ages of tendon examined the mature crosslink concentrations along the rest of the tendon were irregular although at 10cm along the length there was a high concentration of Dpd and a low calcium concentration. Again DHLNL:HLNL was greater than 1 in the portions containing higher concentrations of calcium although the levels are erratic due to experimental error, along the rest of the length.

Figure 3.6 shows the results for a 14 week old tendon. There were higher concentrations of calcium at both ends of the tendon (>180μg/nmol collagen). In both these regions there was a higher DHLNL:HLNL ratio as well as higher concentrations of Dpd (0.008-0.01residues/mol collagen) although the highest concentration of Dpd found at 9cm along the length corresponds to a section with a low calcium concentration. Interestingly this section is similar in distance along the tendon as the high calcium concentration found in a 13-week-old tendon.

A 16-week-old tendon was also examined (Figure 3.7). Here there were high concentrations of calcium at both ends of the tendon (300-450μg/nmol collagen). Again there were corresponding higher concentrations of Dpd (0.03-0.55 residues/mol collagen) and DHLNL:HLNL ratios in these sections also. The levels of Dpd found were far greater than those found in earlier ages of tendon and this pattern of results now starts to resemble those found in fully mineralized tissue. Pyd concentration was still erratic in this age of tendon. From the analysis of all these ages of tendon no indication of intermediate structure could be detected using 1cm sections.

Each age of tendon was examined again using 1mm sections of tissue. The sections were taken from the areas of low concentration calcium to the areas of high

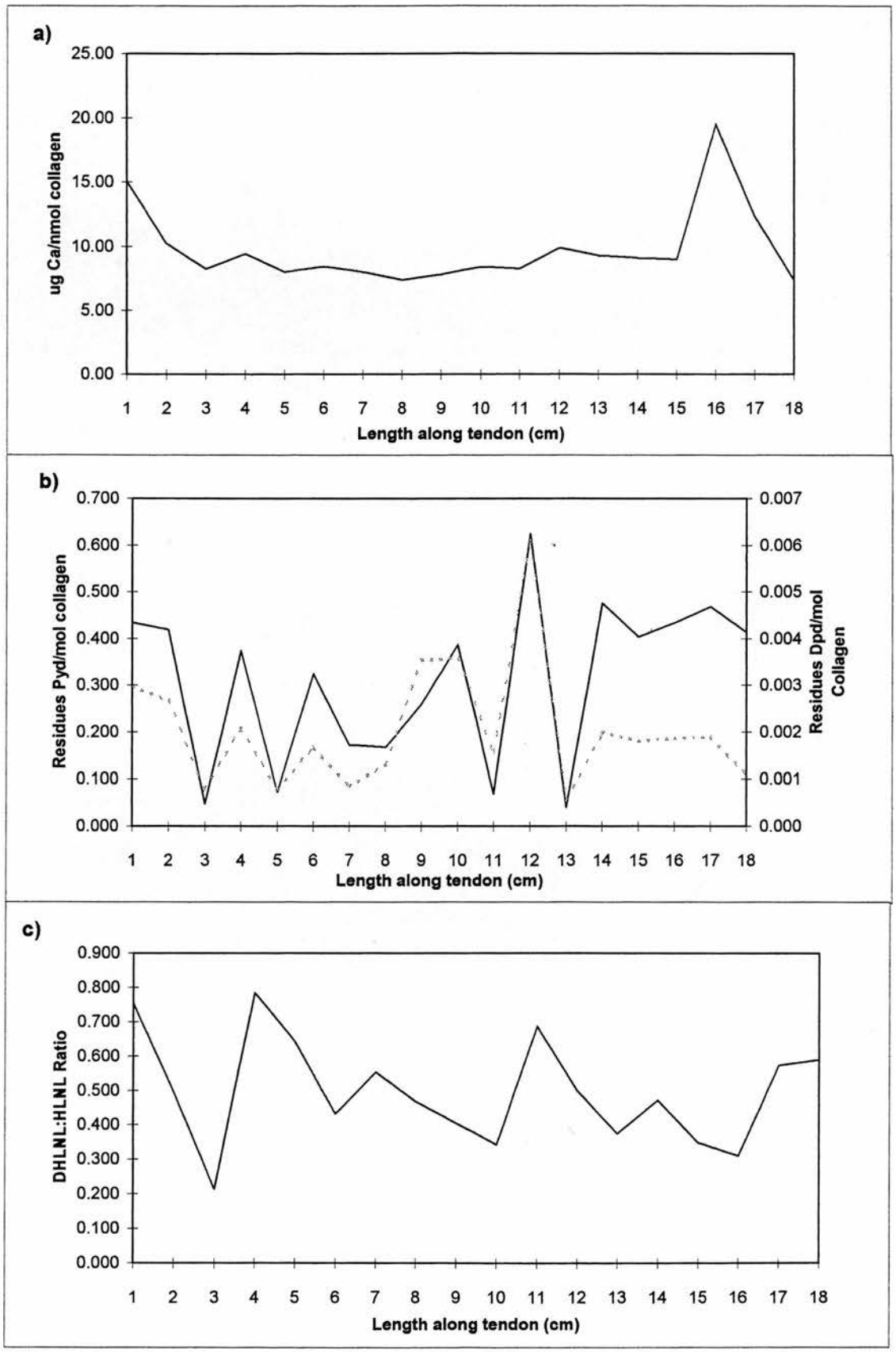

Figure 3.3. a)Calcium concentration, b) Pyd (full line) and Dpd (broken line) concentration and c) DHLNL:HLNL along the length of an 8 week tendon.

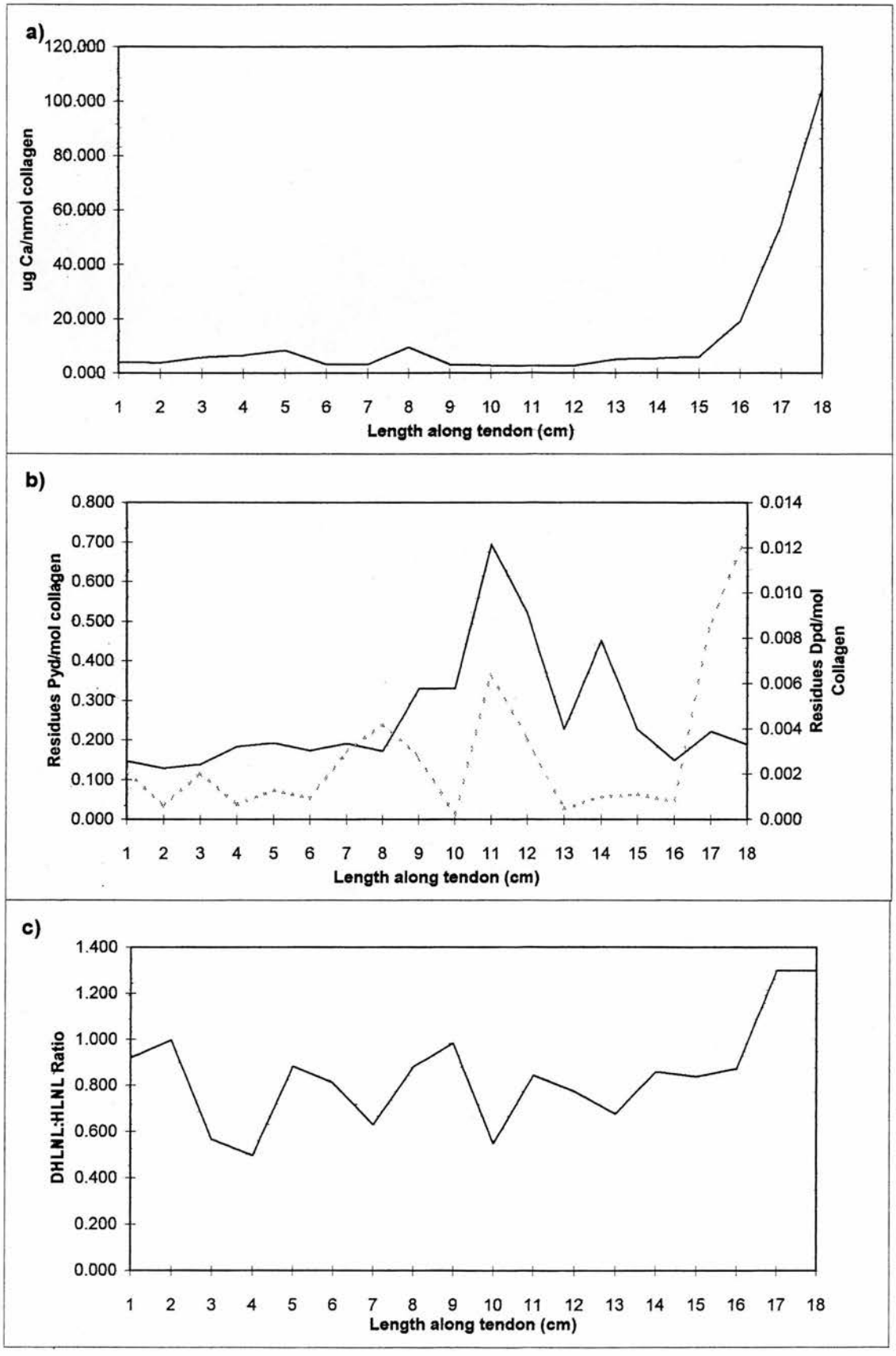

Figure 3.4. a) Calcium concentration, b) Pyd (full line) and Dpd (broken line) concentration and c) DHLNL:HLNL ratio along the length of an 12.5 week tendon

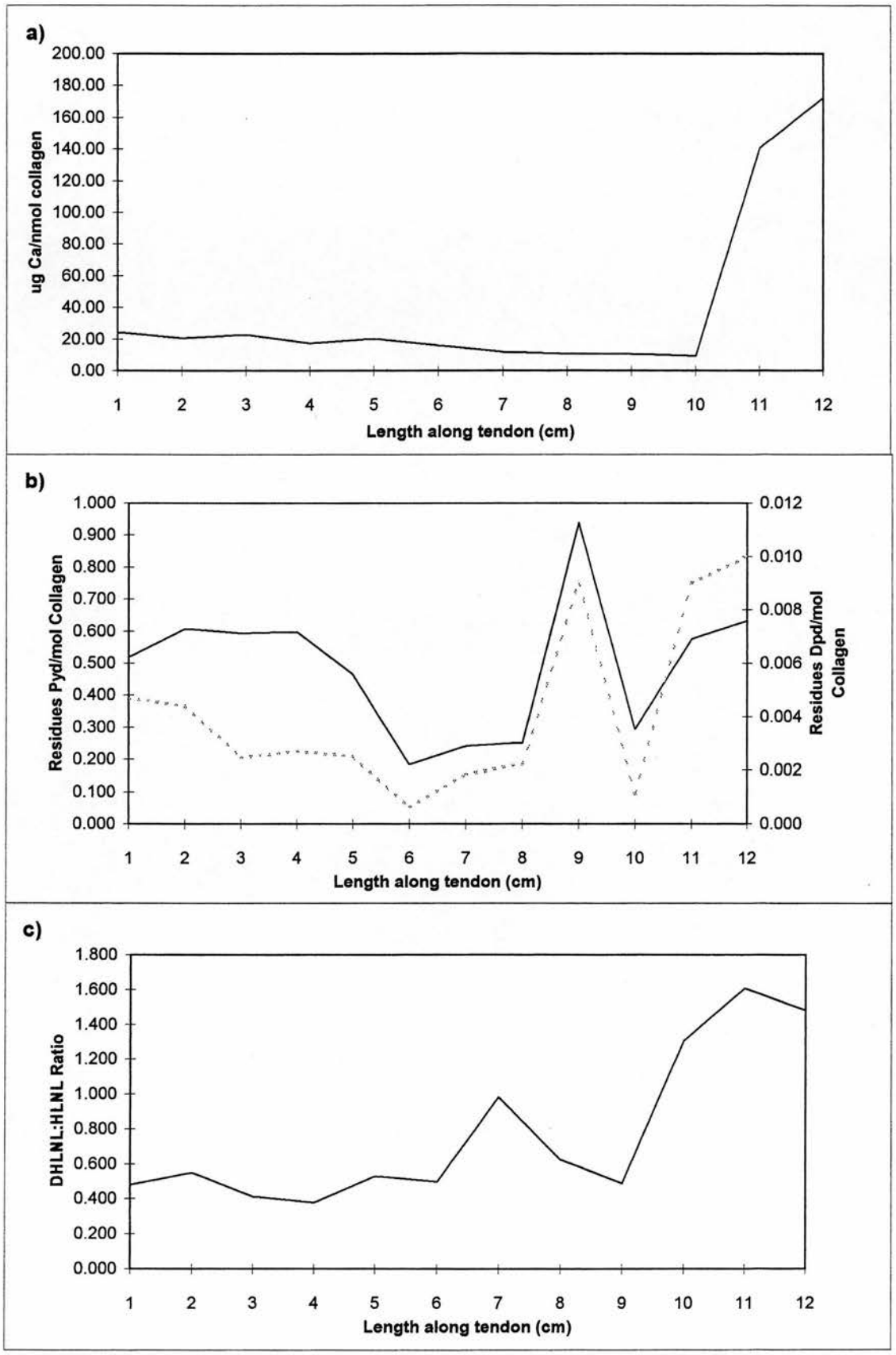

Figure 3.5. a) Calcium concentration, b) Pyd (full line) and Dpd (broken line) concentration and c) DHLNL:HLNL along the length of a 13 week tendon.

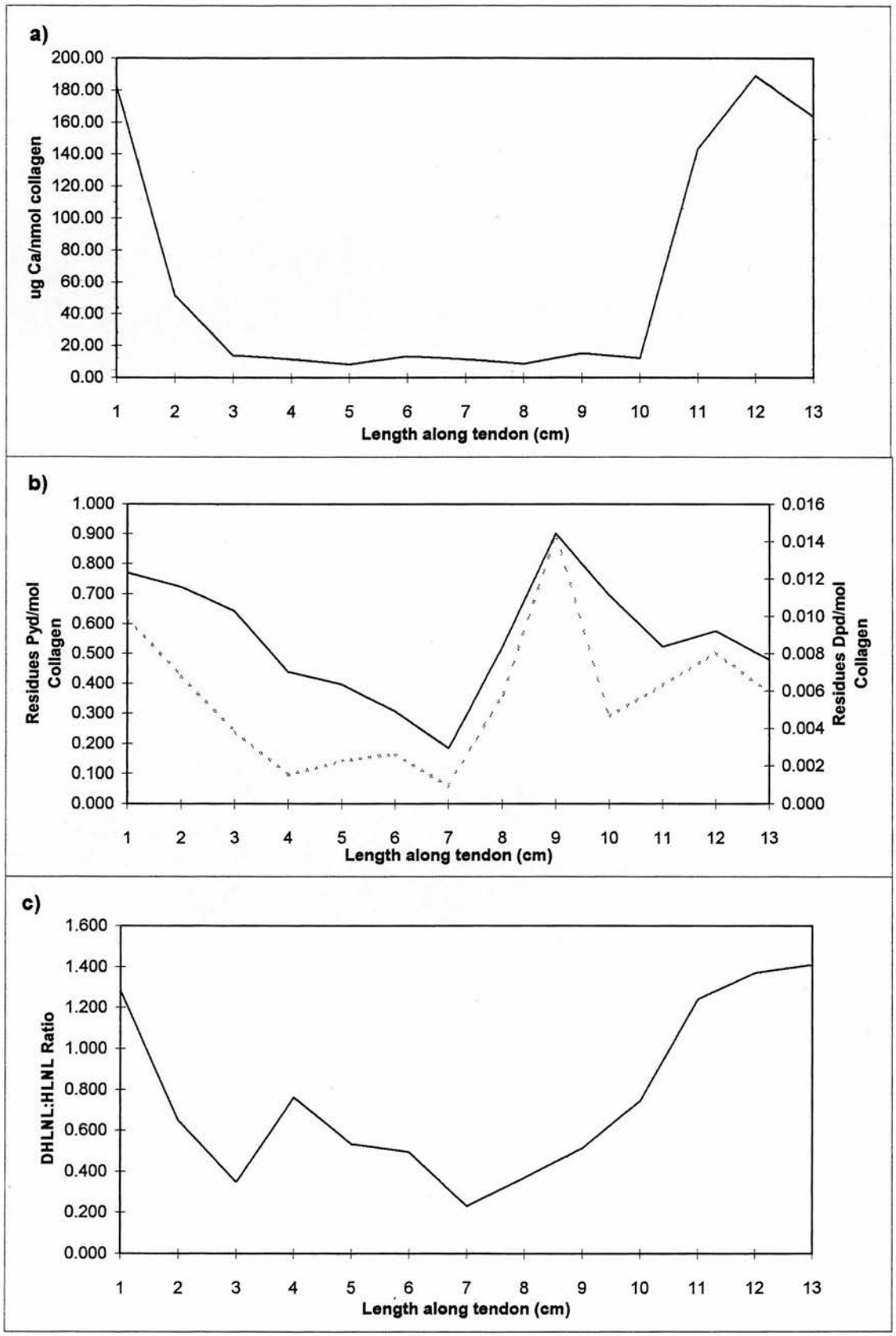

Figure 3.6. a) Calcium concentration, b) Pyd (full line) and Dpd (broken line) concentration and c) DHLNL:HLNL along the length of a 14 week tendon.

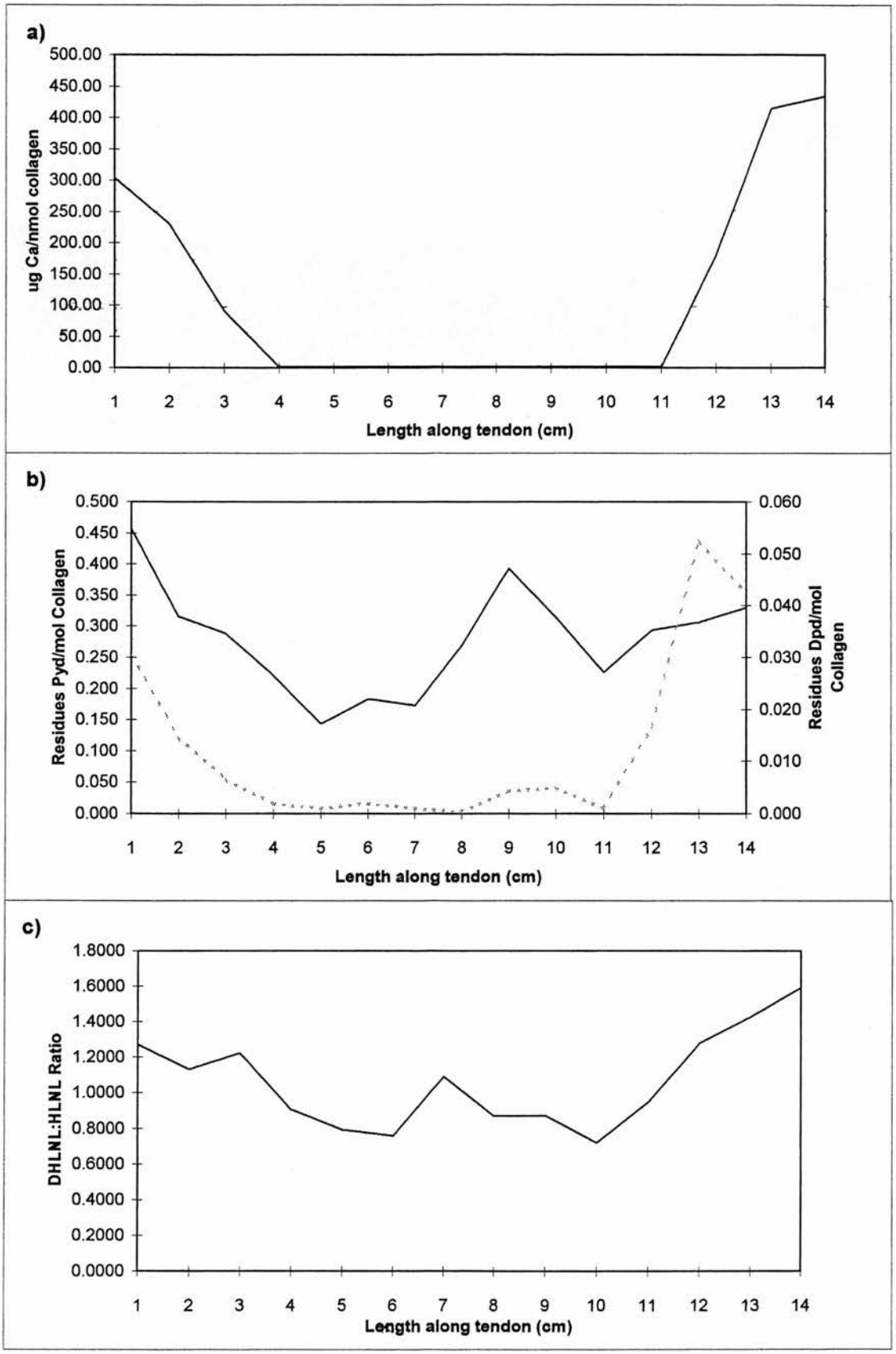

Figure 3.7. a) Calcium concentration, b) Pyd (full line) and Dpd (broken line) concentration and c) DHLNL:HLNL along the length of a 16 week tendon.

concentration of calcium. Figures 3.8, 3.9 and 3.10 show the results of this analysis for 12.5, 13 and 14 week old tendons respectively. The Dpd concentration increased in each case with an increase in calcium concentration. The crosslink levels in the portions of the tendon were erratic with no clear pattern and therefore not considered significant. No evidence of structural changes can be identified except in the presence of high calcium concentrations.

3.3 Investigation into the Edge of Mineralization.

The edge of mineralization in turkey leg tendon is abrupt at a gross anatomical level but has variations in precise locations and fluctuates in the tissue like waves lapping on a beach. A study into a transition zone between the mineralized portion and nonmineralized portion of the tissue was carried out. To minimise the fluctuations within the tissue, pieces of tendon were sectioned longitudinally to 30μm thickness. This was thin enough to minimise the fluctuations but thick enough for the cutting of the sections not to affect the gross structure of the tissue. Five 1mm x 1mm portions were cut from each section. Although smaller sections were possible it proved too little tissue to measure Pyd and Dpd concentrations. Figure 3.11 shows the sampling sites from a 30μm tendon section of turkey leg tendon. Five samples were taken from 12.5, 13, 14 and 60 week old tendon. The concentrations of Pyd, Dpd and calcium were measured. The results for each are in Table 3.3.

These results show once again that appreciable concentrations of Dpd are only present in the mineralized portion of the tendon. Due to the small amounts of tissue being analysed, no Dpd could be detected in the nonmineralized portion, although previous studies of whole tissue samples indicate there are negligible amounts. The Dpd results

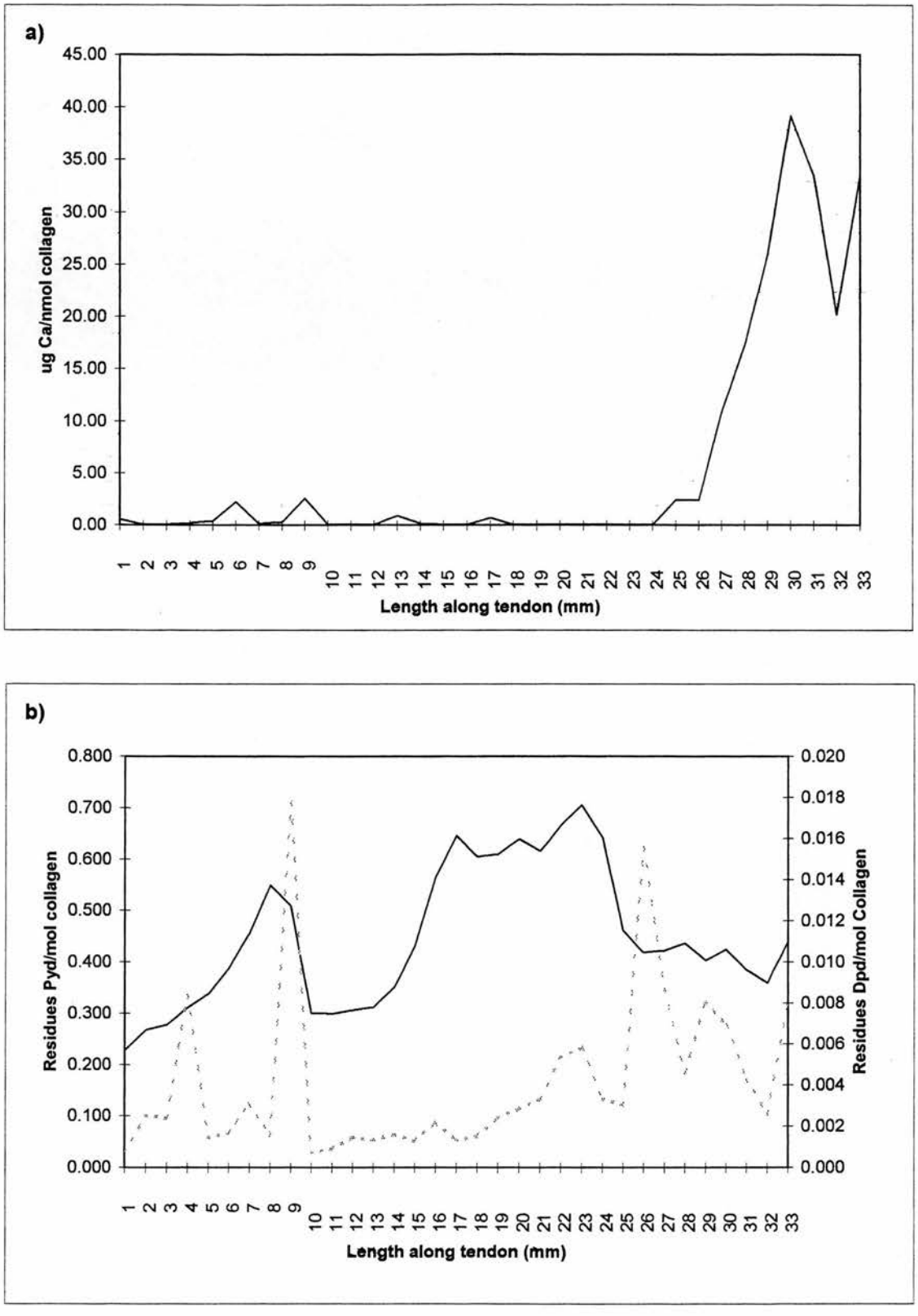

Figure 3.8. a) calcium concentration and b)Pyd (full line) and Dpd (broken line) concentration of mm sections taken along a portion of 12.5 week old tendon.

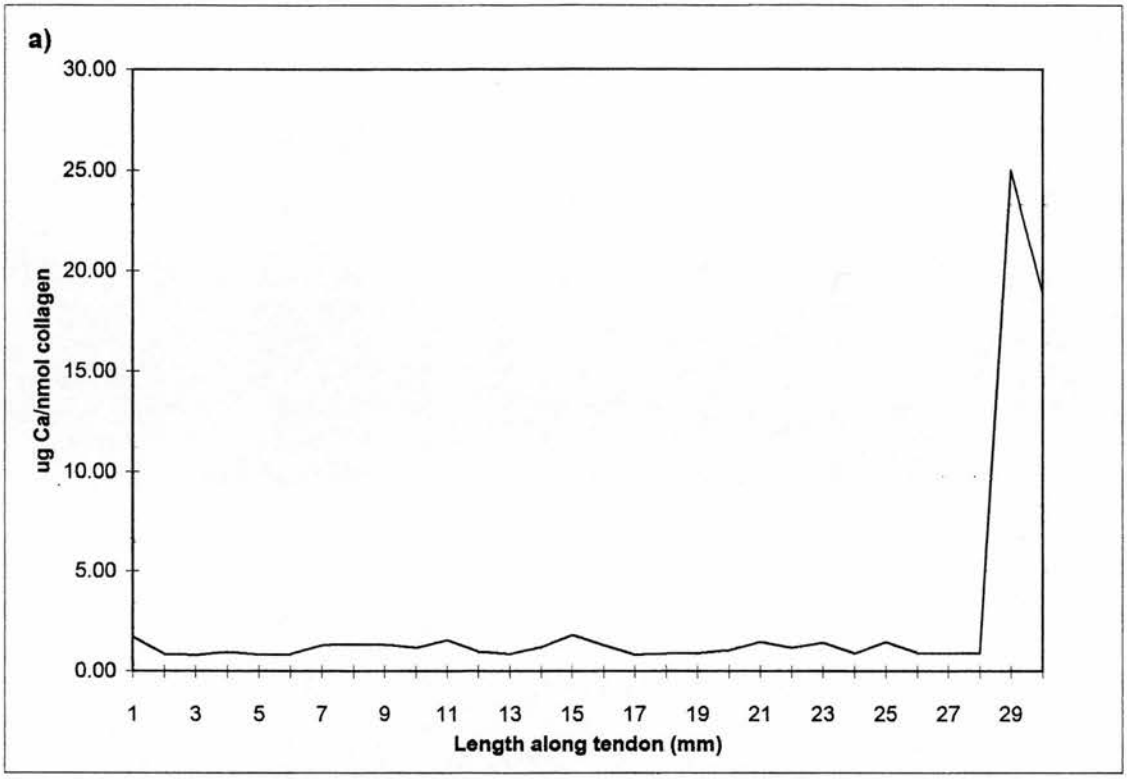

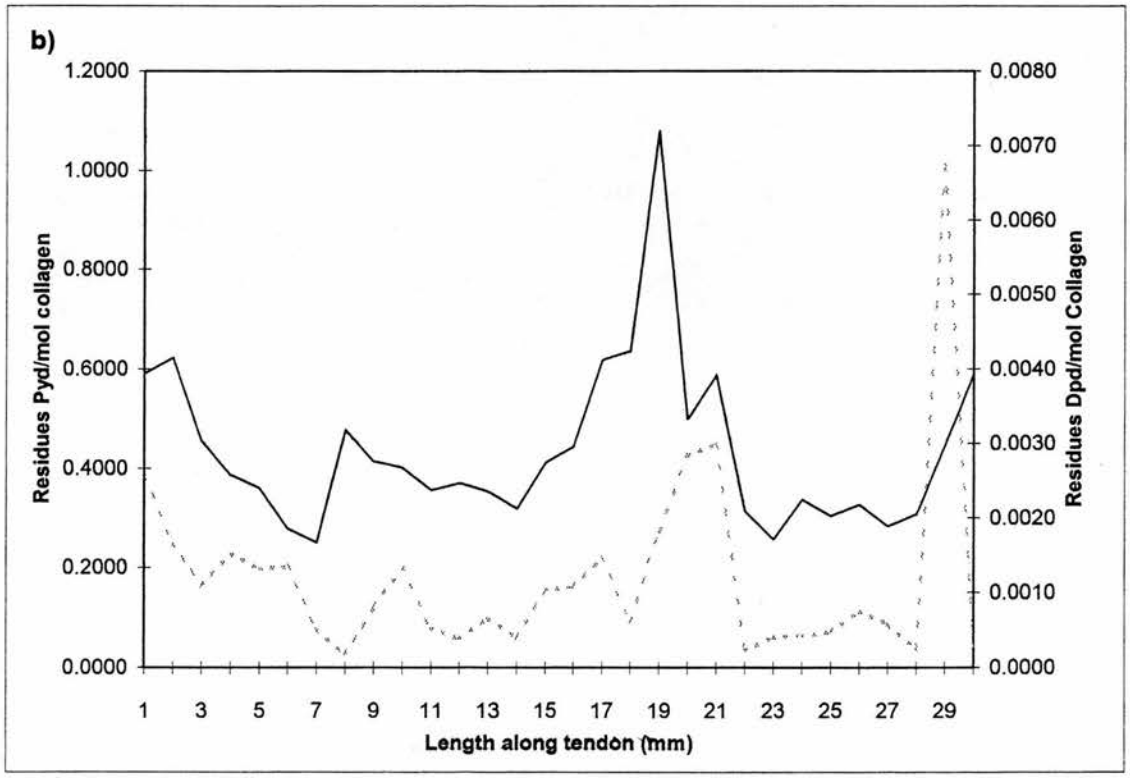

Figure 3.9. a) calcium concentration and b)Pyd (full line) and Dpd (broken line) concentration of mm sections taken along a portion of 13 week old tendon.

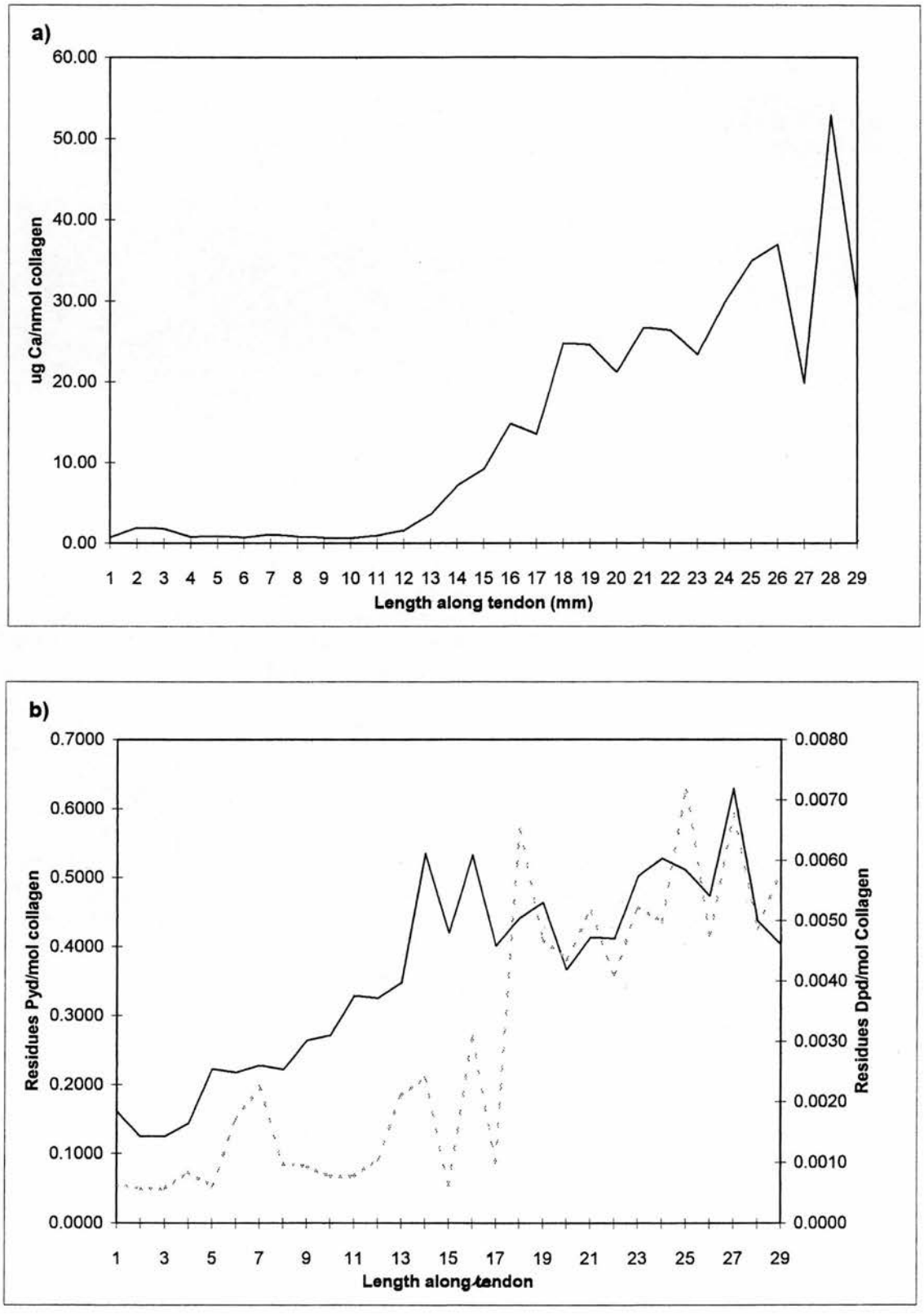

Figure 3.10. a) calcium concentration and b)Pyd (full line) and Dpd (broken line) concentration of mm sections taken along a portion of 14 week old tendon.

from the mineralized portions of the tendon are higher when compared to the results obtained from whole tendon samples sectioned to 1mm, but the 30μm sections taken for this study were from the centre of the tendon where the mineral was located in early mineralization.

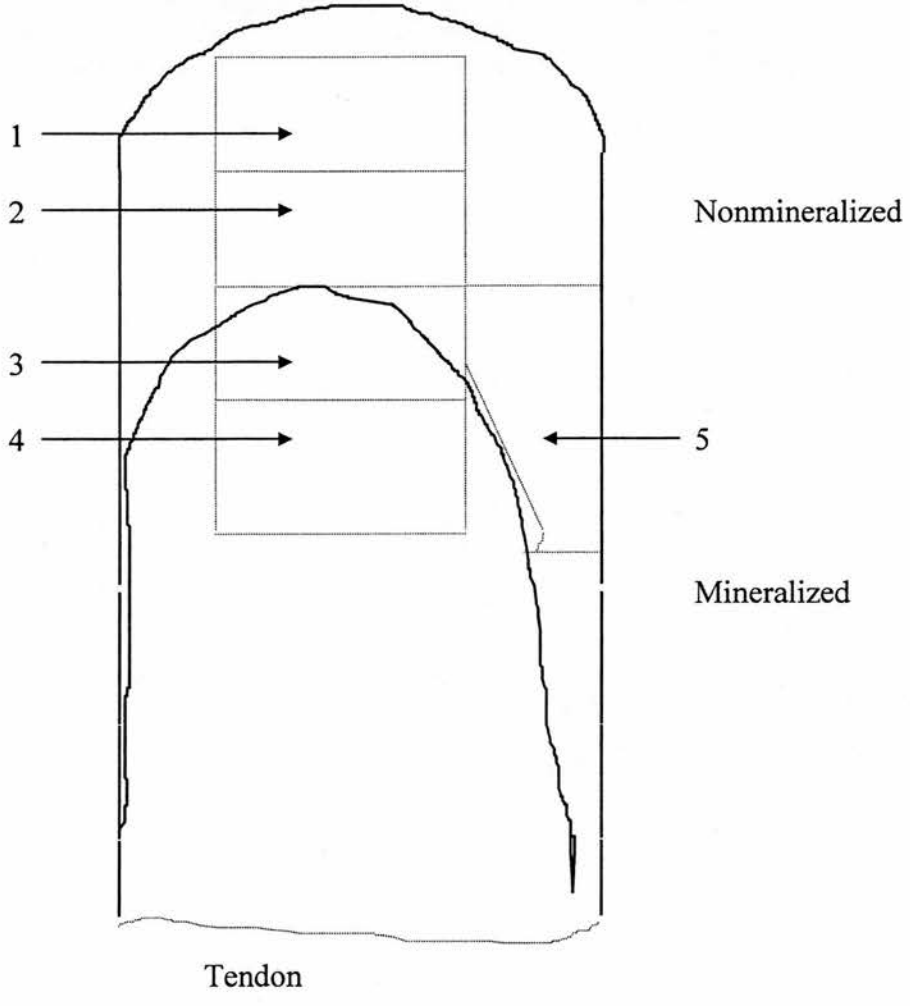

Figure 3.11. Diagram of the sections taken from the 30μm section of turkey leg tendon.

Age	Sample	Pyd (Res/mol)	Dpd (Res/mol)	Calcium (μg/nmol)
12.5 week	1	0.408	0.000	0.2
	2	0.316	0.000	0.1
	3	0.513	0.012	4.3
	4	0.587	0.093	12.4
	5	0.479	0.000	0.6
13 week	1	0.385	0.000	0.1
	2	0.402	0.000	0.1
	3	0.576	0.034	6.4
	4	0.346	0.149	14.8
	5	0.629	0.000	0.4
14 week	1	0.537	0.000	0.2
	2	0.478	0.000	0.2
	3	0.452	0.029	10.4
	4	0.581	0.165	18.7
	5	0.376	0.000	0.1
60 week	1	0.614	0.002	0.5
	2	0.709	0.004	0.3
	3	0.643	0.176	20.8
	4	0.597	0.258	43.6
	5	0.601	0.001	0.4

Table 3.3. Results of crosslink and calcium analysis carried out on samples taken from 30μm sections of 12.5, 13, 14 and 60 week old tendons.

3.4 Discussion.

As mentioned previously, studies carried out by Yamauchi & Katz (1993) showed that in 54 to 56 week old turkey leg tendons, the nonmineralized portions contained negligible concentrations of Dpd; however in the mineralized portions of the same tendons there were appreciable levels of Dpd. This led the investigators to suggest that the post-transitional chemistry and molecular environments are different in these two turkey tendon fibrils.

The aim of this study was to investigate this hypothesis further with a view to studying the edge of mineralization between the mineralized and nonmineralized portions. A 34-week-old tendon was used to investigate the changes in the crosslink pattern (Table 3.1). It was seen that the appearance of Dpd in the mineralized portion was in accordance with the results recorded by Yamauchi and Katz (1993). The reducible crosslink levels, however, differed from those published previously in that although the concentration of HLNL was slightly higher than that of DHLNL in the mineralized portion and vice versa for the nonmineralized portion, these values could not be considered significant within the error of the method used. The previous study found that the concentrations of both reducible crosslinks were far higher in the mineralized portions than in the nonmineralized and the total level of mature crosslinks was higher in the nonmineralized portion of the tendon that in the mineralized portion. In the present study of 34-week-old tendon, the total level of reducible crosslinks was very similar in the sections taken in the middle of both portions (0.875 residues/mol collagen for section 1 in the nonmineralized portion and 0.939 residues/mol collagen in section 5 for the mineralized portion). The concentrations of Pyd in these two portions are also similar (0.728 residues/mol

collagen for the nonmineralized portion and 0.704 residues/mol collagen for the mineralized portion). The other portions taken closer to the edge of mineralization (Sections 2 and 4) have lower concentrations of reducible crosslinks.

All the portions taken in this study were approximately 1cm in length and therefore were taken closer to the mineralizing edge than the portions analysed in the study by Yamauchi & Katz, 1993, which were taken approximately 3 cm from the edge. This could signify that at the edge of mineralization there are changes in the collagen crosslinking profile. From these data and the previously published study it is impossible to tell whether there is a different profile at the edge as mineralized and nonmineralized portions (approximately 5mm of each) are contributing to the overall profile for the 1cm section. In studies carried out on the crosslinking in the COOH-terminus of bovine bone collagen it was seen that with mineralization some of the reducible crosslinks matured but some dissociated back to their precursor form (Allysine and Hydroxyallysine) which is hypothesized to be due to changes in the molecular packing brought about be mineralization (Otsubo *et al.*, 1992). The relatively low levels of reducible crosslinks found in the sections taken either side of the edge and the section, including the edge of mineralization, could be due to a dissociation of the reducible crosslinks to aldehyde precursors but not as a consequence of mineralization but as a preparation for mineralization. The aldehyde concentrations were not measured for any of the tissues in the crosslinking studies and so there is at present no supporting evidence for this suggestion.

A more detailed investigation into the edge of mineralization was carried out on the same age of tissue. Twenty 1mm sections across the edge of mineralization were taken and analysed. The mature crosslinks showed no changes in crosslink profile

except those associated with mineralization. The concentrations of both mature crosslinks in the mineralized portion were similar. The concentrations of Pyd in the nonmineralized portion increase from 0.622 res/mol collagen at the edge of mineralization to 1.124 res/mol collagen at the nonmineralized portion approximately 1 cm from the edge of mineralization. The total level of mature crosslinks over the 2cm of tissue sampled, 1cm either side of the edge of mineralization, was 0.839 ± 0.157 residues/mol collagen. Unfortunately the reducible crosslinks could not be measured as there was insufficient material for analysis.

As no changes in the mature crosslink profiles except those associated with mineralization could be detected in fully mineralized tissue, crosslink studies were performed on ages of tissue which were actively mineralizing along the length. For both the 1cm and 1mm sections taken along the lengths of 8, 12.5, 13, 14 and 16 week old tendons again no changes in the mature crosslink profiles could be detected except those associated with mineralization. The ratio of DHLNL:HLNL for each section showed higher levels of DHLNL in the samples with high calcium content. This is contrary to the results found in the 34-week-old, fully mineralized tendon. One possible explanation for these contrary results is that the mineralized collagen present is of a different hydroxylation state and has therefore been newly laid down, as suggested by Yamauchi and Katz, 1993. In young tissue that is actively mineralizing, the mineral is not apparent by touch as it originates inside the tissue. This leaves an area of mineralized collagen within collagen that has yet to mineralize. These sections have a higher calcium content due to the mineralized collagen but still have nonmineralized collagen present.

Another possible hypothesis is that the changes in the crosslink profile are not due to post-translational changes in newly laid down collagen but are brought about by the mineral crystals compressing the collagen fibrils. This compression breaks some of the reducible crosslinks into their aldehyde precursors (DHLNL precursors are telopeptide hydroxallysine and helical hydroxylysine) which allows the aldehydes to form other crosslinks with other lysine residues that are now available in the deformed, compressed collagen. If not all of the mineral crystals are sufficiently large enough to compress the collagen fibrils in these young mineralized portions studied, many of the reducible crosslinks will not be broken, therefore accounting for higher levels of DHLNL. As the tissue ages and the mineral crystals grow, DHLNL could be broken and HLNL and Dpd formed.

In an attempt to study the edge of mineralization in the centre of the young tendon samples, 30μm sections of samples were taken. These samples included the actual mineralized collagen, as they originated from the centre of the tissue. Unfortunately there was too little material to study the reducible crosslinks. Again all the results demonstrated that the changes in mature crosslink concentrations are only associated with the mineralized portion of the tissue.

From all these results it can be seen that the only change in the mature crosslink profile is the one, previously published, associated with mineralization. The levels of reducible crosslinks suggested some changes in actively mineralizing tissues although due to the levels of detection available and the lack of a robust method of detection for the reducible crosslinks, other experiments were designed to test the following hypotheses:

- Whether collagen with a different lysine hydroxylation state is laid down with mineralization or,
- Whether the mineral crystals themselves deform the collagen fibrils, breaking crosslinks and allowing other crosslinks to form between residues that would not normally be involved.

Further studies on the structure of the collagen and the mineral crystallite have been performed using X-ray diffraction and the telopeptide organisation in nonmineralized and mineralized tissues has been investigated.

Incorporation studies of ^{3}H Proline in actively mineralizing tendon were carried out to investigate the levels of incorporation in collagen as hydroxyproline and proline over the length of the tendon. This was designed to show whether collagen of a different crosslink pattern can be laid down at a great enough rate to account for the changes in crosslink profile with mineralization.

Labelling a mineralizing bovine bone cell culture with ^{14}C-Lysine has been performed to investigate any changes in crosslink and precursors with mineralization.

Chapter 4

X-ray Diffraction Analysis of Turkey Leg Tendon

4 X-ray Diffraction Analysis of Turkey Leg Tendon.

In Chapter 3 crosslink analysis results of turkey leg tendon could not detect any changes in collagen packing except with mineralization. The smallest samples taken were 1mm x 1mm of 30μm thick sections. Although smaller sectioning was possible, the mature and the reducible crosslink concentrations could not be measured due to detection limits of the fluorimeter. It is possible that there is a transition zone, of only a few microns, where the structure of the collagen is different to that of nonmineralized or mineralized collagen, between the mineralized and nonmineralized portions of the tendon. This would be impossible to detect using crosslink studies alone. Another possibility is that there is a change in collagen packing at this transition zone but it is not great enough to change the crosslink profile. For these reasons X-ray diffraction was used in conjunction with crosslink analysis to study the structure of the mineralizing turkey leg tendon.

4.1 Investigation into Changes in the Mineral Crystallite Size with Age.

In Chapter 3 the biochemical results from early mineralized tissue showed that the DHLNL:HLNL ratio was higher in the mineralized portion, suggesting in older, more mineralized tissue there were greater levels of HLNL than DHLNL in those portions. One of the hypotheses put forward by Otsubo *et al.*, 1992, to account for this is that the mineral compresses the collagen fibrils, deforming them and breaking some of the reducible crosslinks into their aldehyde precursors (DHLNL precursors are telopeptide hydroxallysine and helical hydroxlysine). This would allow the aldehydes to form other crosslinks with other lysine residues that would then be available in the deformed, compressed collagen. If the mineral crystals in the young tendon mineralized portions studied were not large enough to

compress the collagen fibrils, many of the reducible crosslinks would not be broken, therefore accounting for higher levels of DHLNL. As the tissue ages and the mineral crystals grow, DHLNL will be broken and HLNL and Dpd formed.

To investigate this hypothesis, the size of the mineral crystals in various ages of tendon were determined. A technique called Small Angle X-ray Scattering (SAXS) was used. This has the advantage of being non-destructive and of providing information with high statistical accuracy due to the averaging over a macroscopic sample volume. Small angle scattering considers a range of sizes sufficiently larger than interatomic distances. The samples can be considered to consist of two sharply separated phases with constant composition, mineral and protein. Porod's Law can be used to calculate the thickness of the mineral crystals for these samples.

The first reference to Porod's law is Porod, 1952 although more accessible explanations are provided by Fratzl *et al.*, 1993; 1996. Due to the sharply separated phases, the sample contains two different scattering length densities. This produces a number of phenomena in scattering profiles that are termed invariants; the first corresponds to the integral intensity. This can be used to give the volume fraction of the two phases and generally corresponds to the very low angle scattering profile. After this region, at slightly higher diffraction angles (but still in the low angle region) the intensity of scatter decays with the forth power of the scattering angle. This relates to the total interface area between the two phases per unit volume of the specimen. The comparison of the two invariants allows the determination of a length scale that defines the two phase mixture. The parameter T can therefore be determined and corresponds to the ratio to volume to surface of one of the phases. This analysis makes no assumption of the shape or arrangement of the phases in the specimen. This technique has been widely used to characterise the structure of bone at the nm level.

4.1.1. Principles of Data Evaluation

Tendons from 12 to 60-week-old birds were examined using a 2.5m camera on beamline 16.1 with a wavelength of 1.488Å at Synchrotron Radiation Source (SRS), Daresbury. Each exposure was for 5 minutes with a beamsize of 500 x 500μm.

Each tendon was diffracted with and without 1mm thickness glassy carbon. Glassy carbon is an isotropic scatterer that enables calibration of the true intensity of the collagen diffraction. Firstly a transmission factor from the spherically averaged intensities of the sample with and without glassy carbon is calculated.

$$\frac{\text{Total Integral of Sample Intensity}}{\text{Total Integral of Intensity + glassy carbon}} = \text{Transmission Factor}$$

$$\text{True Intensity} = \frac{\text{Intensity Value}}{\text{Transmission Factor}} - \text{Background (empty sample cell)}$$

Q is the diffraction vector not dependent on camera length or wavelength. It is calibrated by relating distance to 'D' spacing of rat tail tendon. The pixel location of a recognisable order of diffraction is determined. The D spacing is calculated by dividing the order of diffraction by 67 nm.

$$\text{D spacing} = \frac{\text{Number of Order of Diffraction}}{67\ \text{nm}^{-1}}$$

$$Q = 2\pi \times \text{D spacing}$$

$$\text{The Q value per Pixel} = \frac{Q}{\text{Pixel Number}}$$

The diffraction pattern is re-binned from1 to 100. Assuming a radius of 256 detector points from the origin of diffraction.

$$\text{Q Value per Pixel} = \frac{(Q/\text{Pixel Number})}{2.56}$$

The data is plotted onto a double-logarithmic scale of IQ vs Q (See Figure 4.1 a. for an example). The data decays at Q^{-4} in the Porod region, ie large values of Q, and at Q^{-2} at small values of Q. IQ^2 vs Q is plotted (see Figure 4.1.b.) which gives a curve that tails off. The area below this curve is the total integral intensity, J. The only difficulty in determining J is the fact that the scattering function I(Q) is only known in the finite interval Qmin and Qmax, while J is the integral (area under the curve in Figure 4.1.b) extending from Q=0 to infinity. The total integral intensity constant (K) is calculated as follows.

$$K = J + (P/Q^2)$$

Q^2 is taken as the point at which the scattering intensity decay changes from Q^{-2} to Q^{-4}. The integral intensity is calculated under this section. IQ^4 vs Q is then plotted. The mineral and organic phase are separated by sharp interfaces so I(Q) follows Porod's law where I(Q) = Porod constant (P)/Q^4 for large values of Q. The IQ^4 value at the point of Q^2 (ie the change in decay) is the Porod Constant.

Using Porod's law the thickness (T) can be directly determined from K.

$$\text{Thickness of the Crystal (nm)} = \frac{4K}{\pi P}$$

a)

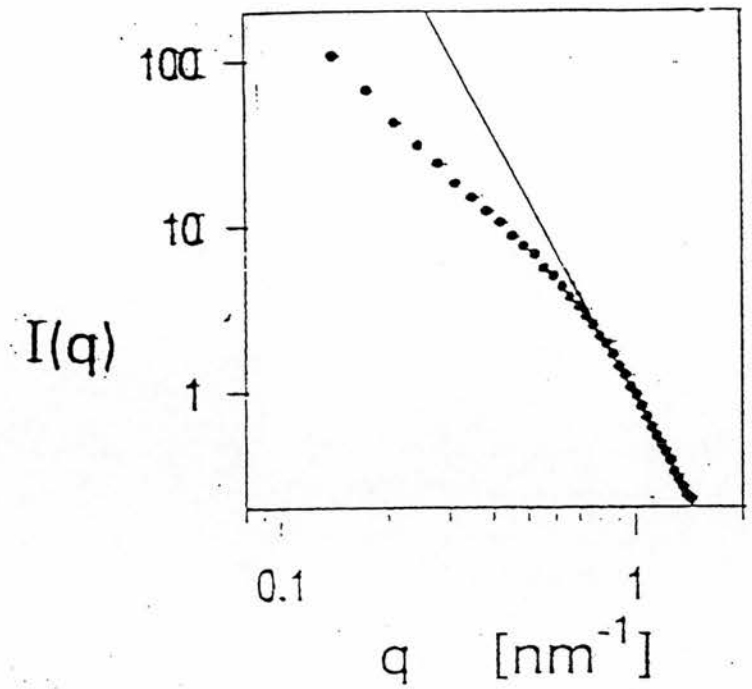

b)

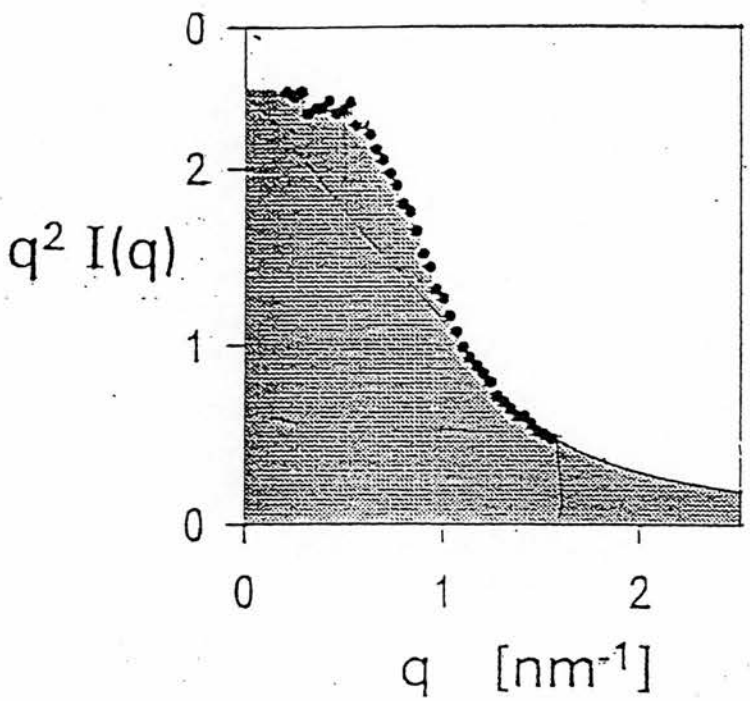

Figure 4.1. shows the plots illustrating Porod's Law and how the thickness of the mineral crystals was calculated. a) shows the equatorial intensity data plotted on a double logarithmic scale against Q. The dots illustrate the intensity data and the line shows the Q^{-4} decay which is the Porod region. b) shows the area of total integral intensity (shaded) on the data plotted on IQ^{-2} vs. Q.

4.1.2. Crystal Thickness with Age

Figure 4.1.c). shows a scatter plot of the crystal thickness from tendons of different ages. It can be seen that from the earliest mineralized tendon at 12 weeks to 22-week-old tendon, the thickness of the mineral increases from the minimum recorded value of 1.48nm to 2.53 ± 0.14nm at 22 weeks. From 22 weeks to 34 weeks the crystal thickness seems to remain constant, increasing again to 3.06 ± 0.02nm at 44 weeks. From this age to 60 weeks the crystal thickness decreases. This shows that for the ages of tendon investigated in Chapter 3 (8 to 16 weeks) the mineral is increasing in size. This is consistent with the proposed hypothesis.

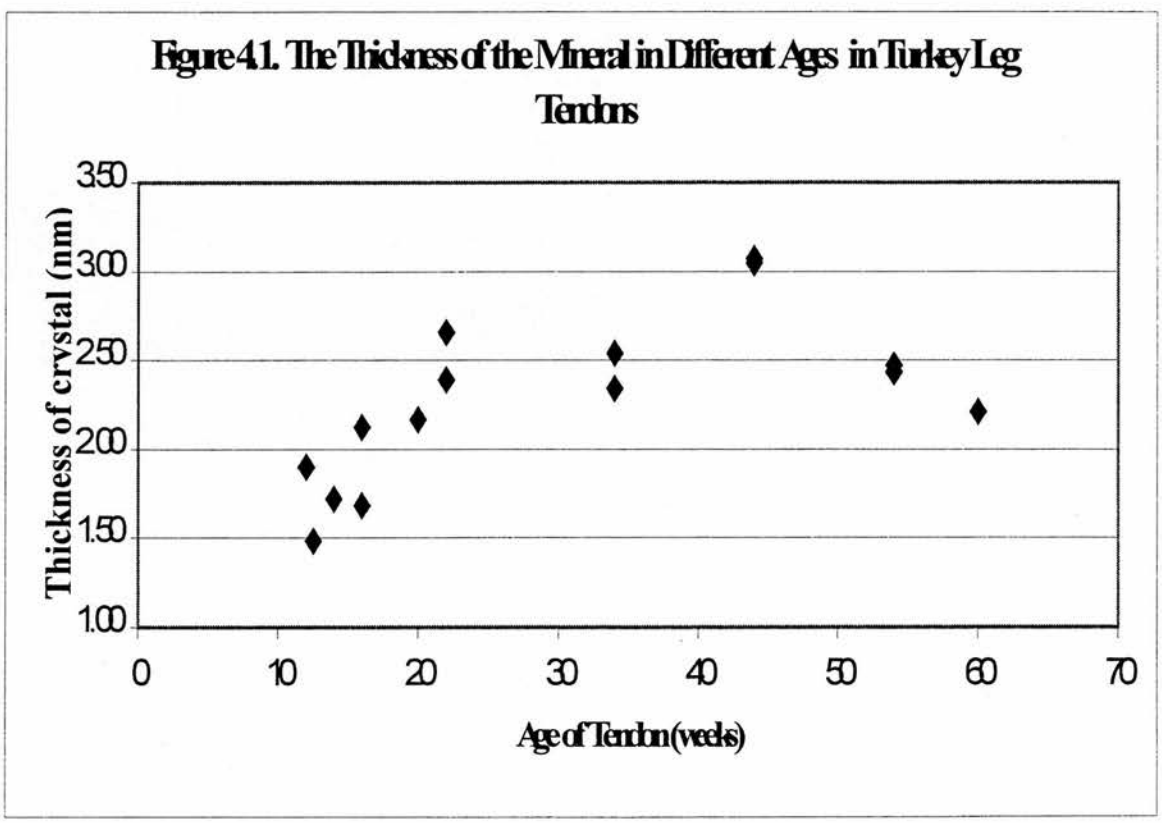

4.2. Investigation into the Axial Structure of Mineralized, Demineralized and Nonmineralized Collagen.

The axial structure of collagen was studied to determine the changes between mineralized and nonmineralized tendon and whether they relate to the changes in the crosslinking profile associated with mineralization. In order to study the post-mineralization distortions of axial structure of turkey leg tendon collagen in mineralized and nonmineralized collagen the mineral must be removed. There are several reasons for this.

The diffraction intensity of mineralized collagen is approximately 10 times greater than nonmineralized collagen due to the effect of the mineral deposited in a D periodic manner. The D periodic mineral phase does not contribute significantly to orders of diffraction above the 10^{th} order. This can be interpreted as a static Debye factor where high-resolution structure cannot be resolved due to deposition variability within the sample. The mineral present makes the diffraction contribution of collagen orders 1 to 10 difficult to observe. The demineralized collagen is compared to nonmineralized collagen and nonmineralized collagen treated with EDTA as permanent distortion of the collagen lattice could arise in the demineralization of the tissue. This will be observed in the nonmineralized collagen treated with EDTA. These diffraction data can give information as to whether the telopeptide structure has been altered and if any material in the gap region has been removed in order for mineralization to occur.

16-week-old mineralized sections of tendon were scraped on each side, using a scalpel to reveal the mineralized collagen in the centre of the tissue, and left in 0.5M EDTA solution overnight to demineralize. Sections of nonmineralized tendon were also treated similarly. All these sections were examined using a 64cm camera at beamline 7.2 at SRS, Daresbury, Warrington, England.

Figure 4.2. shows the diffraction patterns from each of the sections examined. Figure 4.3 shows overlaid graphs of 16-week-old demineralized section, 16-week-old EDTA treated, nonmineralized section and 16-week-old nonmineralized section. From these results it can be seen that the EDTA treated, nonmineralized section and the nonmineralized section are identical over the diffraction range studied showing that the treatment of the sections in EDTA solution overnight does not affect the collagen structure. These results also show that there are no differences in axial structure between demineralized collagen and nonmineralized collagen. Yamauchi and Katz 1993 performed all their crosslink analyses on mineralized tendon that had been demineralized. This still gave the change in crosslink profile associated with the mineralized region. These results suggest that deformation of the collagen, brought about by mineralization, is reversed when the mineral is removed although the crosslinking profile stays the same. However no change in axial telopeptide organisation has been observed by this technique. Modelling indicates that the effect of shortening the telopeptide will have a dramatic effect on the intensities of the orders of diffraction 10 to 19 (Hulmes *et al.*, 1977; 1980).

4.3 Telopeptide Modelling of Nonmineralized and Mineralized Collagen

There are two sites of crosslinking in the telopeptides of collagen type I; one on the N-terminal telopeptide and one on the C-terminal telopeptide. A change in the crosslinking brought about by deformation of the collagen fibrils by the mineral crystals that results in axial or lateral extensions or compressions will effect the meridional intensities of the diffraction patterns (Fraser *et al.*, 1987). Only if the change is a rotation of the telopeptide will there be no change in the axial diffraction pattern (Wess *et al.*, 1998).

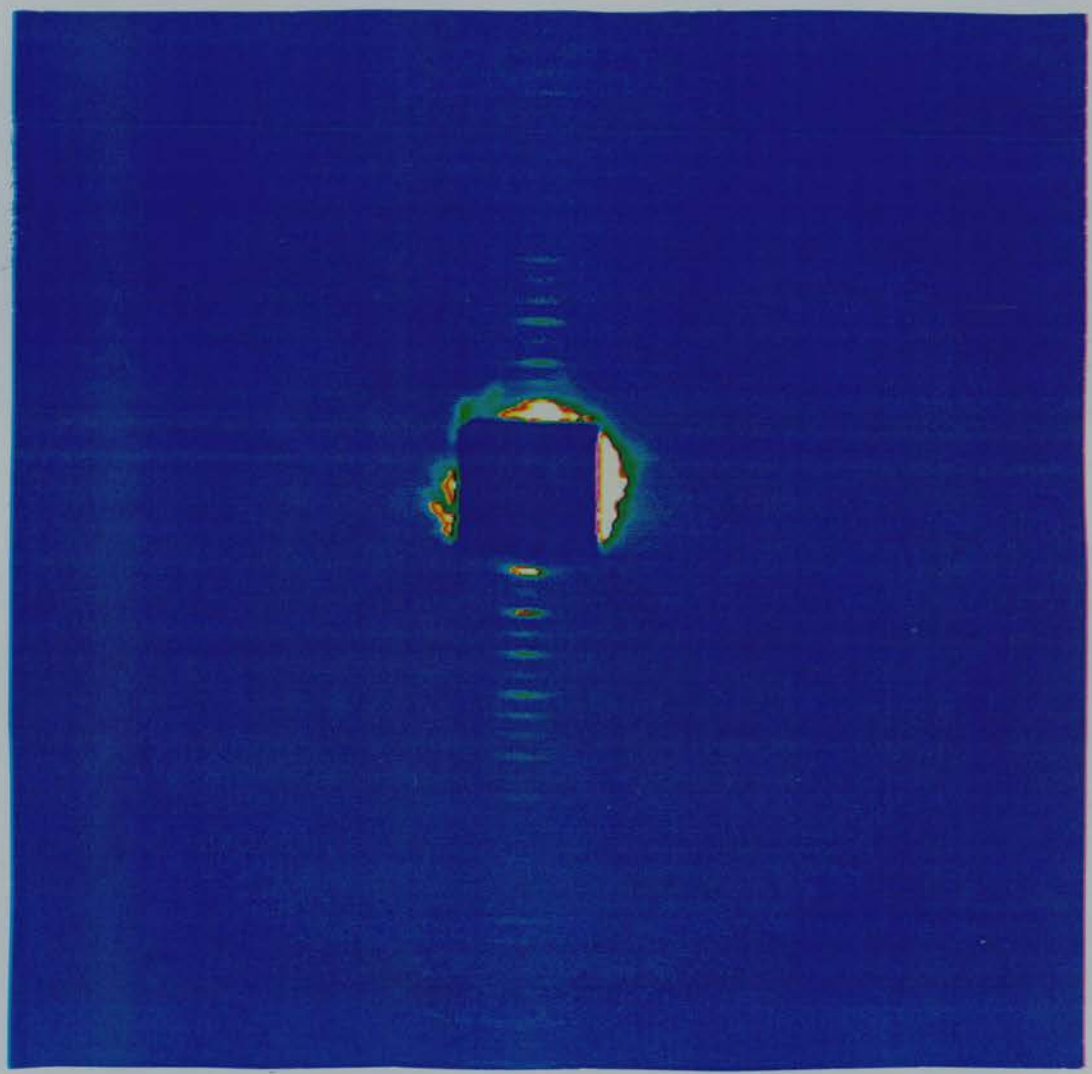

Figure 4.2. The high angle X-ray diffraction patterns for a) 16 week old, nonmineralized tissue

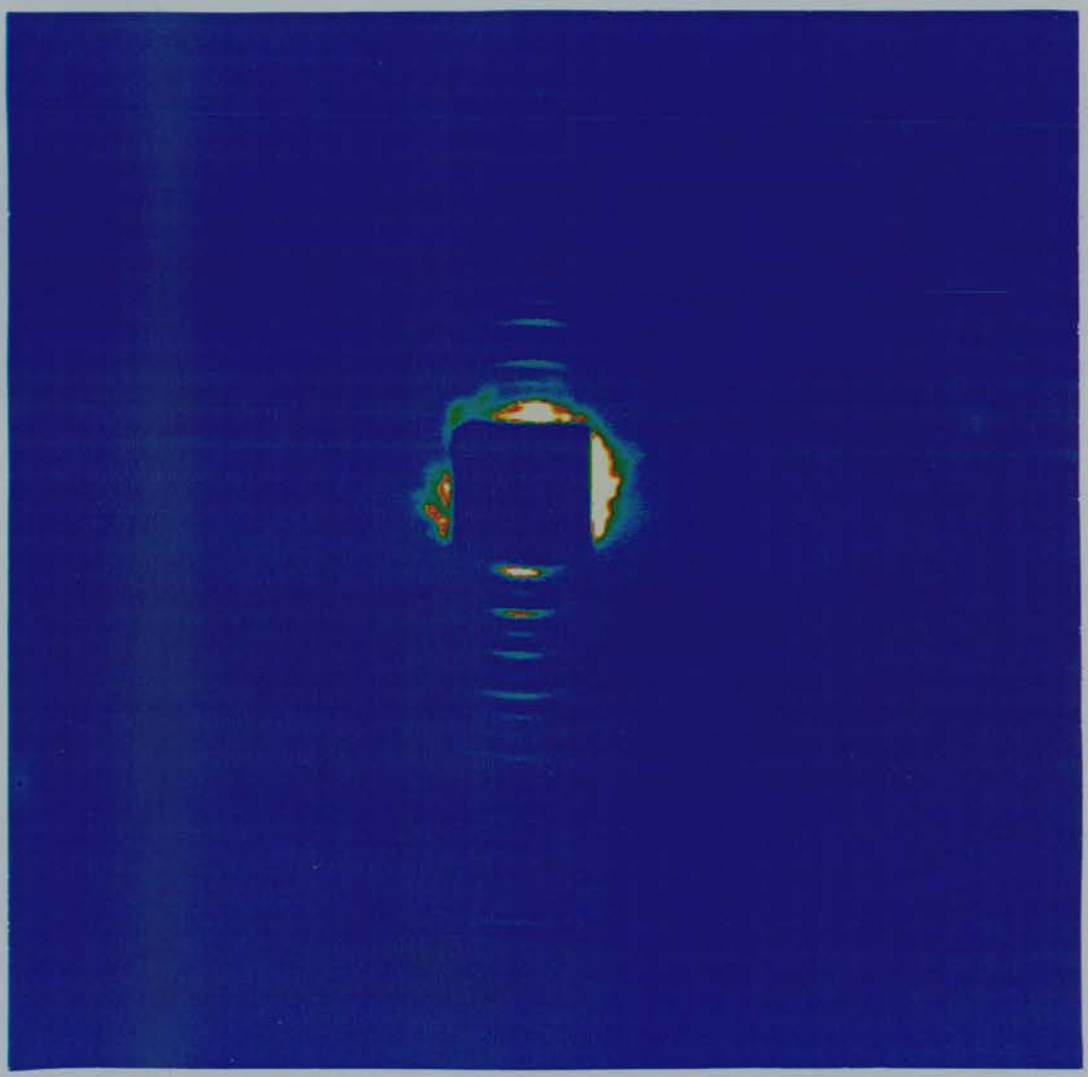

Figure 4.2. The high angle X-ray diffraction patterns for b) 16 week old, nonmineralized tissue treated with EDTA

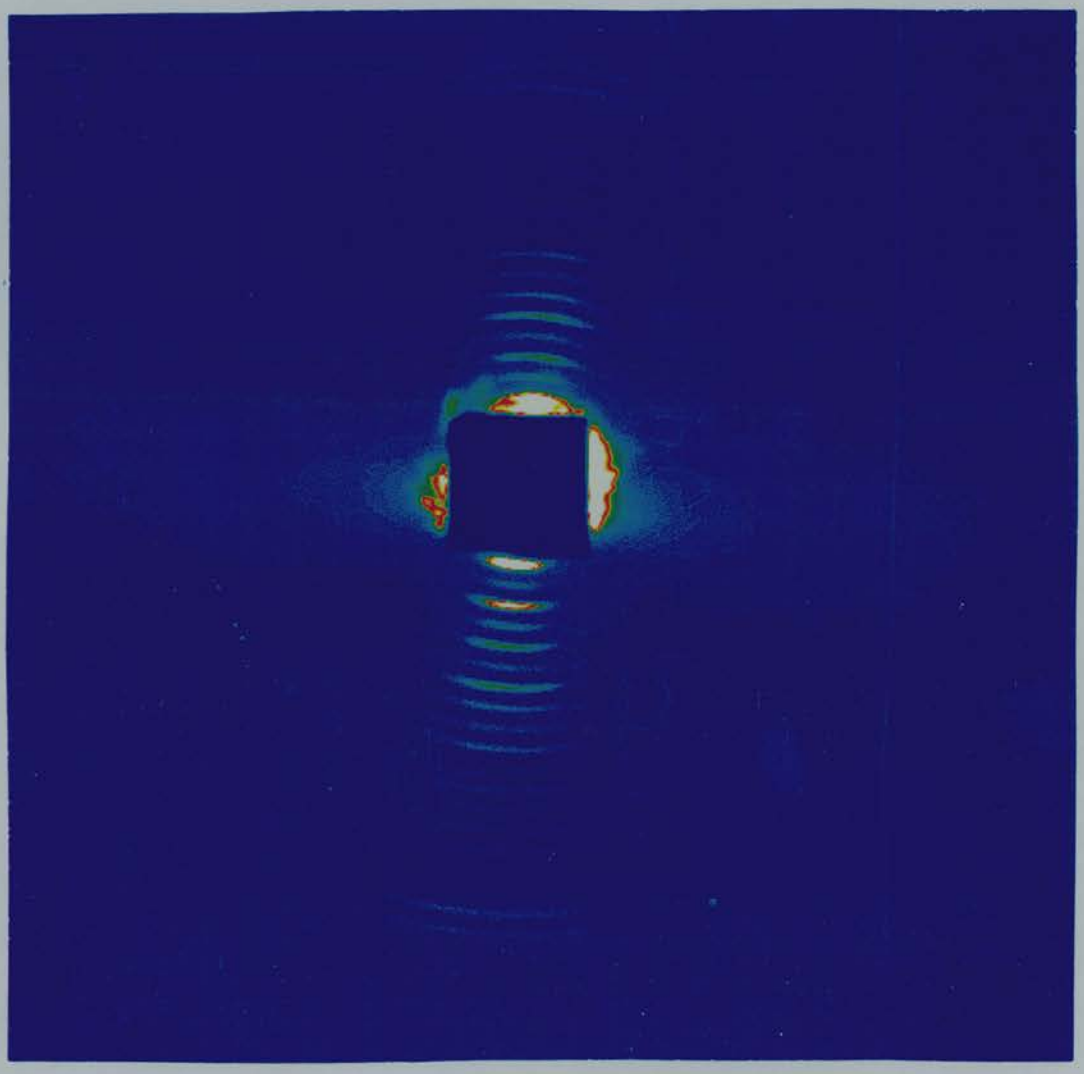

Figure 4.2. The high angle X-ray diffraction pattern for c) 16 week old, demineralized tissue

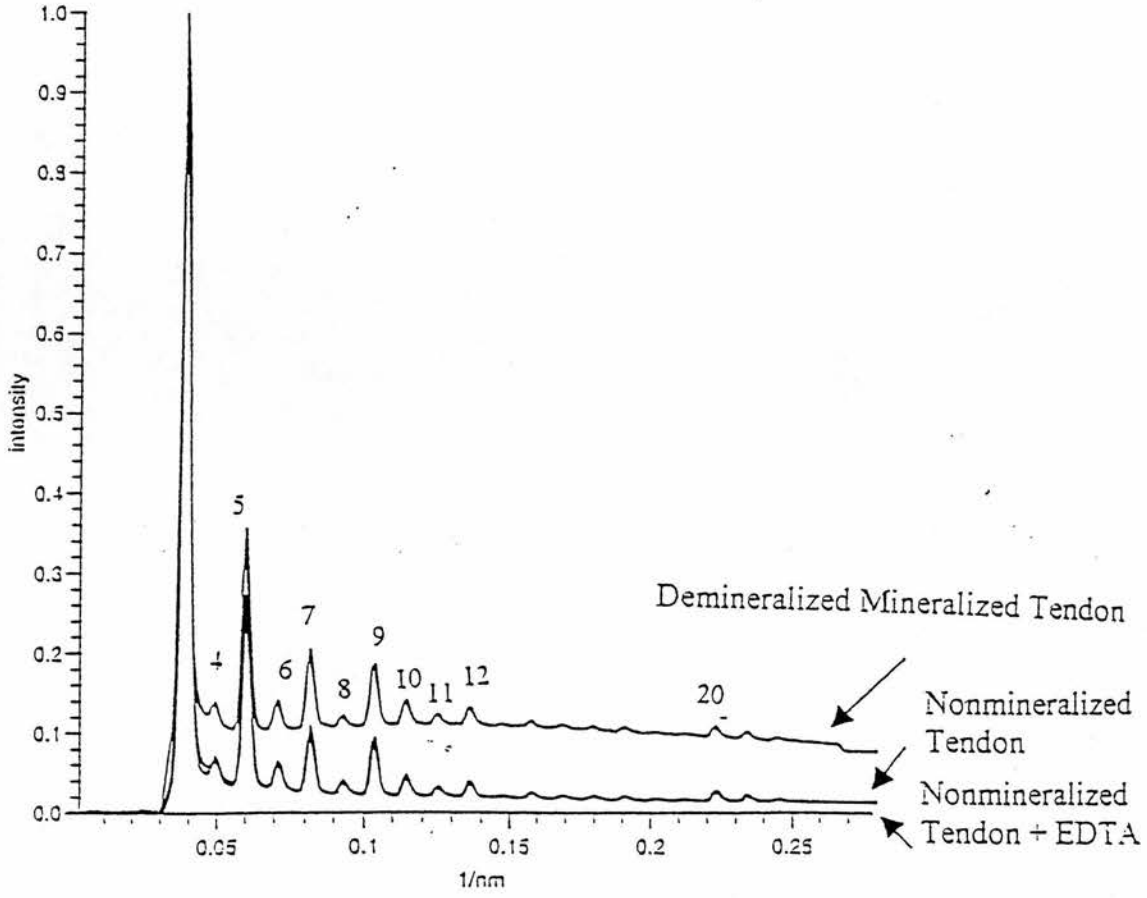

Figure 4.3. Overlaid graphs of the meridional intensities from 16-week-old demineralized mineralized portion; EDTA treated nonmineralized portion and nonmineralized portion.

The telopeptides for nonmineralized and demineralized 16-week-old turkey leg tendon were modelled by alteration of axial and lateral extension from 100% to 10%. The fits for these were compared to observed meridional intensities for these tendons.

4.3.1. Telopeptide Modelling

The meridional diffraction intensities obtained from turkey leg tendon correspond to the Fourier transform of the axially projected D periodic electron density within a fibril. Well separated diffraction intensities obtained on a low angle diffraction camera at the SRS Daresbury allowed the intensity values for the meridional series to be determined using

programs developed in house. No coherence is thought to be found between fibrils. The meridional intensity series has been used by a number of researchers to determine the axially projected electron density profile. A study by Hulmes *et al.,* (1977) examined the effects of changing the number of amino acids in a D period and also the effect of altering the telopeptide conformations which remain poorly resolved. A similar approach was taken in the study here; the amino acid sequence was converted into amino acids scattering factors based on the electron density of each amino acid after correction for the volume of water occupied by each residue; details are available in Hulmes *et al.*, (1977). The amino acid sequence of the chick $\alpha 1$ and a composite chick/rat $\alpha 2$ chain was used to produce the collagen sequence as a discrete array of density functions. The D periodic nature of the collagen was simulated by adding the electron density of an amino acid (i) to those found at (n x 234)+ i, where n is an integer (1-5). This creates an electron density profile that contains the characteristic gap /overlap density contrast. The telopeptides are special regions of the collagen molecule that do not conform to the typical Gly X Y sequence motif. Their conformation remains unresolved and the variation of the axial translation per amino acid was examined by the modelling studies of Hulmes *et al.*, (1977) Wess *et al.*, (1998). The axial locations of the amino acids of the telopeptides was varied and used in the optimisation of the fit to the diffraction data. In the simplest models, the axial translation per amino acid of the N and C terminal telopeptides were examined as a range of possible contracted conformations where the axial translation per amino acid in the main helical region corresponded to 100%. Models were constructed for each possible combination of telopeptide conformation and also including variation in the number of amino acids in each D periodic segment. Fourier inversion of the resultant structure produced a series of structure factors that could be compared to the amplitudes found in the diffraction data. The first order of diffraction of the

collagen tends to dominate the meridional diffraction series and corresponds to the characteristic D periodic step function. In attempting to produce an empirical fit between the data and model intensities, the use of an unweighted first order of diffraction can produce erratic results since a small percentage difference in the amplitude of these factors can dominate the fit. It was found to be most effective if the first order of diffraction was weighted to be 10% of its original value before the goodness of fit, the R factor, was calculated.

$$R= \Sigma(|(ampobs)-(ampcalc)|/ampobs) \quad n=1,20$$

Initial trials revealed that the telopeptide was an important factor in the development of a realistic fit to the diffraction data. In over 400 models, only five produced an R factor of less than 20% and these all corresponded to a local variation of the telopeptide structures. Small differences were found compared to the values for the telopeptide conformation given by Hulmes *et al.*, (1977). This is expected since the low angle intensity profile of turkey leg tendon is similar to rat tail tendon with the exception of the 7^{th} and 14^{th} orders being significantly higher.

Figure 4.4. shows the calculated optimal axial intensities for the telopeptide modelling compared to 16 week old demineralized, nonmineralized and EDTA treated, nonmineralized tendon. The optimal agreement indicated both telopeptides to be contracted. Best agreement was 50% of the original length of the N-terminal telopeptide and 70% of the original length of the C-terminal telopeptide. This is in agreement with Wess *et al.*, 1990, 1998 and Hulmes *et al.*, 1977, 1981.

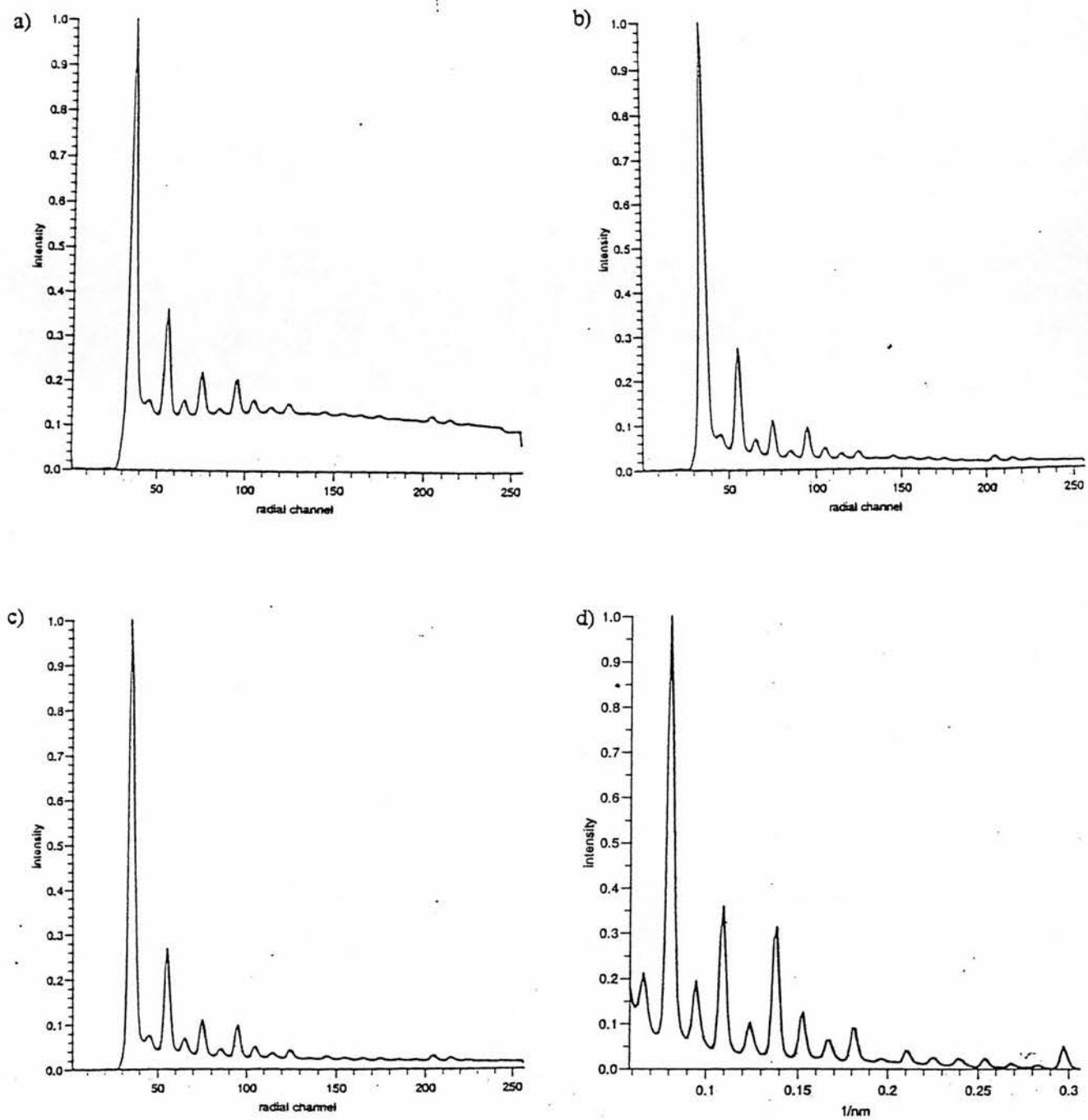

Figure 4.4. The axial scattering intensities for a) 16 week old demineralized tendon, b) 16 week old nonmineralized tendon, c) 16 week old EDTA treated, nonmineralized tendon and d) the optimal agreement for the telopeptide modelling.

4.4. Investigation into the Changes in the Equatorial Packing of Collagen

No changes in crosslink profiles could be detected using crosslink analysis performed over small sections at the edge of mineralization. 30μm thick sections of 60-week-old tendon were prepared as described in chapter 2 and were subjected to medium angle diffraction at SRS, Daresbury using a 200μm beam. A scan was performed through the tissue from the mineralized to the nonmineralized portion in 100μm steps. Further, more detailed analysis of this tissue was performed at ESRF, Grenoble, France on the microfocus beamline ID13, BL1. A 1.5μm full width half maximum (FWHM) beam from Bragg Fresnel optics was used and a scan performed in 10μm steps.

4.4.1. Medium Angle Scan with a 200μm beam in 100μm Steps of 60 Week Old Tendon from Mineralized to Nonmineralized Portions.

A 200μm beam from beamline 7.2 at SRS, Daresbury, UK was used to scan through a 30μm thick 60 week old section of turkey leg tendon. Figure 4.5 shows the diffraction patterns for each of the positions in the scan. Figure 4.6. shows the overlaid graphs of the scan through the edge of mineralization. From these data it can be seen that the position of the collagen triplet, the major molecular interference peak at approximately 1.3nm spacing, does not change from the mineralized to the nonmineralized portions. The position of the highest intensity of the collagen diffraction peak for both the nonmineralized and mineralized sections is the same. Previously published data shows the position of the Bragg reflections for mineralized collagen to be further from the centre of the beam than nonmineralized collagen. As this is in reciprocal space it can therefore be interpreted as the collagen fibrils are more compressed in the mineralized tissue than in the nonmineralized tissue (Lees *et al.*, 1984; Lees, 1987; Fratzl *et al.*, 1993). There are two possible explanations for the current

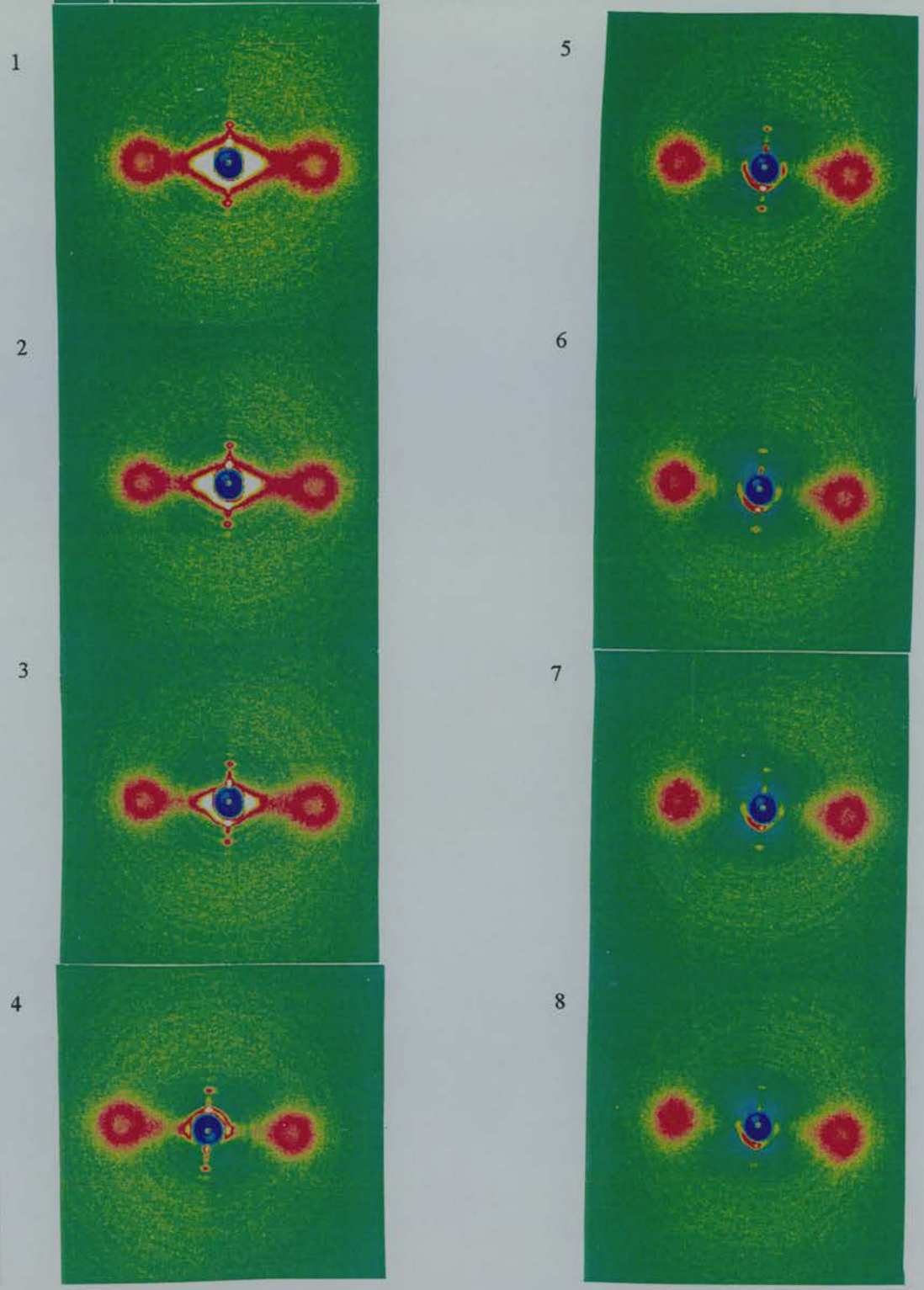

Figure 4.5. The high angle X-ray diffraction patterns for a scan of 200μm beam in 100μm steps from the mineralized to the nonmineralized portions of a 60-week-old tendon. Each pattern shows the characteristic equatorial scatter from the collagen although the meridional intensities cannot be clearly observed as all the frames in the plot have been scaled to frame 1 so these relatively low intensity reflections are not seen.
Diffraction patterns 1and 2 show the high intensity (white) scattering from the mineral crystal around the beam centre. 3 shows mineral but less than observed in 1 & 2, whilst in 4 only a small amount of mineral can be seen, this can be considered the edge region. 5-8 are diffraction patterns from nonmineralized, from 100μm after the edge region (5) to 300μm (8).

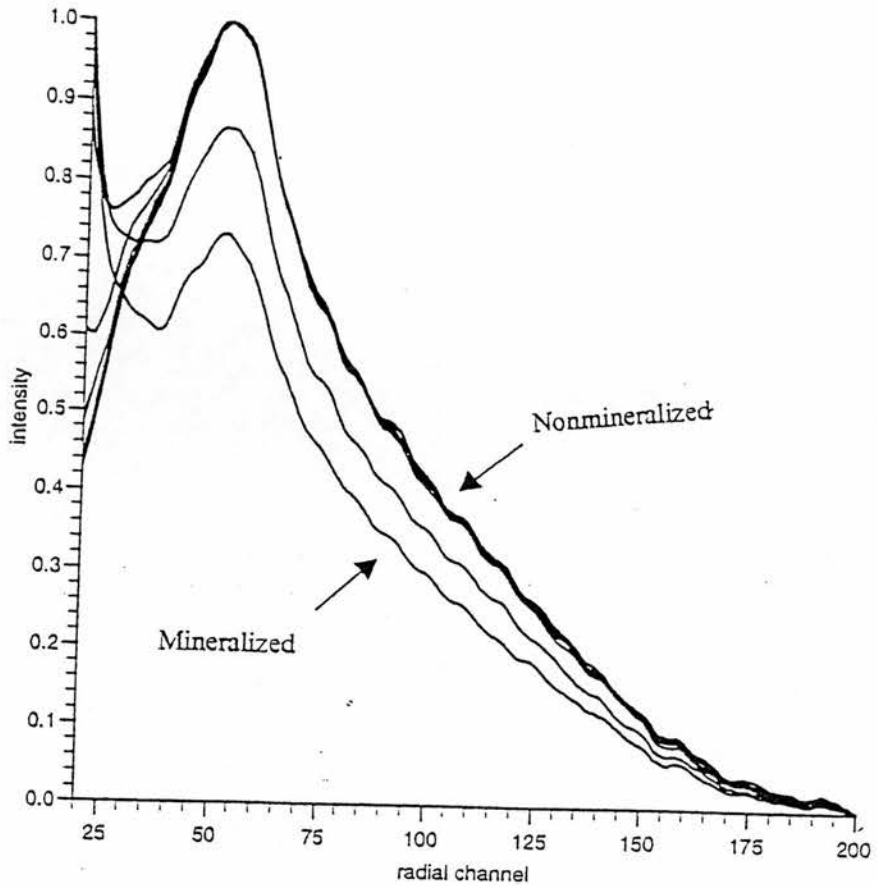

Figure 4.6. Overlaid plots of the scan through the edge of mineralization of 60-week-old tendon. The data are normalized for each sample to show the relative position of the equatorial reflections.

observation: Mineral diffracts X-rays approximately ten times more than collagen. This could mean that the mineral observed in the diffraction patterns at the beginning of the scan is very little and the majority of the collagen present in this is unmineralized. Another explanation is that the tissue has dried which would reduce the spacing between the collagen fibrils as seen previously (Fratzl *et al.*, 1993). If this were the case, however, it would be expected that the reflection became sharper than for fully hydrated tissue, which is not the case.

Figure 4.7 shows the equatorial scattering intensity of each scan plotted on double logarithmic scales versus $Q = (4\pi/\lambda)\sin(\theta/2)$ where θ is the scattering angle and λ the wavelength of the incident X-ray beam. From this data it can be seen that all the curves are behaving as PQ^{-4} according to Porod's law where P is the Porod constant. All the diffraction patterns taken through the scan show no different collagen packing at the edge of mineralization indicating that the parameter T does not change with distance into the mineralized portion of the sample.

4.4.2. A Medium Angle Scan of a 30μm Thick 60-Week Old Turkey Leg Tendon using a 1.5μm FWHM beam in 10μm steps.

A more detailed study of the edge of mineralization was performed using the microfocus beamline BL1 at ESRF, Grenoble, France using Bragg Fresnel Optics. Previous work done with these optics and beamline showed that the first 22 meridional reflections were resolved from 200μm thick sections of turkey leg tendon (Snigirev *et al.*, 1993). The aim of our experiment was to use this technology to study the edge of mineralization in more detail than has previously been possible. Figure 4.8 shows the diffraction patterns obtained from a scan from the mineralized portion through to the nonmineralized portion of a sample. Unfortunately the beam flux was low for the entire duration of our experiments but despite this images could still be obtained. Figure 4.9. shows the equatorial scattering intensity of each scan plotted versus Q (see section 4.4.1. for a definition of Q). No differences can be seen between the mineralized and nonmineralized collagen due to the poor images obtained. The experiment overall was not successful due to the low beam flux.

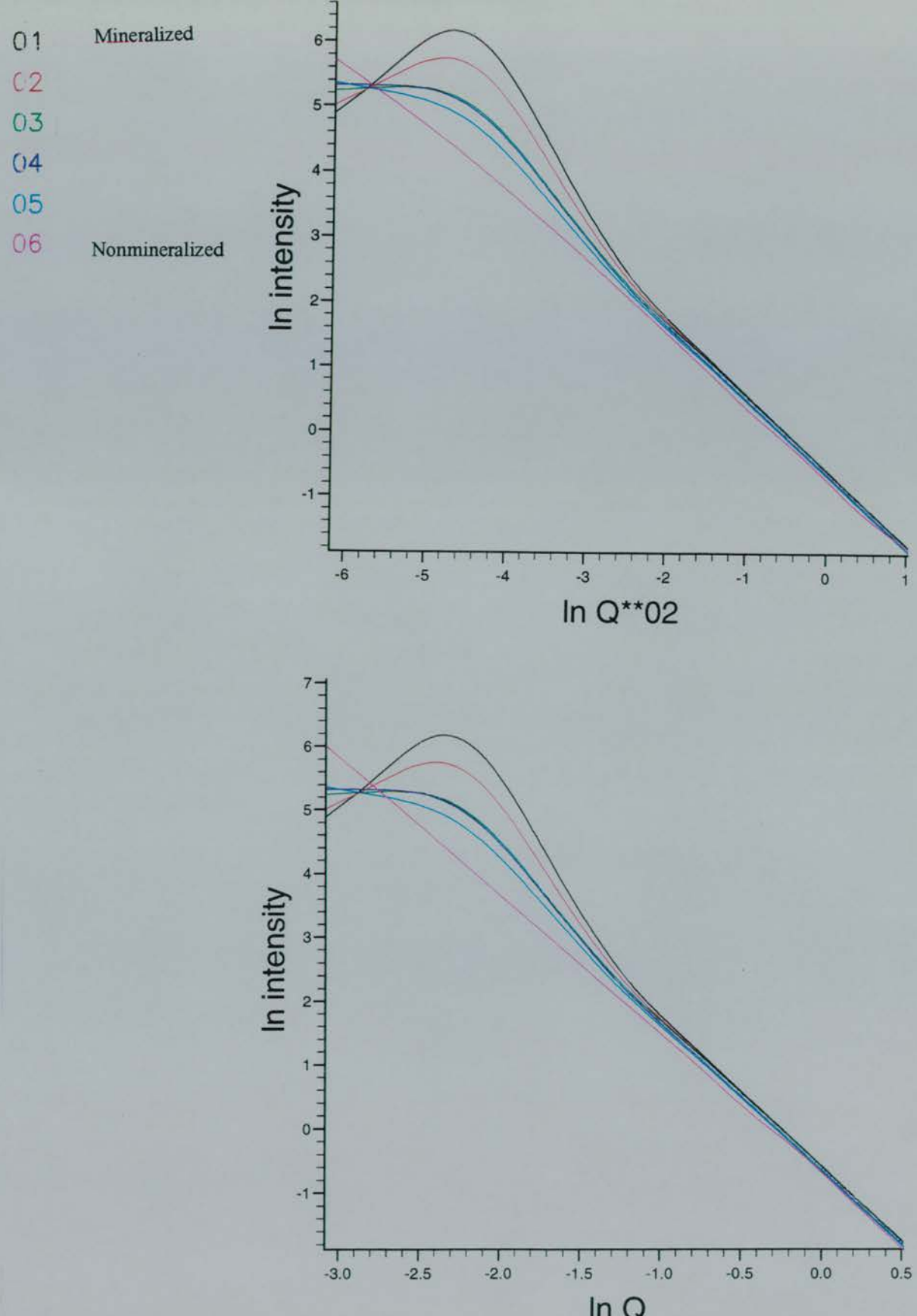

Figure 4.7 The equatorial scattering intensity from scans using a 200μm beam in 100μm steps from the mineralized to nonmineralized portions of 60 week old tendon. The key shows that line 1 is from within the mineralized portion of the tendon and number 6 is within the nonmineralized portion. These sections are 500μm apart over the mineralizing edge. No changes can be seen between the intensity apart from the gradual loss of mineral in the Porod region ie. no contrast between the mineral and protein components.

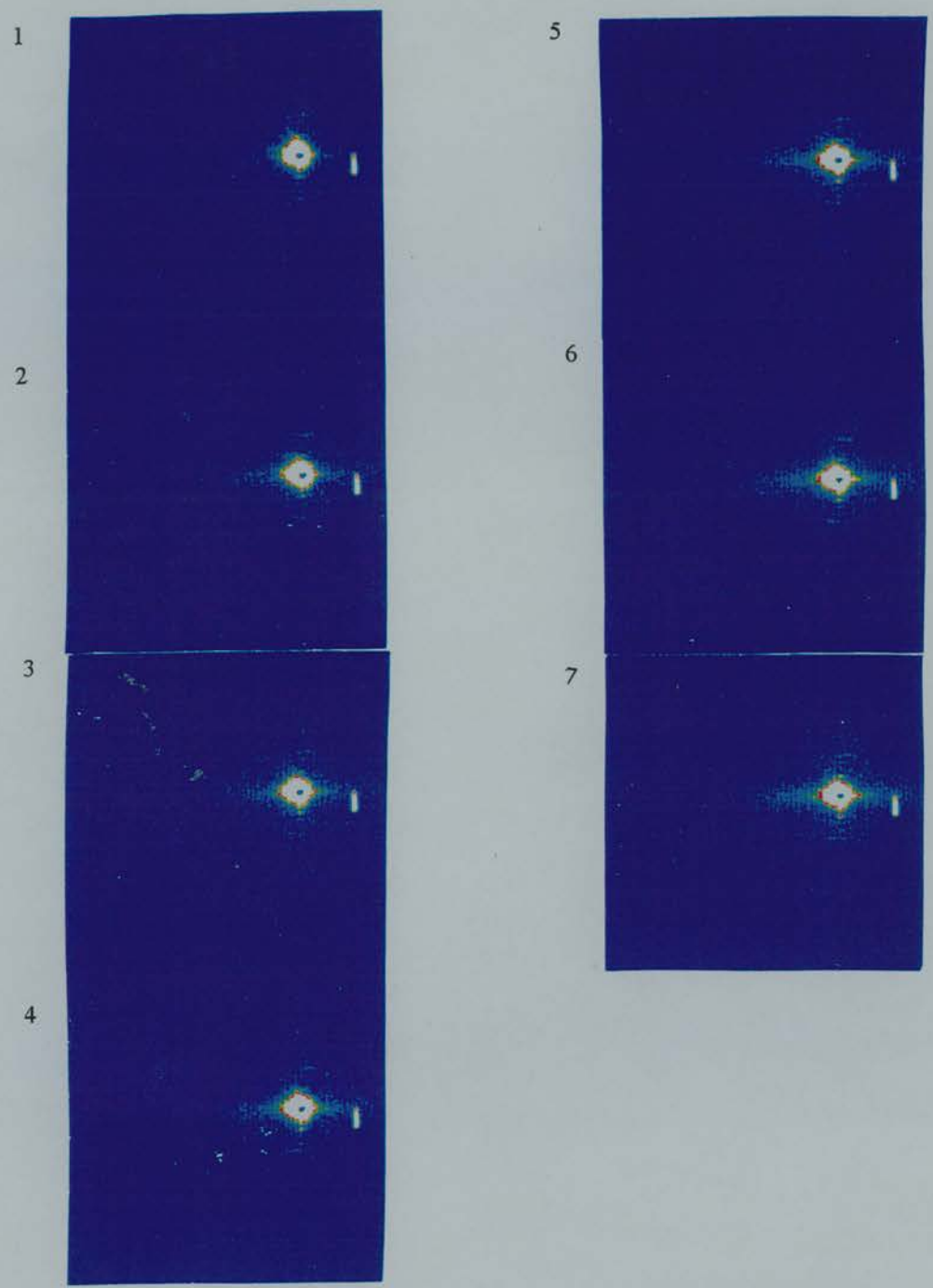

Figure 4.8. The medium angle X-ray diffraction patterns from 1.5μm FWHM beam in 10μm steps from a scan through the mineralized portion (scan 1) to the nonmineralized portion (scan 7) of a 60-week-old tendon. Due to low beam flux very little can be seen in this scan. The mineral crystallite that was evident in the mineralized portion of the scan in Figure 4.5 as high intensity cannot be seen in the scans of the mineralized portion here. The shape is faintly seen in scan 1 as a pale blue colour surrounding the beam (in the centre). The intensities in each of the scans are scaled individually so the equatorial intensity cannot be seen in this scan due to the presence of the mineral. The "fan-shaped" equatorial intensity can be seen only faintly in the other scans. Meridional intensities from the collagen can be seen more clearly towards the nonmineralized portions (5-7 inclusive).

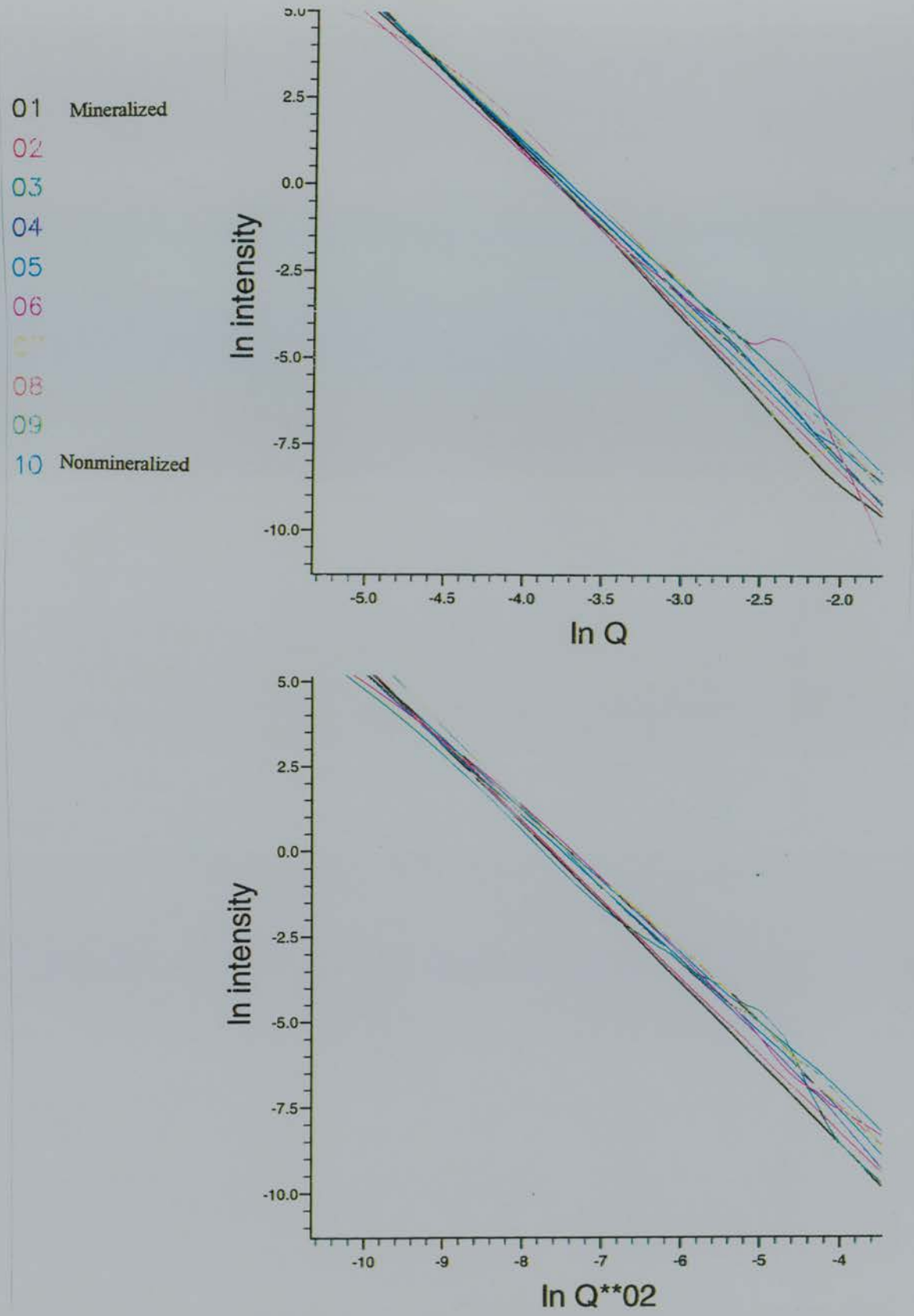

Figure 4.9. The equatorial scattering from the scans shown in Figure 4.8, using a 1.5 FWHM μm beam in 10μm steps from the mineralized to nonmineralized portions of 60 week old tendon. No difference can be seen between the equatorial intensity of the mineralized to the nonmineralized. Not even the characteristic shape of the mineral can be seen here due to low beam flux when these data were collected.

4.5. Discussion.

X-ray diffraction was used to study the collagen structure in mineralizing turkey leg tendon. In Chapter 3, crosslink analysis was unable to detect any changes in collagen structure except those associated with mineralization. X-ray diffraction was used to investigate the changes in mineral crystallite size with age. It was seen that the mineral crystal size in tendons from 12 to 22 weeks old increases with age from 1.48 nm to 2.53 nm. From 22 to 44 weeks the mineral size increases more slowly to 3.06 nm. From this age onwards to 60 weeks old the mineral crystal decreases to 2.2 nm. A previous study carried out using Small Angle X-ray Scattering (SAXS) measured the thickness of 14 week old mineralized turkey leg tendon to be in the order of 2 nm (Fratzl *et al.*, 1992). This value is consistent with the results observed in this study. Other studies using different techniques to measure the crystallite size have given varying results. The thickness observed from high voltage electron microscopic tomography was 4-6 nm (Landis *et al.*, 1996) which is greater than any calculated thickness in the present study. A comparative study between TEM and X-ray diffraction was carried out on dispersed bone crystals. In this study TEM was considered the most reliable method in this instance, although the inherent drawbacks of preparing the samples in this manner were noted by the authors. It was also concluded that the study may be biased towards smaller values than the larger *in vivo* ones (Ziv & Weiner, 1994). X-ray diffraction was favoured in this study as the crystals measured are *in vivo* with the tissue having minimal sample preparation. The crystal thickness measured for all the ages of tendon can all be accommodated within the gap regions of the collagen although only if a slight compression of the fibril structure between the crystals is assumed. This is observed in 8 to 54 week old mineralized tissues where the equatorial spacing of collagen decreases with increasing mineralization (Bigi *et al.*, 1988).

The decrease of the crystal size detected in older birds could be due to calcium resorption, possibly due to testosterone levels and a type of osteoporosis. Testosterone is known to have similar effects to estrogen in increasing intestinal absorption of calcium, decreasing bone resorption rate and (usually) increasing bone formation rate. This has been established generally by studies of hypogonadism (Wang *et al* 1996).

It has been hypothesised in this study that the observed compression of the collagen fibril structure may deform the collagen fibrils enough breaking some of the reducible crosslinks into their aldehyde precursors. In order to study this deformation the telopeptide organisation was investigated in mineralized and nonmineralized tendons.

Mineralized 16-week-old tendon portions were demineralized with EDTA. These tendons were compared to nonmineralized tendon and nonmineralized tendon that had been treated with EDTA. The results showed that EDTA treatment did not permanently distort the collagen molecules. They also showed that there are no differences in the axial structure between the demineralized collagen and the nonmineralized collagen seen in the first 20 orders. Telopeptide modelling indicates that shortening or lengthening the telopeptide will have a dramatic effect on the intensities of the orders of diffraction 10 to 19 (Hulmes *et al.*, 1977). No change in the axial telopeptide organisation has been observed by this technique. It could be argued that if the collagen distortion is not permanent, removal of the mineral will reverse this distortion and leave the structure similar to that in the nonmineralized environment. Crosslink analysis performed on demineralized tendon gives the same change in crosslink profile associated with the mineralized region (Yamauchi & Katz, 1993). Therefore if the compression of the collagen fibrils brought about by mineralization was responsible for the changes in crosslink profile associated with mineralization, one of two things would happen:

1) Once demineralized the telopeptide organisation would be different to the nonmineralized collagen to maintain the crosslink profile seen or

2) The collagen would revert back to its native, nonmineralized organisation and there would be a further change in crosslink profile.

The axial structure data obtained in the present study does not support the hypothesis that the distortion of the collagen by the mineral is responsible for the change in collagen crosslinks. Further study of the telopeptide organisation was carried out by modelling the data for the nonmineralized tendon and the demineralized tendon.

The method employed involved an alteration of the axial extension of the telopeptides from 100 to 10% (Hulmes *et al.*, 1977). Due to the sensitivity in the meridional orders 10-19 when altering the telopeptide length this method is considered valid for axial changes, however, there are three drawbacks: 1) if any rotational changes of the telopeptide occur, they are not detected as they will only effect the lateral scattering intensity; 2) if using the telopeptide length to predict crosslinking sites, changes from inter- to intra-molecular crosslinks and vice versa cannot be accounted for and 3) when minimizing the given parameter in the model a better fit will be produced. This does not prove that the telopeptide is actually in the position you find at the minimum.

The results from the modelling of the telopeptides indicated that they are contracted. The best agreement was 50% of the original length of the N-terminal telopeptide and 70% of the original length of the C-terminal telopeptide. This is in agreement with Wess *et al.*, 1990; 1998 and Hulmes *et al.*, 1977, 1981. Figure 4.10 shows the amino acid sequences for the C-terminal telopeptide and its four neighbouring collagen molecule segments. At 67% contraction of the C-telopeptide, Lysine (Lys) at position 16 of the C-telopeptide is adjacent Hydroxylysine (Hyl) 87. This suggests that this is the position of the crosslinks in both

mineralized and nonmineralized collagen. The only other possible site for crosslinking is Lys 327, which is not normally involved in crosslinking. The telopeptide contraction necessary for this crosslinking site is 91%. This is not in agreement with the present data.

The position of the C-terminal crosslink at Hyl 87 in both mineralized and nonmineralized collagen is in agreement with Yamauchi & Katz, 1993 where the crosslinks involved in both the mineralized and nonmineralized collagen were found to tie together the same peptides involving Hyl 87. Figure 4.11. shows the amino acid sequences for the N-terminal telopeptide and its four neighbouring collagen molecule segments. The telopeptide has been calculated to be at 50% of its original length in both mineralized and nonmineralized collagen. There appears to be no sites of crosslinking between the N-terminal telopeptide that fit the present data. The only possible site of crosslinking that leads to a contraction of the telopeptide is at Hyl 930. In previously published data using bovine dentin collagen evidence was provided that Pyd is located between the N-terminal telopeptide and Hyl 930 (Kuboki *et al.*, 1993). This crosslink would necessitate the telopeptide being 87% of its original length which does not fit the present data on turkey leg tendon. A distinct feature of mineralized tissues is a relative paucity of N-terminal crosslinks, both before and after mineralization (Yamauchi *et al.*, 1989; Otsubo *et al.*, 1992 & Yamauchi *et al.*, 1992). This may account for the organisation of the telopeptide, as it may not be crosslinked at all. This is in agreement with the previously published data where it was seen that most, if not all, the aldehyde present throughout the turkey tendons seems to be associated with the two C-terminal Lys 16 sites. From all the telopeptide data collected it can be seen that there is no axial change in the organisation of the telopeptide between nonmineralized collagen and mineralized collagen of the turkey leg tendon. Due to limitations in the modelling method, as mentioned earlier, rotational changes in the telopeptide between these two environments cannot be ruled out as

Figure 4.10. The Amino Acid Sequences for C-Terminal Telopeptide and its Four Neighbouring Collagen Molecule Segments.

Telopeptide Region

gly	gly	gly		val	phe	val		leu	pro	leu		ser	ser	ser		thr	thr	thr	
gly	gly	gly		val	leu	val		gln	hyp	gln		arg	arg	arg		ala	hyp	ala	
tyr	tyr	tyr		gly	gly	gly		gly	gly	gly		gly	gly	gly		gly	gly	gly	
asp	glu	asp		leu	leu	leu		met	met	met		phe	leu	phe		leu	leu	leu	
leu	phe	leu		hyp	hyp	hyp		hyp	hyp	hyp		hyp	hyp	hyp		hyp	hyp	hyp	
ser		ser		gly	gly	gly		gly	gly	gly		gly	gly	gly		gly	gly	gly	
phe		phe		gln	ser	gln		glu	glu	glu		ala	ala	ala		met	phe	met	
leu		leu		arg	arg	arg		arg	arg	arg		asp	asp	asp	67% of Length	HYL	HYL	HYL	87
pro		pro		gly	gly	gly		gly	gly	gly		gly	gly	gly		gly	gly	gly	
gln		gln		glu	glu	glu		ala	val	ala		val	arg	val		his	ile	his	
pro		pro		arg	arg	arg		ala	ala	ala		ala	ala	ala		arg	arg	arg	
pro		pro		gly	gly	gly		gly	gly	gly		gly	gly	gly		gly	gly	gly	
gln		gln		phe	leu	phe		leu	val	leu		pro	val	pro		phe	his	phe	
gln		gln		hyp	hyp	hyp		hyp	hyp	hyp	91% of Length	LYS	met	LYS	327	ser	asn	ser	
glx		glx		gly	gly	gly		gly	gly	gly		gly	gly	gly		gly	gly	gly	
LYS		LYS	16C	leu	val	leu		pro	gly	pro		pro	pro	pro		leu	leu	leu	
ala		ala		hyp	ala	hyp	Extension	LYS	LYS	LYS	564	ala	ala	ala		asp	asp	asp	
his		his		gly	gly	gly		gly	gly	gly		gly	gly	gly		gly	gly	gly	
asp		asp		pro	ser	pro		asp	glu	asp		glu	ser	glu		ala	leu	ala	
gly		gly		ser	val	ser		arg	LYS	arg		arg	arg	arg		LYS	the	LYS	
gly		gly		gly	gly	gly		gly	gly	gly		gly	gly	gly		gly	gly	gly	
arg		arg		glu	glu	glu		asp	ala	asp		ser	thr	ser		asp	gln	asp	
tyr		tyr		hyp	hyp	hyp		ala	hyp	ala		hyp	ser	hyp		ala	hyp	ala	
tyr		tyr		gly	gly	gly		gly	gly	gly		gly	gly	gly		gly	gly	gly	
				LYS	pro	LYS		pro	leu	pro		pro	pro	pro		pro	ala	pro	
End of Molecule				gln	leu	gln		LYS	arg	LYS		ala	ala	ala		ala	hyp	ala	
				gly	gly	gly		gly	gly	gly		gly	gly	gly		gly	gly	gly	
				pro	gly	pro		ala	gly	ala		pro	pro	pro		pro	pro	pro	
				1D				2D				3D				4D			

Figure 4.11. The Amino Acid Sequences for the N-Terminal Telopeptide and its Four Neighbouring Collagen Molecule Segments.

4D				3D				2D				1D			
asp	asp	asp		pro	pro	pro		pro	val	pro		gln	leu	gln	
HYL	asp	HYL	918	HYL	ala	HYL	684	ala	gln	ala		hyp	hyp	hyp	
gly	gly	gly		gly	gly	gly		gly	gly	gly		gly	gly	gly	
glu	glu	glu		ala	pro	ala		glu	glu	glu		ala	ala	ala	
thr	hyp	thr		arg	arg	arg		arg	LYS	arg	453	LYS	HYL	LYS	219
gly	gly	gly		gly	gly	gly		gly	gly	gly		gly	gly	gly	
glu	asp	glu		ser	asp	ser		glu	glu	glu		ala	ala	ala	
glu	LYS	glu	924	ala	ala	ala		gln	gln	gln		asn	ala	asn	
gly	gly	gly		gly	gly	gly		gly	gly	gly		gly	gly	gly	
asp	asp	asp		pro	pro	pro		pro	pro	pro		ala	leu	ala	
arg	HYL	arg	927	hyp	thr	hyp		ala	ala	ala		hyp	hyp	hyp	
gly	gly	gly	Extension	gly	gly	gly		gly	gly	gly		gly	gly	gly	
ile	leu	ile		ala	met	ala		ser	pro	ser		ile	val	ile	
HYL	HYL	HYL	930	thr	thr	thr		hyp	hyp	hyp		ala	ala	ala	
gly	gly	gly	87% of Length	gly	gly	gly		gly	gly	gly		gly	gly	gly	
his	asp	his		phe	phe	phe		phe	phe	phe		ala	ala	ala	
arg	arg	arg		hyp	hyp	hyp		gln	gln	gln		hyp	hyp	hyp	
gly	gly	gly		gly	gly	gly		gly	gly	gly		gly	gly	gly	
phe	his	phe		arg	arg	arg		leu	leu	leu		phe	leu	phe	
ser	asn	ser		val	thr	val		hyp	hyp	hyp		hyp	hyp	hyp	
gly	gly	gly		gly	gly	gly		gly	gly	gly		gly	gly	gly	
leu	leu	leu		pro	pro	pro		pro	pro	pro		ala	pro	ala	
gln	gln	gln		hyp	hyp	hyp		ala	ala	ala		arg	arg	arg	
gly	gly	gly		gly	gly	gly		gly	gly	gly		gly	gly	gly	
pro	leu	pro		pro	pro	pro		pro	pro	pro		pro	ile	pro	
hyp	hyp	hyp		ser	ser	ser		hyp	ala	hyp		ser	hyp	ser	
gly	gly	gly		gly	gly	gly		gly	gly	gly		gly	gly	gly	
pro	leu	pro		asn	leu	asn		glu	glu	glu		pro	pro	pro	

Telopeptide Region

End of Molecule

glu		glu	
leu		leu	
ser		ser	
gly		gly	
tyr		tyr	
asp		asp	
glu	glu	glu	
LYS	pro	LYS	9N
ser	asp	ser	
thr	ala	thr	
gly	LYS	gly	5N
ile	gly	ile	
ser	gly	ser	
val	gly	val	
pro	pro	pro	
gly	gly	gly	

can any changes between intra- and inter-molecular crosslinks that may occur. This seems unlikely, however, as the data generated in this study is in agreement with results obtained from other tissues (Wess *et al.*, 1990; 1998: Hulmes *et al.*, 1977; 1981) and with crosslink results from turkey leg tendon and other mineralized tissues (mineralization (Yamauchi *et al.*, 1989; 1992; 1993: Otsubo *et al.*, 1992). These data suggest that the change in crosslinking profile associated with mineralization is not due to distortion of the collagen molecules by the mineral crystals, breaking crosslinks and forming others.

A further investigation of the edge of mineralization revealed that there were no changes detectable using a scan through the tissue in 100μm steps using a 200μm beam between the mineralized and nonmineralized portions. The only unexpected result was that position of the collagen triplet peak for both the nonmineralized and mineralized sections is at the same position. Previously published data shows the position of the Bragg reflections for mineralized collagen to be further from the centre of the beam than nonmineralized collagen. As this is in reciprocal space it can therefore be interpreted as the collagen fibrils are more compressed in the mineralized tissue than in the nonmineralized tissue (Lees *et al.*, 1984; Lees, 1987; Fratzl *et al.*, 1993). There are two possible explanations for the current observation: Mineral diffracts X-rays approximately ten times more than collagen. This could mean that the mineral observed in the diffraction patterns at the beginning of the scan is very little and the majority of the collagen present in this is unmineralized. Another explanation is that the tissue, in ethylene glycol, has dried which would reduce the spacing between the collagen fibrils as seen previously (Fratzl *et al.*, 1993). If this were the case, however, it would be expected that the reflection become sharper than for fully hydrated tissue, which is not the case.

A more detailed study of the edge of mineralization was attempted using a 1.5μm FWHM beam in 10μm steps. This method should have enabled the most detailed study that has ever been carried out on the edge of mineralization in turkey leg tendon. Unfortunately due to low beam flux poor images were generated. The data collected showed again that there were no changes in collagen packing at the edge of mineralization and that the maximum crystallite axis size does not change with distance into the mineralized portion of the sample. Both crosslink analysis and X-ray diffraction cannot detect any changes between the nonmineralized and mineralized portions of the turkey leg tendon. The section scans for both were as small as is allowed with present technology; therefore it must be assumed that there were no changes in collagen packing between the nonmineralized and mineralized portions at the edge of mineralization.

Chapter 5

Investigation of *In Vivo* Collagen Production

5. Investigation into Collagen Turnover in Turkey Leg Tendon.

The crosslink analyses and X-ray diffraction investigations on the edge of mineralization in turkey leg tendon suggest that the changes in collagen packing occur as a consequence of mineralization. An investigation into the telopeptide organisation, however, showed that they are the same in both nonmineralized and mineralized tendon which suggests that the changes in crosslinking profile associated with mineralization was not a consequence of the mineral crystal distorting the collagen breaking the existing crosslinks and forming new crosslinks. If these changes are taking place before mineralization as suggested by Yamauchi and Katz, 1993 as a consequence of some intracellular post-translational event, it would imply there would be a high turnover rate of the collagen during mineralization.

An experiment was therefore designed to establish the pattern of collagen turnover in turkey leg tendons during mineralization. The incorporation of tritiated proline into collagen hydroxyproline was assessed in a bird receiving the radiolabel at a time when active mineralization of the tendon was occurring (12-13 weeks of age). This experiment was designed to determine whether the differences observed in the crosslinking pattern between the mineralized and nonmineralized portions are linked to the rate of collagen production in each portion. This could suggest that the changes observed in the crosslinking pattern are due to the production of collagen with different mature crosslink precursors.

a)

Section (1cm)	Calcium (µg/nmol collagen)	^{3}H (CPM/nmol collagen)	Section (1cm)	Calcium (µg/nmol collagen)	^{3}H (CPM/nmol collagen)
1	23.45	185.4	11	1.42	68.8
2	34.71	198.8	12	1.16	69.7
3	20.35	163.0	13	1.35	68.8
4	36.41	126.9	14	1.07	81.3
5	39.3	165.7	15	2.53	102.5
6	34.8	165.9	16	20.32	310.7
7	54.41	267.5	17	23.18	278.3
8	45.14	183.5	18	26.91	250.6
9	1.82	98.7	19	30.9	302.8
10	1.31	55.6	20	33.43	259.0

b)

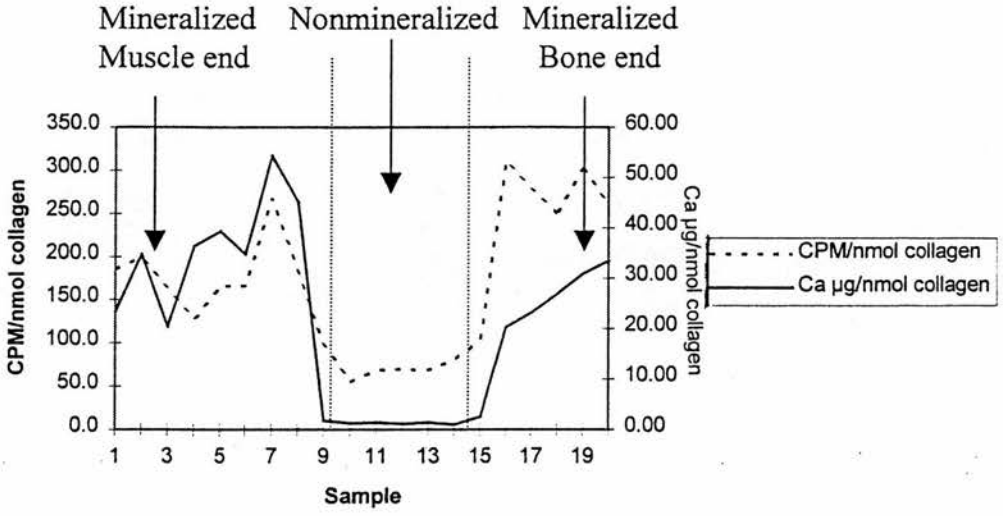

Figure 5.1 shows the ^{3}H CPM per nmol of collagen present along the length (1cm sections) of a turkey leg tendon as a table (a) and as a graph (b). These counts are related to the calcium content per nmol of collagen along the length of the tendon as a measure of whether mineralization has started in early, actively mineralizing tendon. It can be seen that high ^{3}H CPM are associated with higher calcium concentration suggesting that there is a higher rate of production of collagen in the mineralizing portions of the tendon.

5.1 The Level of Incorporation of Tritiated Proline

Following labelling *in vivo* and preparation of the tissue as described in section 2.2, the number of ^{3}H CPM present along the excised tissue was measured. One of the excised tendons was sectioned into 1cm portions along its length from distal to proximal. After the redissolution of the dried acid hydrolysates in water (1ml), an (20µl) aliquot of each was taken to measure ^{3}H. Another aliquot (300µl) was used to measure the calcium concentration in each sample.

Figure 5.1 a) and b) show the results for each of the 1cm sections. Each measurement was related to collagen concentration and a quenching correction applied to each of the radioactive counts, refer to section 2.2.2.3 B. It can be seen that the CPM/nmol collagen is greater in the sections of the tendon with high calcium concentration ie. the mineralized sections, than in the nonmineralized portions of the tendon. There is a greater concentration of ^{3}H in these portions but it is not clear from these results what form the ^{3}H is in, whether it is ^{3}H-proline or ^{3}H-hydroxyproline. All the samples, before being redissolved in a known volume of water were dried under vacuum completely, therefore eliminating the possible presence of residual tritiated water.

5.2 Separation of ^{3}H-Proline and ^{3}H-Hydroxyproline.

As mentioned in chapter 2, section 2.2.2.3.A, initial trials to separate the proline and hydroxyproline were performed on a Locarte ion exchange column. Only 500 nMoles of hydroxyproline could be applied to the column which did not result in sufficient ^{3}H CPM. Dowex mini columns were used which allowed 4µmoles of hydroxyproline to be applied to the column. An aliquot equivalent to 4µmoles of hydroxyproline from

six of the tendons in the legs of the turkey were analysed and a quenching correction applied (chapter 2, section 2.2.2.3.B.).

Figure 5.2 a) to f) shows all the results of the separation of ^{3}H-hydroxyproline and ^{3}H-proline from the mineralized to the nonmineralized portions of each tendon. It can be seen from each result that there is more ^{3}H-hydroxyproline and ^{3}H-proline in the mineralized portion of each tendon than in the nonmineralized portion. This implies that there is a greater rate of proline incorporation in the mineralized portion of a tendon than in the nonmineralized portion of the same tendon. Another observation of the nonmineralized sample separations was the relatively large amounts of radioactivity eluted in the early fractions of the chromatogram. As this could have been caused by column overloading these fractions were pooled and re-run on a Dowex mini-column. Figure 5.3 shows the results of one of these runs; most of the CPM are still present in the first fraction and can therefore be discounted as being ^{3}H-hydroxyproline or ^{3}H-proline.

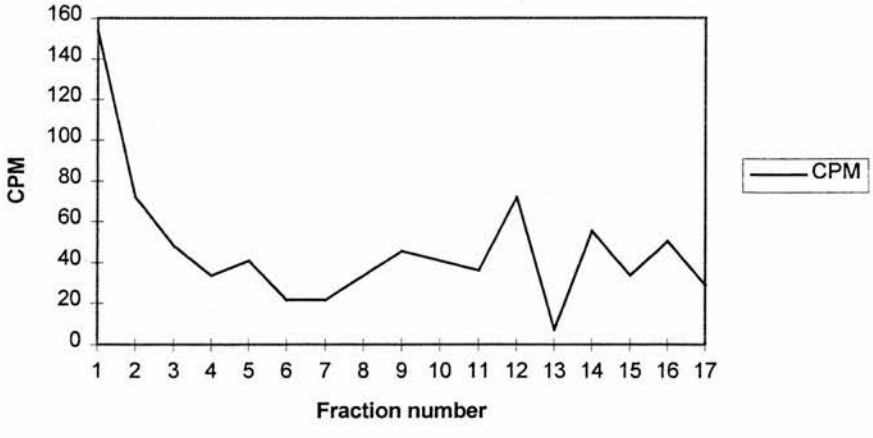

Figure 5.3. The first three fractions from the nonmineralized portion of tendon a) pooled and re-run on a Dowex mini-column.

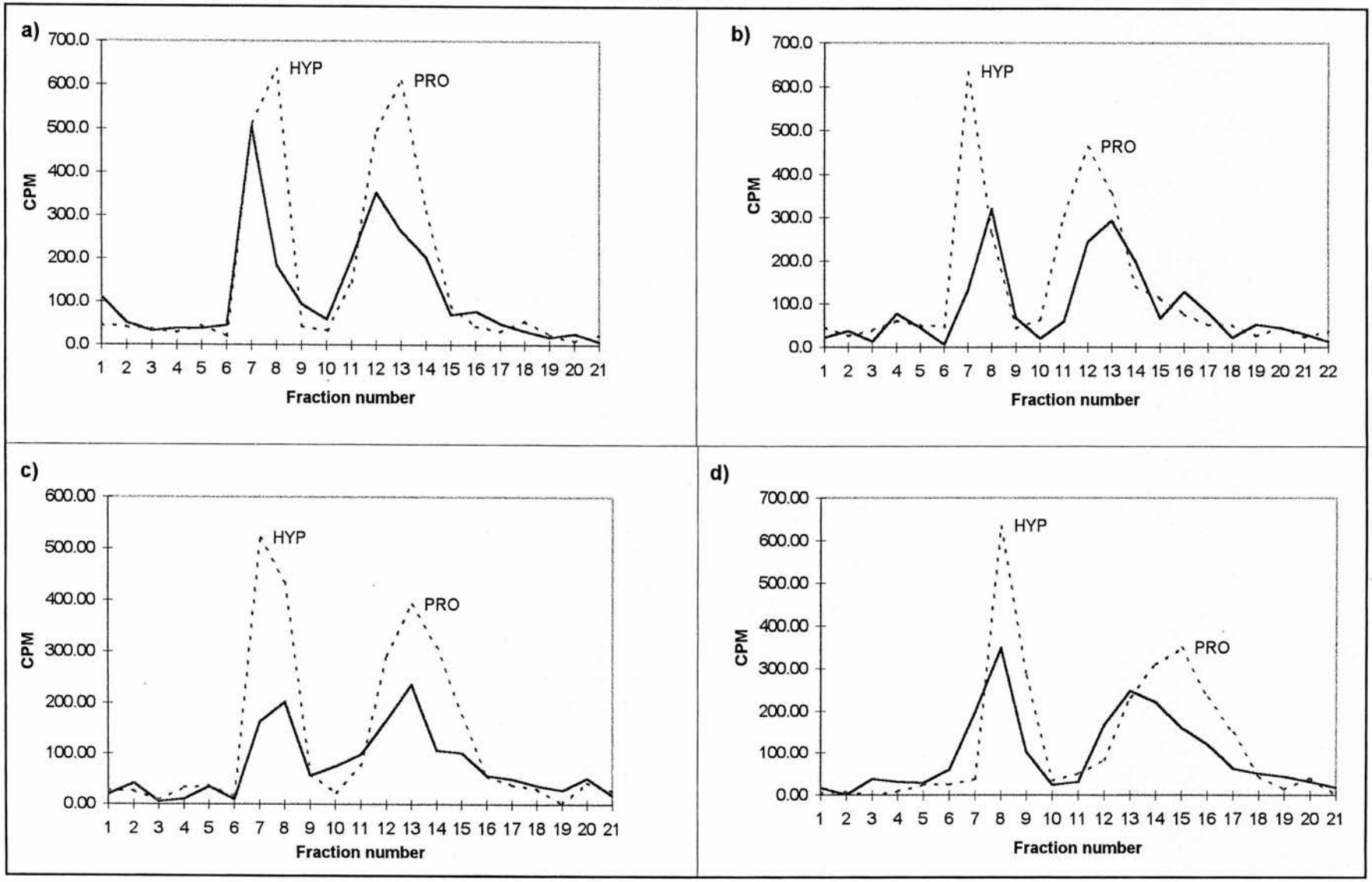
a)
700.0
600.0
500.0
400.0
300.0
200.0
100.0
0.0
CPM
HYP
PRO
1 2 3 4 5 6 7 8 9 10 11 12 13 14 15 16 17 18 19 20 21
Fraction number
b)
700.0
600.0
500.0
400.0
300.0
200.0
100.0
0.0
CPM
HYP
PRO
1 2 3 4 5 6 7 8 9 10 11 12 13 14 15 16 17 18 19 20 21 22
Fraction number
c)
600.00
500.00
400.00
300.00
200.00
100.00
0.00
CPM
HYP
PRO
1 2 3 4 5 6 7 8 9 10 11 12 13 14 15 16 17 18 19 20 21
Fraction number
d)
700.00
600.00
500.00
400.00
300.00
200.00
100.00
0.00
CPM
HYP
PRO
1 2 3 4 5 6 7 8 9 10 11 12 13 14 15 16 17 18 19 20 21
Fraction number

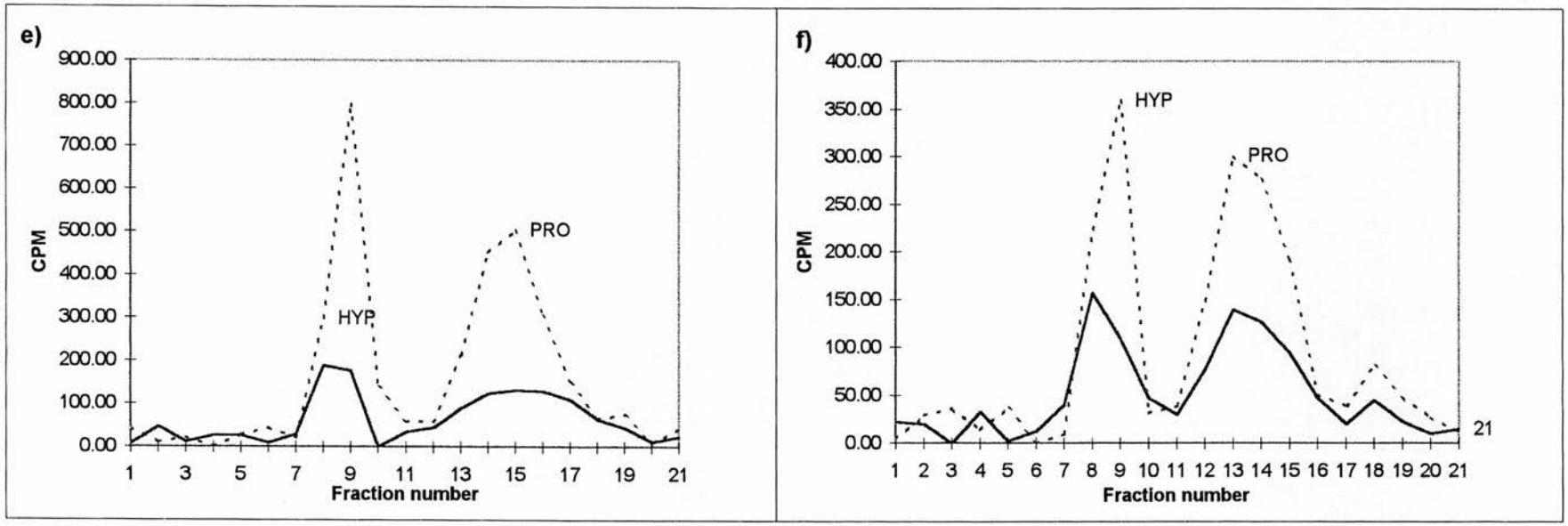

Figure 5.2. hydroxyproline and proline from nonmineralized and mineralized portions of tendons a) to f) separated on Dowex mini-columns. The broken line is from the mineralized portion and the full line is from the nonmineralized portion of each tendon

Table 5.1 shows the ^{3}H CPM values for the hydroxyproline and proline in the nonmineralized portion and mineralized portion of each tendon. The calculated ratios between hydroxyproline and proline the nonmineralized portion and the mineralized portion are 0.680 ± 0.08 and 0.792 ± 0.06, respectively. The ratio between hydroxyproline and proline for bovine type I collagen is 0.875 which suggests that it is not only collagen turning over in the tendon but some noncollagenous proteins also.

	Nonmineralized			Mineralized		
Tendon	CPM Hyp	CPM Pro	Hyp:Pro	CPM Hyp	CPM Pro	Hyp:Pro
a	692.5	1024.9	0.675	1148.9	1564.2	0.734
b	455.7	737.8	0.617	897.1	1125.6	0.797
c	368.22	612.4	0.601	954.9	1173.5	0.810
d	653.2	921.8	0.708	917.5	1124.4	0.816
e	365.6	495.0	0.739	1236.4	1476.7	0.837
f	266.3	360.8	0.738	583.3	770.5	0.758

Table 5.1. Comparison of the ratios of CPM for ^{3}H-hydroxyproline to the CPM for ^{3}H-proline for the nonmineralized and mineralized portions of each tendon showed in Figure 5.2.

5.3 Crosslink Analysis of ^{3}H-Proline Labelled Turkey Leg Tendon.

Another tendon from the ^{3}H-proline labelled turkey was reduced with KBH_4 and sectioned into mineralized portion and nonmineralized portion. Samples were also

taken of the nonmineralized portion and mineralized portion directly either side of the edge of mineralization (Figure 5.4).

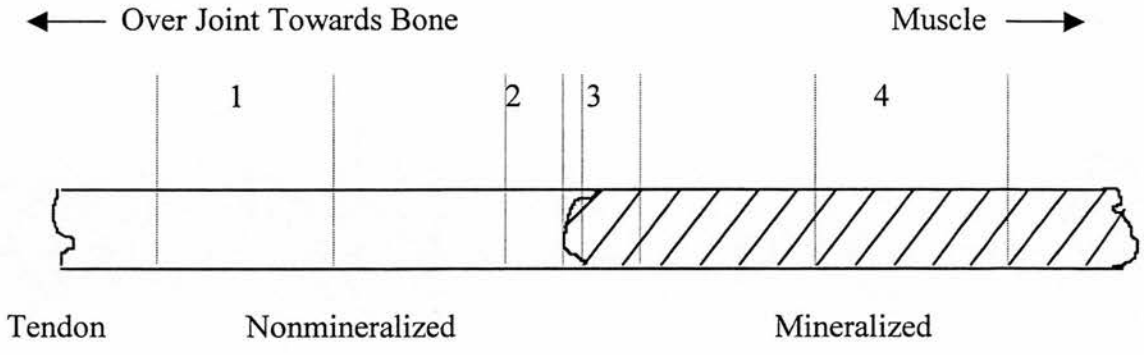

Figure 5.4. Illustration of the sampling of the turkey leg tendon for analysis.

1, Nonmineralized portion

2, Nonmineralized portion at the edge of mineralization

3, Mineralized portion at the edge of mineralization

4, Mineralized portion.

Sample	Pyd (res/mol)	Dpd (res/mol)
Nonmin	0.551	0.0069
Nonmin at edge	0.342	0.0033
Min at edge	0.413	0.1152
Min	0.320	0.1712

Table 5.2. Table showing the crosslink results for a reduced, ^{3}H-proline labelled turkey leg tendon.

The pyridinium crosslink analyses crosslink results for this tendon (Table 5.2) showed similar patterns to other tendons investigated in chapter 3. In the mineralized portion of the tendon, at the edge or in the middle, there are appreciable levels of deoxypyridinoline (Dpd) and in the nonmineralized portions, at the edge or in the middle, there was negligible Dpd. These results imply that there is no change in the normal collagen packing brought about by the labelling of the collagen. The reducible crosslink concentrations were not determined as there was insufficient material for analyses.

5.4 Discussion

From the results of crosslink analyses and a scan of the edge of mineralization using X-ray diffraction it can be seen that the changes that occur in the crosslinking profile cannot be detected with age or at the edge of mineralization, only with the mineral itself. This implied that the mineral was causing the change in collagen packing. Studies carried out on the telopeptide organisation, however, detected no changes in the telopeptide axial length between the mineralized and nonmineralized tendon samples. This indicated that the observed change in the crosslinking pattern with mineralization cannot be a consequence of distortion of the collagen with mineralization so that existing crosslinks are broken and new crosslinks formed. The aim of the present experiment was to determine whether the collagen in the mineralizing portion of the turkey leg tendon turns over at a great enough rate to account for the changes in crosslink profile. If this were the case it would imply that newly synthesized collagen is being produced to account for these changes as suggested previously (Yamauchi & Katz, 1993).

The results from this experiment showed that for aliquots containing 4μmoles of hydroxyproline, the levels of ^{3}H-hydroxyproline and ^{3}H-proline in the mineralized portion were greater than those found in the nonmineralized portions of the same tendons (n=6). The ratios of ^{3}H-hydroxyproline to ^{3}H-proline for each portion were 0.680 ± 0.08 for the nonmineralized portion and 0.792 ± 0.06 for the mineralized portion. Both these ratios differ from the ratio of hydroxyproline to proline for bovine type I collagen (0.875) suggesting other, noncollagenous proteins are being produced with the collagen. The difference in the Hyp:Pro ratios between the nonmineralized and mineralized portions also suggest that different noncollagenous components or different quantities of a noncollagenous component are turning over besides the collagen in the nonmineralized portion compared to the mineralized portion. This may suggest that the noncollagenous proteins being produced are involved in mineralization. There appears to be a greater production of noncollagenous proteins in the nonmineralized portion of the tendon. It could be hypothesized that perhaps these proteins inhibit mineralization, although there is no direct evidence for this.

The results from this experiment can be interpreted in two ways: A higher level of ^{3}H-hydroxyproline and ^{3}H-proline present in the mineralized portions suggests that more collagen was being produced in this portion at 12 to 14 weeks than in the nonmineralized portion. However if the tissue turned over rapidly enough the label would be lost again. Therefore either;

1) More collagen is being produced in the mineralized portion of the tendon accounting for the higher levels of incorporation ^{3}H label, or

2) The turnover of the collagen is greater in the nonmineralized portion as the level of ^{3}H label has been incorporated and lost again.

The reason for using a relatively short labelling time (2 weeks) was to ensure that little of the labelled collagen was degraded again; therefore it is unlikely that the nonmineralized collagen turns over rapidly enough to lose the ^{3}H label. A recently published paper also supports this assumption. The levels of MMP-2, an enzyme that degrades collagen, were measured in 11, 14 and 22-week-old turkey leg tendons. The investigators studied nonmineralized tendon (distal) and tendon as yet unmineralized in 11 and 14 weeks but mineralized in 22 weeks (proximal). The levels of active MMP-2 in the proximal area increases from 11 to 14 weeks and decreases slightly in 22 week old mineralized section (Knott *et al.*, 1997). These higher levels of MMP-2 in the mineralizing portion at 14 weeks are consistent with the hypothesis that existing collagen is degraded and newly synthesized is produced. There is no direct evidence for the newly synthesized collagen having lower levels of lysine hydroxylation than the existing collagen although there is no evidence to discount this theory.

From the concentrations of ^{3}H hydroxyproline and ^{3}H proline in the nonmineralized and mineralized portions the apparent differences in the production of collagen between these portions do not appear to be great enough to account for the changes in crosslinking profiles. It must be remembered, however, that the mineral in these portions at this early age is not throughout the whole cross section of the tissue. If the higher production of collagen is only associated with the small amount of mineral then the collagen in the rest of the section will have the nonmineralized crosslink profile. Therefore the levels of production could be sufficient to support the hypothesis that collagen of a different lysine hydroxylation state is being produced to account for the changes in crosslinking profile.

In summary, these data lend weight to the hypothesis that more collagen is being produced in mineralizing tissues with a resorption of the existing collagen. Whether the collagen has a different level of lysine hydroxylation cannot be determined from these data. Although the new collagen being synthesized in this portion appears to be too little to contribute to structural modifications, it may only be associated with the actual mineral present in the whole section, which would be very little. Therefore this mechanism could represent the major process by which mineralization occurs. Further experiments on different ages of birds should be carried out to test this hypothesis. The results of incorporation experiments with ^{14}C-lysine are presented in Chapter 6. This experiment was designed to determine the lysine hydroxylation state of newly synthesized collagen produced during mineralization and the existing collagen present before mineralization.

Chapter 6

Investigation of Lysine Hydroxylation State *In Vitro*

6. Investigation into Lysine Hydroxylation *In Vitro.*

In order to investigate the hydroxylation of lysine residues in collagen with mineralization, an experiment was designed using foetal bovine bone cell culture which produces a sheet of mineral as opposed to discrete nodules of mineral (Whitson *et al.*, 1992). ^{14}C-lysine was used in a pulse chase experiment to label the collagen being produced in the cultures before being chased by the appropriate, unlabelled media after 48h or 24h depending upon the experiment. The full method used for this experiment is described in section 2.3. Three experiments were carried out, one to investigate lysine hydroxylation in existing collagen when mineralizing, one to investigate the lysine hydroxylation of the newly synthesized collagen being produced with mineralization and a time course experiment to determine when any changes in lysine hydroxylation occur.

6.1 The Foetal Bovine Bone Cell Culture.

The foetal bovine osteoblasts, after isolation, were initially plated out at the minimum seeding efficiency of 1 x 10^4 bone cells per 22 mm^2 coverslip as stated in Whitson *et al.*, 1992. Six days after initial seeding the cells were trypsinized and seeded at 300 cells mm^{-2}. On day 7 after the first passage, all the cells had reached confluence with multilayering and the cells that were to mineralize were transferred to mineralizing media (section 2.3.2.1). On day 9 after first passage the cells started to curl off the bottom of each well and by day 11 all the cells had formed a ball. All the cultures were maintained in active culture to the conclusion of the experiment at day 16 after first passage. Although mineralization could not be seen with the cells in this form

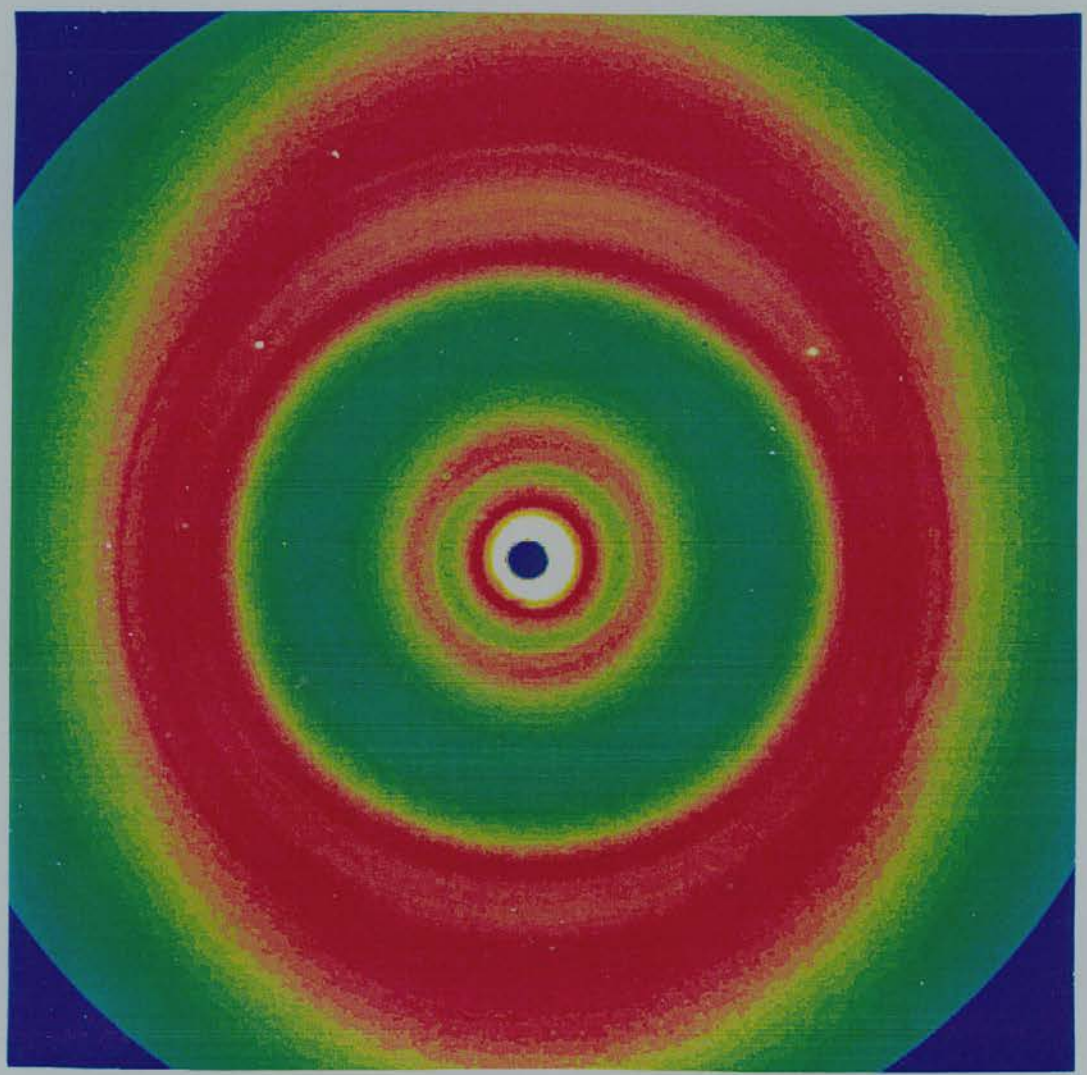

Figure 6.1. a) The X-ray diffraction pattern from one of the foetal bovine bone cell cultures used in these experiments. The cells and extracellular matrix were taken whole from their culture well into a sample cell, kept hydrated and placed in an X-ray beam.

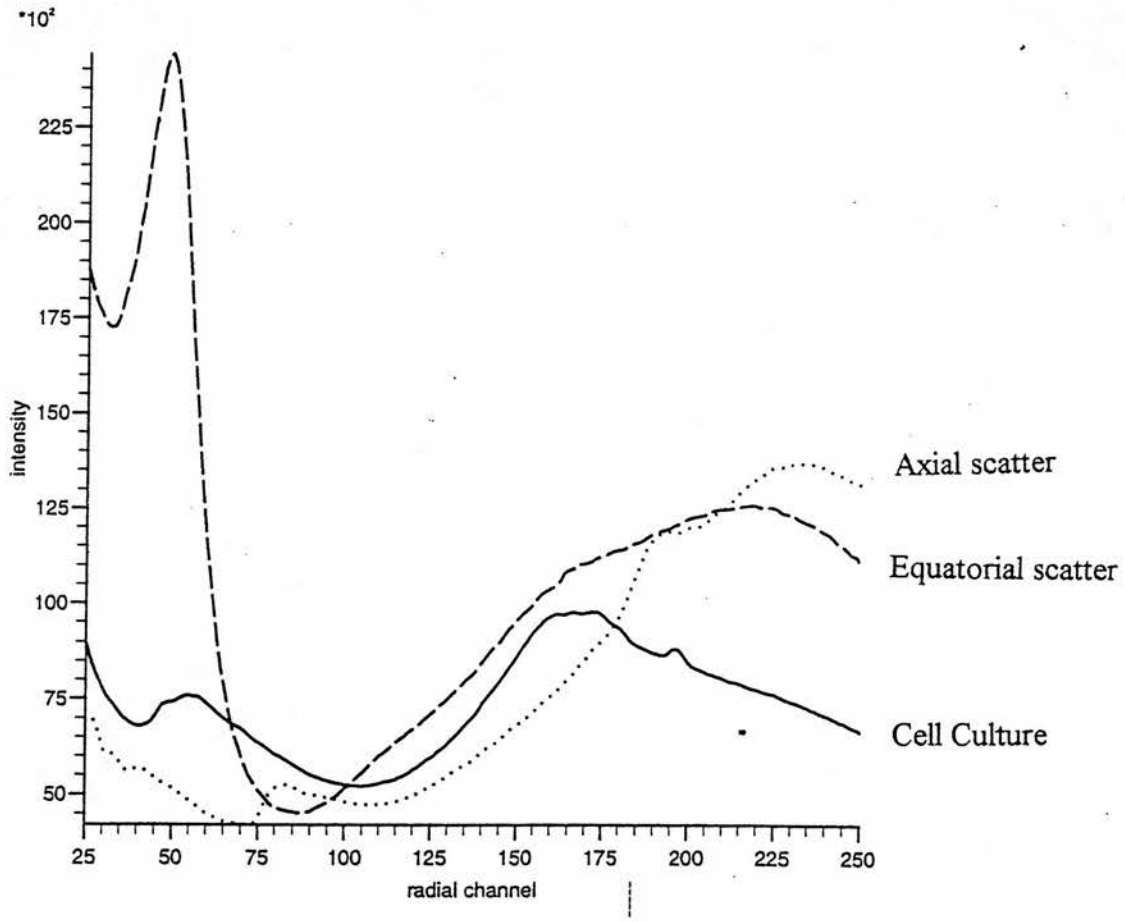

Figure 6.1. b) A plot showing the integrated scattering intensity from the cell culture compared to the equatorial and axial scatter from a 16-week-old nonmineralized turkey leg tendon.

Sample	Treatment
1	Cultures were labelled in GROWTH media and chased with unlabelled GROWTH media 48h later. GROWTH media was changed every 24h.
2	Cultures were labelled in GROWTH media and chased with unlabelled MIN media 48h later. MIN media was changed every 24h.
3	Cultures were labelled in MIN media and chased with unlabelled MIN media 48h later. MIN media was changed every 24h.
	Time Course (Day 1 starts after second seeding, all media changed every 24h and all cell cultures were reduced and hydrolysed on day 16)
4	Labelled in GROWTH on day 4, chased with unlabelled GROWTH after 24h on day 5 and transferred to MIN on day 6.
5	Labelled in GROWTH on day 5, chased with unlabelled MIN after 24h on day 6.
6	Labelled in MIN on day 6, chased with unlabelled MIN after 24h on day 7.
7	Labelled in MIN on day 7, chased with unlabelled MIN after 24h on day 8.
8	Labelled in MIN on day 8, chased with unlabelled MIN after 24h on day 9.
9	Labelled in MIN on day 9, chased with unlabelled MIN after 24h on day 10
10	Labelled in MIN on day 10, chased with unlabelled MIN after 24h on day 11.
11	Labelled in MIN on day 11, chased with unlabelled MIN after 24h on day 12.
12	Labelled in MIN on day 12, chased with unlabelled MIN after 24h on day 13.
13	Labelled in MIN on day 13, chased with unlabelled MIN after 24h on day 14.
14	Labelled in MIN on day 14, chased with unlabelled MIN after 24h on day 15.
15	Labelled in MIN on day 15, chased with unlabelled MIN after 24h on day 16.

Table 6.1. Table summarising each treatment for samples 1-15.

some of the non-labelled test cultures were used for X-ray diffraction analysis (Figure 6.1). Although the characteristic diffraction rings for hydroxyapatite are not present there is some order present in the culture due to the collagen. The characteristic diffraction produced by aligned fibrils of collagen cannot be seen.

The small size of the cultures meant that the duplicate cultures had to be combined for analysis. Table 6.1 summarises the treatments of the samples that were analysed, for a more detailed diagram see Figure 2.2. After culturing each of these samples was reduced and hydrolysed as described in section 2.3.2.5.

6.2 Hydroxyproline Analysis

As previously stated in section 2.4.2.1, a different method of hydroxyproline analysis was performed to minimise the amount of sample needed. This RP-HPLC method can detect pmoles of hydroxyproline compared to a detection limit of several nmoles for the colorimetric method. Table 6.2 shows the results from the hydroxyproline analysis and the collagen content of each sample. These results confirm that collagen has been produced by the cells in all the cell cultures.

Sample	Hyp (pmoles)	Collagen (pmoles)
1	344	1.2
2	12890	43.0
3	50436	168.1
4	24091	80.3
5	18682	62.3
6	15632	52.1
7	15676	52.3
8	14942	49.8
9	17823	59.4
10	17033	56.8
11	13190	44.0
12	28267	94.2
13	18937	63.1
14	13722	45.8
15	26190	87.3

Table 6.2. Table showing the hydroxyproline and the collagen content for each sample.

6.3. Separation of Collagen Crosslinks.

Each sample hydrolysate was subjected to a cleanup step on P11 mini-columns to remove mainly acidic and neutral amino acids prior to the separation as described in section 2.1.2.4.A. The resulting eluate was dried. The separation of the crosslinks was carried out using a cation exchange column as described in section 2.4.2.2. B. Standards of Pyd and Dpd, ^{3}H-DHLNL and ^{3}H-HLNL were run on the column. Pyd and Dpd eluted at 45-60 minutes, ^{3}H-DHLNL eluted at 90-105 minutes and ^{3}H-HLNL eluted at 140-155 minutes at 0.6ml min^{-1} flow rate.

6.3.1. Results for Non-Mineralizing Cells.

Figure 6.2 shows the results for sample 1, the cells labelled and maintained in growth media. A significant quantity of the ^{14}C CPM eluted in the positions of the Pyd and Dpd standards, but there was insufficient sample to confirm the identity of this material. There was also a peak eluting at the same time as HLNL standard together with another ^{14}C-labelled component eluting at 120-125 minutes, which does not correspond to any of the crosslink standards.

6.3.2. Results from Existing Collagen with Mineralization.

Figure 6.3 shows the ^{14}C-labelled crosslink separation for sample 2, cells labelled in growth media and transferred to mineralizing media. The early eluting peak at 45-65 minutes and the peak that elutes at the same position as HLNL standard are also present in this sample. Again there was no identifiable DHLNL peak but the unidentifiable peak eluting at 120-125 minutes that is seen in Figure 6.4 was also not

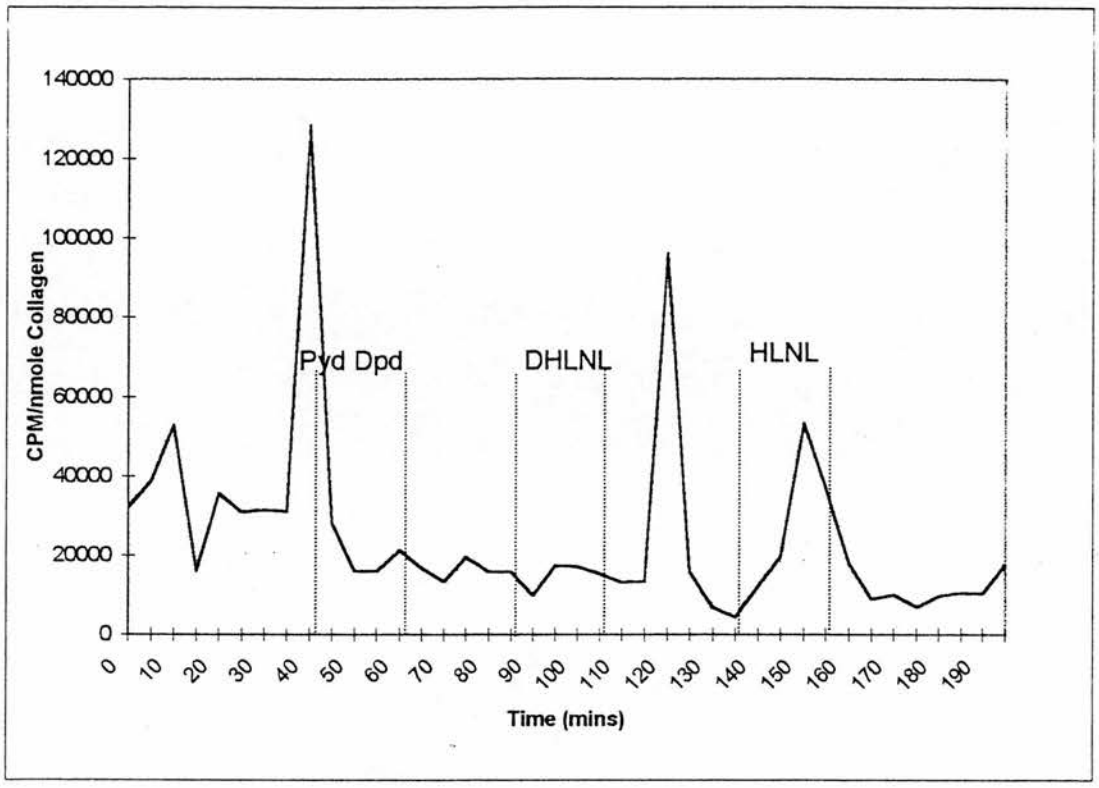

Figure 6.2. Separation of ^{14}C-labelled crosslinks from Sample 1, by ion-exchange chromatography. The positions of crosslink standards are indicated.

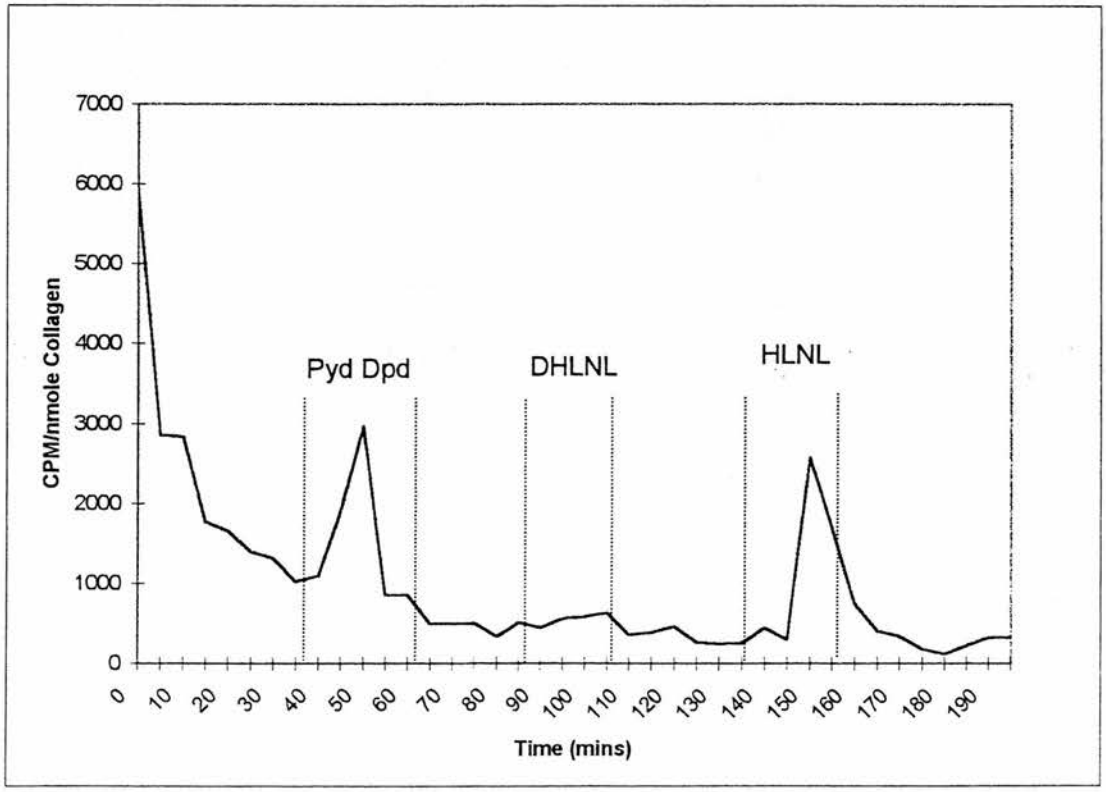

Figure 6.3. Separation of ^{14}C-labelled crosslinks from sample 2, by ion-exchange chromatography. The positions of crosslink standards are indicated.

present. The maximum CPM/nmole of the early eluting peak is less than that observed in sample 1 for the nonmineralizing collagen.

6.3.3. Results for Newly Synthesized Collagen with Mineralization.

Figure 6.4. shows the results of ^{14}C-crosslink separation for sample 3, cells labelled upon transferring to mineralizing media. The results from this separation are quite different from the previous two. A far higher level of ^{14}C-labelled lysine/nmole collagen has been incorporated. The majority of the ^{14}C-labelled component eluted at the same time as HLNL standard. The early eluting peak and a peak that elutes at the same position as DHLNL standard were also observed. HLNL is the proposed precursor of Dpd and could suggest that the newly synthesized collagen produced

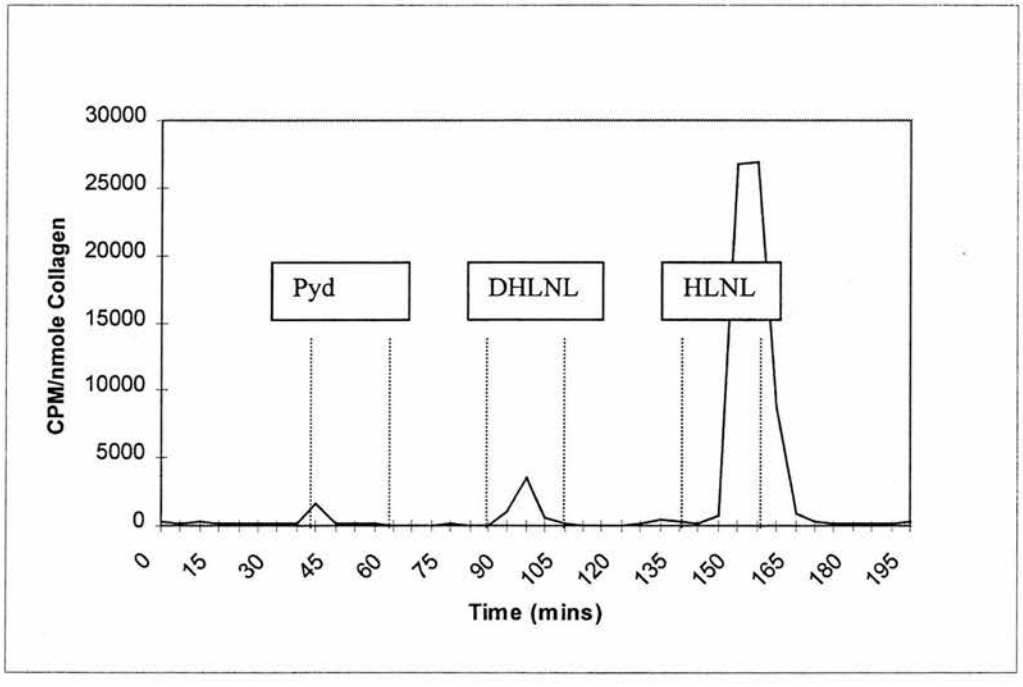

Figure 6.4. Separation of ^{14}C-labelled crosslinks from Sample3 by ion exchange chromatography. The positions of crosslink standards are indicated.

from mineralizing cells has a different hydroxylation state to the existing collagen or nonmineralizing collagen.

6.3.4. Time Course Experiment to Determine when the Changes in Crosslinking Occur.

A time course experiment was carried out from 3 days before mineralizing media was added to 13 days after as set out in Table 6.1. A culture was labelled for twenty-four hours every day. Figure 6.5. a) to l) shows the separations for each of the samples cultured for 16 days. It can be seen from these results that before mineralizing media is added there is very little of the peak eluting at the same time as HLNL standards. In the 24 hour period after mineralizing media is added there is a large increase in this peak, which remains high for the following 72 hours. After this time the level drops slightly but still remains far higher than that separated for the existing collagen labelled.

6.4. Validation of Labelled Components Separated on Ion Exchange.

In order to validate that the ^{14}C labelled components that elute at the same time as DHLNL and HLNL standards were DHLNL and HLNL, fractions containing these peaks were collected and pooled and then subjected to further analysis.

6.4.1 Reverse Phase HPLC Analysis of Dansylated Periodate Cleavage Products of the Pooled Fractions.

Periodate cleavage of HLNL from bone results in Proline and Hydroxynorvaline (HNV). Each pooled fraction was periodate cleaved and dansylated before running on

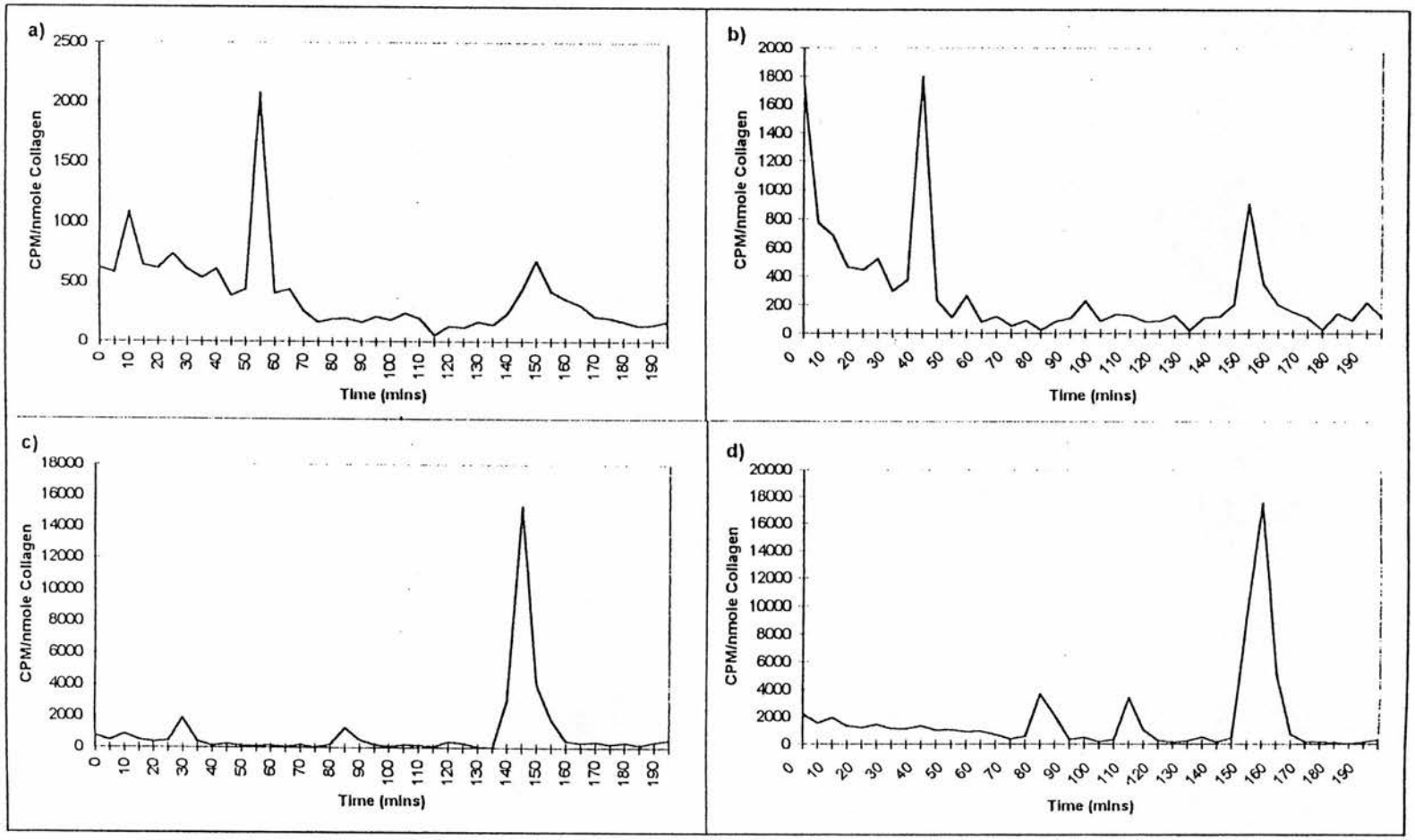
a)
CPM/nmole Collagen
Time (mins)
b)
CPM/nmole Collagen
Time (mins)
c)
CPM/nmole Collagen
Time (mins)
d)
CPM/nmole Collagen
Time (mins)

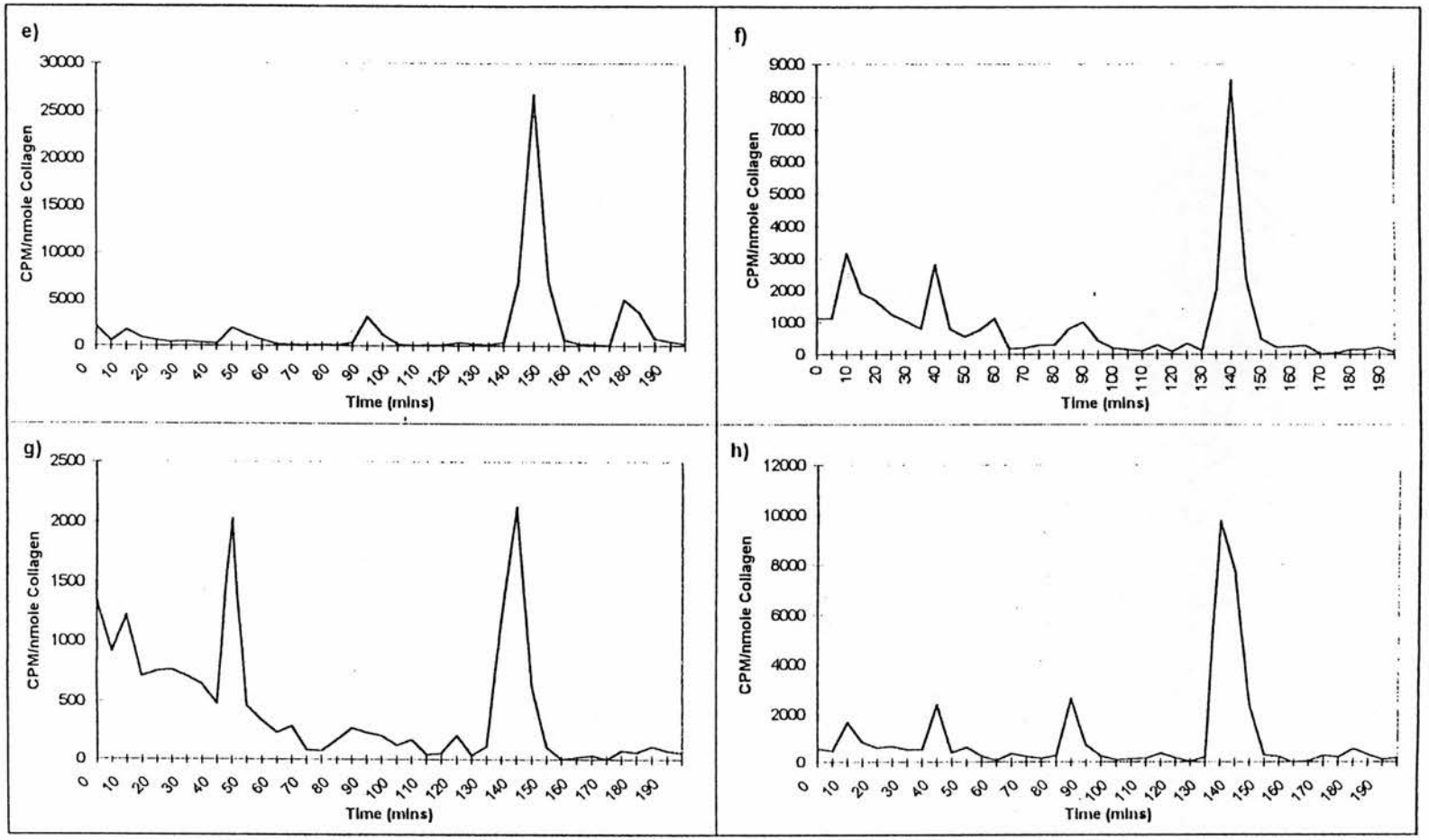
e)
CPM/nmole Collagen
Time (mins)
f)
CPM/nmole Collagen
Time (mins)
g)
CPM/nmole Collagen
Time (mins)
h)
CPM/nmole Collagen
Time (mins)

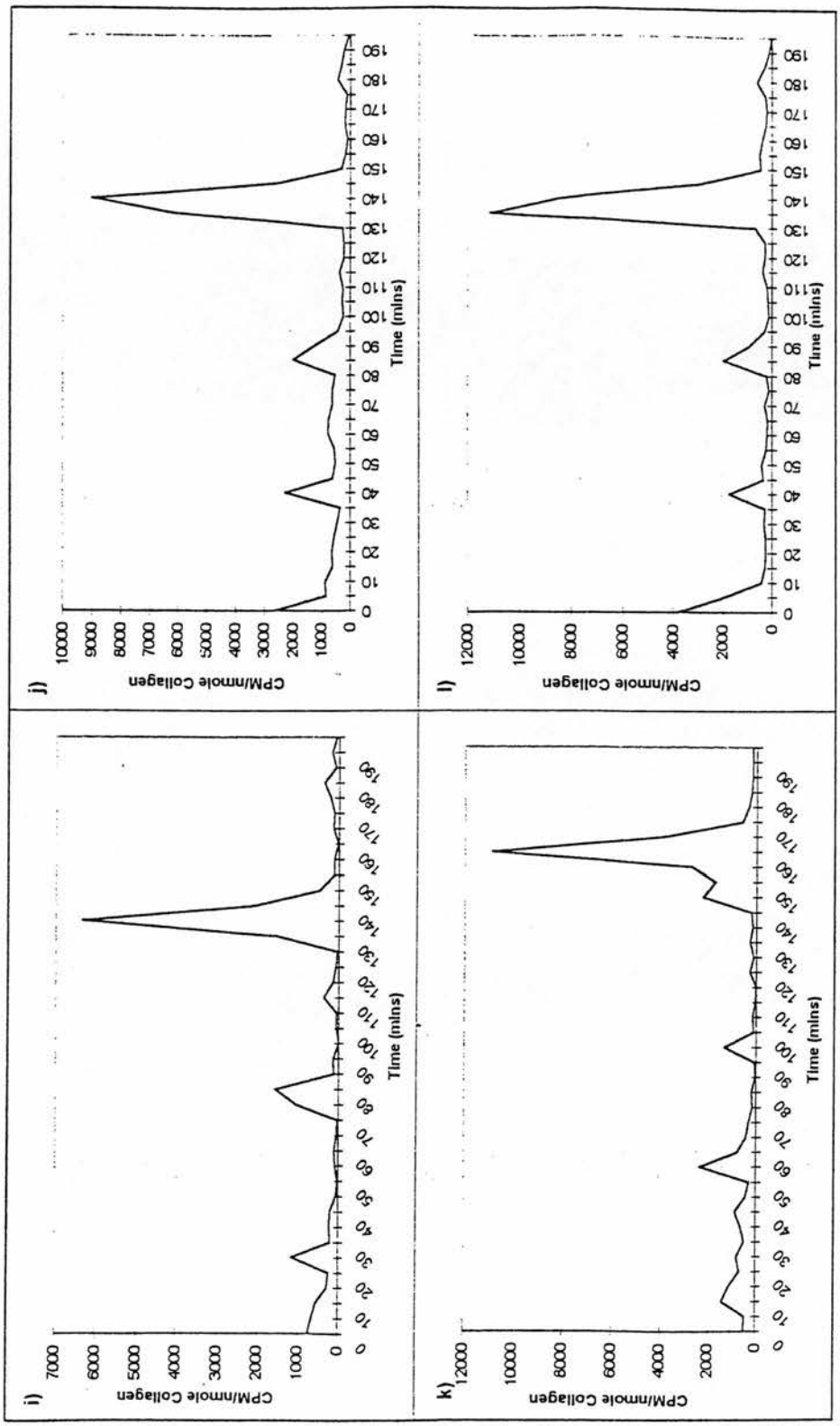

Figure 6.5. a) to l) show the separations of ^{3}H-Hydroxyproline and ^{3}H-Proline on Dowex Mini Columns for samples cultured for 16 days

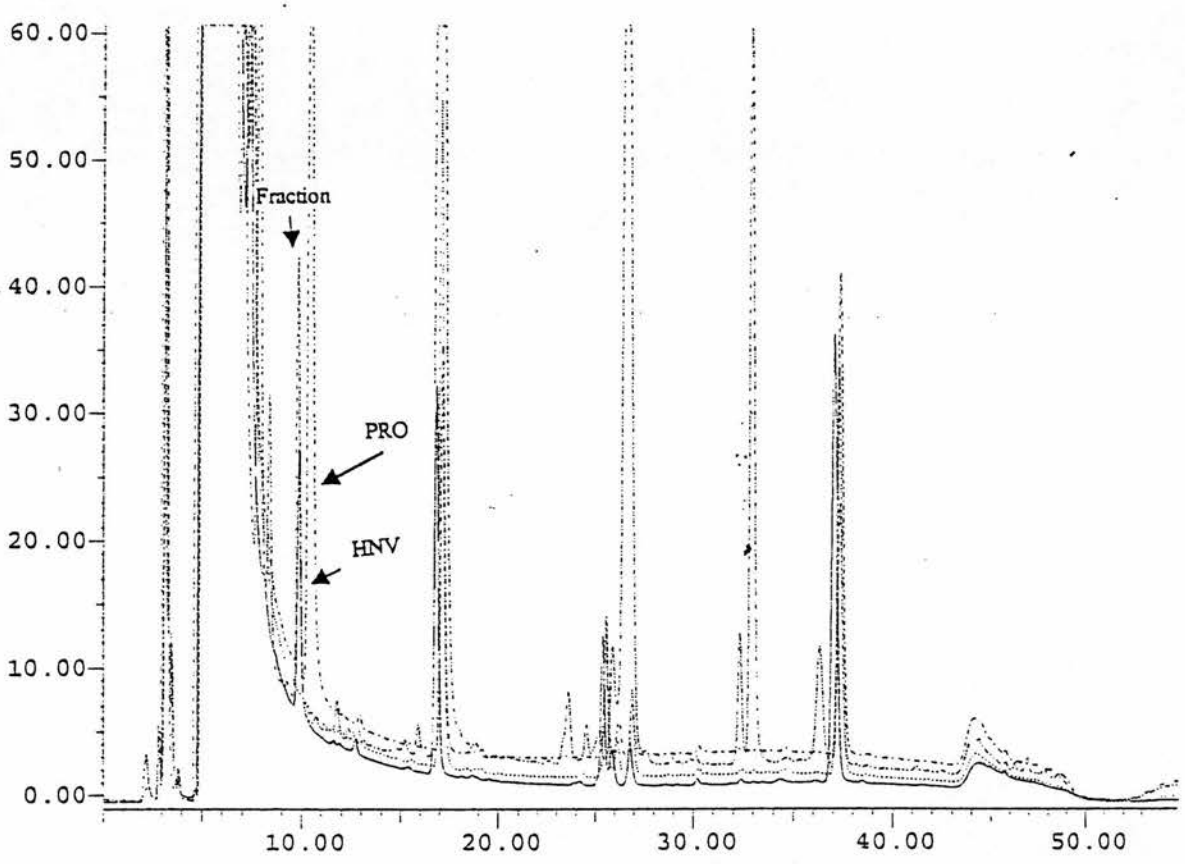

Figure 6.6. Overlaid chromatograms of dansylated Proline, HNV, a blank and the periodate cleaved pooled ^{14}C labelled fractions that elute at the same time as HLNL.

_____HNV

.....Blank

-.-.-.-. Proline

-..-..-.. Periodate Cleaved Fraction.

RP HPLC. Dansylated proline, HLNL and HNV were also run. Figure 6.6 shows overlaid chromatograms of all three standards and the periodate-cleaved fractions. The periodate-cleaved fractions correspond to HNV, although no proline was present, indicating that the fractions do not contain HLNL.

6.5. Discussion

From the all the previous experiments carried out in this study, evidence was found for both of the following hypotheses.

1) In agreement with Yamauchi and Katz, 1993, collagen produced with mineralization has a different lysine hydroxylation state accounting for the different crosslink profiles between mineralized and nonmineralized portions of turkey leg tendon.

2) Changes associated with mineralization are brought about by the mineral crystal itself. Mineral distorts the collagen, breaking reducible crosslinks back to their aldehyde precursors and allowing them to reform with other residues they would not normally be able to (Otsubo *et al.*, 1992).

The aim of this study was to investigate hydroxylation of lysine in mineralizing bone cell cultures. Three different experiments were carried out primarily: 1) Investigation into the hydroxylation of lysine in nonmineralizing collagen

2) Investigation into the hydroxylation of lysine in collagen present before mineralization and

3) Investigation into the hydroxylation of lysine in collagen newly synthesized during mineralization.

In all these experiments the CPM for each fraction was divided by the nmole collagen calculated for each sample in order to compare each sample. The results from these preliminary experiments showed interesting results. The labelled collagen in a nonmineralizing cell culture in experiment 1 had very high levels of CPM/nmole collagen. These levels were far higher than the levels of CPM/nmole collagen observed in experiments 2 and 3, labelling of collagen before addition of mineralizing media and after. In turn, the levels of CPM/nmole collagen in the labelling of collagen after the addition of mineralizing media were far higher than those found when labelling of collagen was carried out before the addition of mineralizing media. These results suggest that with the addition of mineralizing media there was a resorption of the existing collagen before production of newly synthesized collagen with a different lysine hydroxylation. Collagen produced before the addition of mineralizing media remained in the cell culture if no mineralizing media was added, as indicated by the high levels of ^{14}C-labelled collagen in experiment 1. If mineralizing media was added a resorption of the existing labelled collagen occurred resulting in a loss of label, as was seen in experiment 2. Labelling of the cultures after the addition of mineralizing media demonstrated that collagen was being produced but had a different distribution of ^{14}C-lysine to that seen in the nonmineralized collagen in experiment 1 and the existing collagen in experiment 2.

The main difference in the ^{14}C-Lysine distribution between collagen labelled in growth media and that labelled in mineralizing media was the large increase in a peak that elutes at the same time as HLNL standard. The fractions containing this peak were collected and subjected to Smith degradation periodate cleavage. The periodate cleavage products of HLNL (ketoamine form) are proline and hydroxynorvaline

(HNV). In bone it has been shown that 67% of HLNL is in the keto-form (Robins & Bailey, 1975). Analysis of periodate cleavage products showed that although HNV was present, no proline could be detected. It must be concluded from this that the peak that elutes at the same time as HLNL is not HLNL. In fact, from other analyses carried out no Pyd, Dpd or DHLNL could be detected in any of the cell culture hydrolysates. None of the peaks present in the ion-exchange of the cell culture analyses that elute with the crosslink standards was identified in this study. Although it cannot be concluded that newly synthesized collagen with mineralization has less lysine hydroxylation to account for the changes in the crosslink profile associated with mineralization, the results of these experiments do show that there is difference in the ^{14}C label distribution between the nonmineralized and mineralized collagen. A time course experiment was carried out to determine when the collagen with a different distribution of ^{14}C-Lysine is synthesized in relation to mineralization. From the results of this experiment it can be seen that as soon as mineralizing media was added to the cultures, changes in the distribution of ^{14}C-Lysine with mineralization were seen. After 72 hours it appears that the levels of incorporation of ^{14}C-Lysine decrease. This indicates that there was an increased production of collagen with a different ^{14}C-Lysine distribution for the first 72 hours after the mineralizing media was added and then the rate of production decreases after this time. From X-ray diffraction analysis of one of the cultures it was seen that there was no hydroxyapatite present in the cultures. This time course experiment shows that the changes occurring in the newly synthesized collagen are not dependent on the presence of hydroxyapatite. It can be hypothesized that they are perhaps brought about by the

presence of a component of the mineralizing media such as ascorbic acid (50μg/ml), β-glycerol phosphate (10mM), insulin (5μg), transferrin (5μg) or selenium (5ng/ml). All the results from this experiment support the hypothesis that a collagen of a different hydroxylation state is synthesized with mineralization. This experiment did not provide direct evidence of decreased levels of lysine hydroxylation in the newly synthesized collagen. It does, however, provide evidence that confirms the results obtained in Chapter 5; there is a corresponding resorption of the nonmineralized collagen with a high level of production of collagen with a different ^{14}C-Lysine distribution associated with mineralization. Although there is evidence to suggest that in bone the growing mineral crystal breaks reducible crosslinks into their aldehyde precursors (Otsubo *et al.*, 1992), the change in the ^{14}C-Lysine distribution happened in the newly synthesized collagen in the first 24 hours after mineralizing media was added. This implies that it is the media itself that triggers the change and not the mineral crystal.

Chapter 7

Discussion

7.0 Discussion.

The packing of collagen type I molecules in mineralized tissues is different to those found in nonmineralized tissues. Many studies have been carried out to investigate the structures in these two environments, with turkey leg tendon being used as a model system in which to study both nonmineralized and mineralized tissue. A study was performed on the crosslink profiles of turkey leg tendon. It was found that in the nonmineralized portion of the tendon the predominant mature crosslink was Pyridinoline (Pyd), the levels of Deoxypyridinoline (Dpd) were negligible. In the mineralized portion of the tendon, however, significant levels of Dpd are present. The molecular loci of Pyd in nonmineralized collagen and Dpd in the mineralized collagen were found to be identical. As the precursors of both these crosslinks are different, the authors tentatively concluded that the post-translational chemistry and molecular environments of the fibrils are different in these two portions of turkey leg tendon (Yamauchi & Katz, 1993). This result implies that with mineralization, there is resorption of existing collagen and the newly synthesized collagen produced has a different lysine hydroxylation state.

In studies carried out on the crosslinking in the COOH-terminus in bovine bone, however, it was seen that with mineralization some of the reducible crosslinks matured but some dissociated back to their precursor form (allysine and hydroxyallysine) (Otsubo *et al.*, 1992). This work suggests that the crosslink changes observed in mineralized tissue are brought about as a consequence of the mineral crystal itself, distorting the collagen packing, breaking existing crosslinks and reforming different crosslinks.

The aim of the present study was to further investigate the changes in the collagen packing in nonmineralized and mineralized tissues and to resolve whether the change in the collagen crosslink profile occurs before mineralization as suggested by Yamauchi and Katz, 1993 or whether they are a due to the mineralization process itself (Otsubo *et al.*, 1992).

To achieve this, crosslink analysis and X-ray diffraction were used to investigate changes in collagen packing in different ages of turkey leg tendon and at the edge of mineralization. X-ray diffraction was also used to study the changes in mineral crystallite size with different ages of turkey leg tendon and the organisation of the telopeptide in nonmineralized and demineralized tissue.

Other experiments were designed to investigate the turnover of collagen *in vivo* in nonmineralized and mineralized turkey leg tendon by incorporating ^{3}H proline into the collagen of actively mineralizing tendon.

An *in vitro* model system was also used in this study. An experiment was designed to investigate the lysine hydroxylation state in nonmineralized and mineralizing foetal bovine bone cell culture by incorporating ^{14}C Lysine into the collagen.

The first study conducted used crosslink analysis to investigate the crosslinking profiles in turkey leg tendon. The previous study by Yamauchi & Katz, (1993) only used fully mineralized tendon of 54 weeks of age and the mineralized portions of the tissue analysed had been demineralized with 0.5M EDTA. It was decided that to investigate the crosslinking profile in turkey leg tendon it should be done on different ages of tissue and particular attention to the edge of mineralization should be paid. This was done to investigate the hypothesis that a collagen with a different lysine hydroxylation state is being produced with mineralization. It was assumed that the

newly synthesized collagen would be laid down before mineralization so at the edge of mineralization in actively mineralizing tissue there may be collagen of a different crosslinking pattern that is not mineralized. The results for all the crosslinking studies carried out in this study showed that although there was evidence for both hypotheses no changes in the crosslinking profile could be detected except those associated with mineralization.

Several problems in detection limits determined the smallest size of tissue analysed. The levels of Pyd and Dpd could be measured in all the small sections used in this study, however, the levels of reducible crosslinks were unable to be measured in the smaller, more detailed sectioning and the method of detection used proved not to be robust. An attempt was made to develop a more sensitive method of detection for the reducible crosslinks involving derivatization with a fluorescent compound, dansyl chloride. Limited progress was made as the detection sensitivity was increased but DHLNL eluted from a reversed phase HPLC column at the same time as lysine. Future work in this field should develop successful, robust, sensitive methods of detection for the reducible crosslinks to enable a full and reliable study of the reducible crosslinks in turkey leg tendon with age.

In the present study analysing the crosslinks of mineralizing turkey leg tendon, the mature pyrrolic crosslink concentrations were not measured. This was due to the inherent difficulties in isolating the crosslink as it is modified under acid hydrolysis. The pyrrole crosslink has been shown to be associated with mineralized tissues and a study conducted on osteoporotic avian bone showed that an increase in lysyl hydroxylation resulted in a decrease in the pyrrole content of the bone (Knott *et al.*, 1995). Analysis of the pyrrole crosslink, in a simialr manner to that which has been

conducted in the present study, would be useful to gain an insight inot the changes in the levels of crosslink with mineralization.

It should be noted that all the mineralized sections of tendon used in this study were native, not demineralized. It had been reported that the levels of allysine and hydroxyallysine increase in mineralized tendon and in bone (Otsubo *et al.*, 1992). It has subsequently been suggested that the rise in the levels of these free aldehydes is artifactual, due to the treatment of the tissue with EDTA (Knott *et al.*, 1997). This was avoided in the present study and proved to be of assistance in the analysis of small sections of tissue at the edge of mineralization. The levels of calcium easily enabled the identification of 1mm x 1mm sections of nonmineralized tissue at the edge of mineralization and ensured that no mineralized tissue had been included in the fine sectioning.

Although there was evidence for both hypotheses derived from the reducible crosslink data, the overall data suggested that as no detectable changes in collagen crosslinking could be detected, except those associated with mineralization, the mineral itself is distorting the collagen packing, breaking crosslinks and forming new crosslinks. It was decided to investigate the thickness of the mineral crystallite in different ages of tendon. If not all of the mineral crystals in the young mineralized portions studied, are large enough to compress the collagen fibrils, many of the reducible crosslinks will not be broken therefore accounting for higher levels of DHLNL. As the tissue ages and the mineral crystals grow, DHLNL will be broken and HLNL and Dpd formed. X-ray diffraction was used to study the mineral crystallite thickness. The minimum thickness measured for the youngest tendon examined was 1.69 ± 0.22 nm at 12 weeks of age. The size of the "gap" in the gap region is approximately 1.5 nm (Veis & Sabsay, 1987). Even at 12 weeks of age the average mineral crystal thickness is

greater than the gap region suggesting that the collagen is compressed even at this early stage of mineralization. These results supported the hypothesis that the change in crosslink profile is a result of the mineral itself.

X-ray diffraction was another method used to study the collagen structure at the edge of mineralization. X-ray scans through the mineralized to the nonmineralized portions of the tendon were performed using a 200μm beam in 100μm steps and a 1.5μm beam in 10μm steps. Problems were encountered with the latter scan. This experiment was an attempt to study the edge of mineralization in the greatest detail that has ever been performed. Unfortunately the beam flux during the allotted experimental time was low which only produced poor images. Due to competition for beamtime at ESRF the experiment could not be repeated. Further work should include a comprehensive study of the edge of mineralization using this technology. The results from the 200μm scan showed that no detectable changes in the collagen structure could be detected and the thickness of the mineral crystals through the mineralized portion did not change. These results support the crosslink analyses of the different ages of tendon and lend evidence to the hypothesis that the mineral itself is responsible for the change in the crosslinking profile.

X-ray analysis was also the tool used to study any changes in the telopeptides of the collagen molecules in mineralized and nonmineralized tendons and their organisation within these tissues. It was decided to investigate the telopeptides in both the mineralized and nonmineralized tissues, as any changes in the position of the telopeptide between the two environments would be apparent from the intensities of the axial meridional reflections of the collagen. If, as suggested from the crosslink analysis and x-ray diffraction analysis, the change in crosslink profile is due to the mineral distorting the collagen molecules, breaking existing crosslinks and forming

other crosslinks, there would be a difference between the telopeptide organisation in nonmineralized and mineralized tissues. The results from this study showed that there was no difference in the telopeptide organisation between mineralized and nonmineralized collagen. This evidence was the first in this study to suggest that the mineral did not distort the collagen, breaking crosslinks, but in fact collagen of a different lysine hydroxylation state was being produced with mineralization. Further modelling of the telopeptides was performed using the observed axial intensities for the mineralized and nonmineralized tendons. The modelling results suggested that the C-terminal telopeptide in both environments is 70% of it's original length. This was in agreement with a crosslink between Lys 16C and Hyl 87 (Yamauchi & Katz, 1993). The $\propto$1(I) N-terminal telopeptide in both environments is calculated to being 50% of it's original length. At this length there are no available sites for crosslinking. Present data support previous studies that have reported a lack of crosslinks at the N-terminus of mineralized tissues (Yamauchi *et al.*, 1989; Otsubo *et al.*, 1992 & Yamauchi *et al.*, 1992). Other studies conducted on bone, however, have located crosslinks at the N-terminal end. 85% of pyrrole and 66% of dpd have been reported to be concentrated at the N-terminal end in human bone (Hanson & Eyre, 1996). The results from the present study do not support this finding.

Due to the telopeptide results further experiments were designed to test the hypothesis. It was assumed that if newly synthesized collagen is being produced with mineralization then there is also a resorption of the nonmineralized collagen. ^{3}H Proline was used in an incorporation experiment using a 12-week-old female turkey. The levels of ^{3}H proline and ^{3}H hydroxyproline were measured in the nonmineralized and mineralized portions of the same tendons to indicate the relative levels of collagen production. The results of this study showed that the levels of both the ^{3}H

proline and ^{3}H hydroxyproline are higher in the mineralized portions of the tendons. This implies that more collagen is being produced in the mineralized portion of the tendon than in the nonmineralized portion. The ratios of ^{3}H hydroxyproline to ^{3}H proline in the portions are different to each other and to that of bovine type I collagen. This implies that it is not only collagen that is being produced but also noncollagenous proteins. The levels and possibly the types of these noncollagenous proteins are different in each portion.

No progressive change in the levels of ^{3}H hydroxyproline and ^{3}H proline were observed along the length of the mineralizing tendon. This would be expected if the rate of turnover was indicative of increased synthesis of a new type of matrix for mineralization. The increase in ^{3}H CPM in the tendon correlated with the increase in calcium levels. This evidence alone suggests that the observed increase in the rate of collagen production is as a consequence of mineralization.

The present results are in agreement with other published data where the levels of MMP-2, an enzyme that degrades collagen, were measured. In young, mineralizing tendon there were increased levels of this enzyme (Knott *et al.*, 1997). This is consistent with the hypothesis that existing collagen is degraded and newly synthesized collagen is produced.

From the present data there is no direct evidence to support the hypothesis that the newly synthesized collagen has a different lysine hydroxylation state, however it does not discount the theory either. Although the difference in the ^{3}H hydroxyproline and the ^{3}H proline in the mineralized portions does not appear to be great enough to account for the changes observed in the crosslink profile, it must be remembered that the mineral in these portions at this early age (12-14 weeks) is not throughout the whole cross section of the tissue. If the higher production of collagen is only

associated with the small amount of mineral (as seen previously in this study) then the collagen in the rest of the section will have the nonmineralized crosslink profile presumably the same collagen production level as the nonmineralized tissue. Although the number of tendons analysed in this experiment was 6, they all originated from the same turkey. Lack of time prevented this experiment being carried out in another bird. Further work could investigate the levels of collagen production in the mineralized and nonmineralized portions of different ages of birds, both younger and older and finer sectioning of the tissue would help clarify whether the changes observed are determined pre- or post-mineralization.

The final experiment carried out in the present study was designed to investigate the levels of lysine hydroxylation in nonmineralized and mineralizing foetal bovine bone cell culture. The levels of incorporation from the results of the initial experiments showed that there was a resorption of the existing nonmineralized collagen with mineralization that did not take place unless the mineralizing media was added. There was also a high level of production of collagen with mineralization. These results also showed that newly synthesized collagen with mineralizing media had a very high increase in a labelled ^{14}C labelled component that eluted at the same time as HLNL standards, compared to the collagen already present in mineralizing cell cultures and nonmineralizing cell cultures. On further analysis of the ^{14}C labelled peaks that elute with the crosslink standards it was shown that they did not contain the crosslinks. Periodate cleavage of the peak that eluted at the same time as HLNL standard yielded only one of the expected products, hydroxynorvaline. Due to the lack of time, further characterization and identification of these peaks was not possible. Further work should be undertaken to identify the ^{14}C-labelled peaks. Although it cannot be determined whether there is a decrease in the level of lysine hydroxylation in the

newly synthesized collagen it can be seen that there is a difference in the distribution of the ^{14}C-label in this collagen compared to that in collagen that was synthesized before mineralizing media.

It cannot be determined from this data alone that the mineral crystal definitely does not distort the collagen, breaking and reforming crosslinks. There appeared to be no mature crosslinks detectable in any of the cell cultures and no poorly, crystalline hydroxyapatite can be observed in the X-ray diffraction pattern of a cell culture. If no mineral crystals are present then the collagen cannot be distorted in this model system. Further work should be carried out repeating this experiment and ensuring hydroxyapatite is formed and the cultures are left for longer periods of time.

A time course experiment was carried out using this *in vitro* model system to investigate when the newly synthesized collagen with a different distribution of ^{14}C-lysine was being produced in relation to the mineralization. The results of this experiment showed that as soon as the mineralizing media was added to the cultures there was a large increase in the level of ^{14}C labelled peak that elutes at the same time as the HLNL standard. These results suggested the possibility that a constituent of the mineralizing media initiates the production of the collagen with a different ^{14}C lysine distribution. The constituents include ascorbic acid (50μg/ml), β-glycerol phosphate (10mM), insulin (5μg/ml) and selenium (5ng/ml). Ascorbic acid and β-glycerol phosphate are well known constituents of cell culture media for mineralizing cells. It has been shown that the presence of long acting ascorbate analogue Asc-2-P in cell culture media for animal bone-derived cells allows the formation and mineralization of nodules in the absence of β-glycerol phosphate (Beresford *et al.*, 1993).

Further work should concentrate on examining these constituents on the lysine hydroxylation state of newly produced collagen and the levels of lysyl oxidase and lysyl hydroxylase mRNA.

With the lack of ^{14}C-labelled crosslinks it cannot be concluded whether the resorption of the existing collagen and the apparent increase in collagen synthesis with mineralization is a product of this crosslink deficit. In studies carried out using chick osteoblasts it was seen that when an inhibitor of lysyl oxidase was included in the cultures there was a 2 fold increase in the amount of collagen accumulated and 80% loss of existing labelled collagen over 16 days (Gerstenfeld *et al.*, 1993). Although the increase in collagen synthesis and concomitant resorption of existing collagen can be attributed to the lack of crosslinks it must be remembered that there was a change in the distribution of the ^{14}C-lysine for the newly synthesized collagen and that there was an increase in the rate of collagen produced in the mineralized portion of turkey leg tendon.

In conclusion, two hypotheses concerning the change in crosslink profile observed in mineralized tissues compared to nonmineralized tissues were investigated in this study, the aim being to resolve which of the hypotheses was true. The results generated from the experiments carried out suggest an agreement with the hypothesis that collagen with a decreased level of lysine hydroxylation is produced with mineralization. The major points are:

1) The change in the crosslink profile in turkey leg tendon was only detected associated with mineralized collagen.

2) There was no difference in the organisation of telopeptides in mineralized and nonmineralized turkey leg tendon. The C-terminal telopeptide Lysine 16 crosslinked

to Hydroxylysine 87 regardless of the hydroxylation state of the telopeptide Lysine. The N-terminal telopeptide was not involved in crosslinking in either the mineralized or nonmineralized portions.

3) The level of collagen production in the mineralized portion was greater than that in the nonmineralized portion of a turkey leg tendon.

4) The distribution of ^{14}C-lysine was different in newly synthesized collagen during mineralization than in existing collagen present during mineralization in foetal bovine bone cell culture.

The next series of experiments that would have been carried out to further elucidate this hypothesis would have been:

1) To develop a more sensitive and robust method for detection of reducible crosslinks. Although no other changes in the mature crosslink levels were detected, except those associated with mineralization, the reducible crosslinks could not be investigated in the small sections used in this investigation. As reducible crosslinks are the precursors of mature crosslinks it is important to investigate the concentrations of these crosslinks to the same extent.
2) To analyse the concentrations of hydroxylysine, lysine, aldehyde precursors and Pyrrole in actively mineralizing tendons through to mature tendons. An insight into the lysine hydroxylation state of the telopeptide and helix with mineralization would be gained as well as a possible correlation between another mature crosslink, pyrrole and pyridinoline, deoxypyridinoline and mineralization.
3) Repeat the investigation into the edge of mineralization using the microfocus beam at ESRF, France. As this experiment was unsuccessful due to low beam

flux, a repeat of this would provide the most detailed study of the collagen and mineral crystallite that has ever been performed.

4) To investigate the cause of the decrease in mineral crystallite thickness in the tendons of older turkeys. A study of the thickness of the mineral in the bones of these birds compared to those of younger would indicate whether the decrease in crystallite size in the tendon is also observed in the bones. Analysis of hormone levels could determine whether the decrease in mineral thickness is as a result of a form of osteoporosis.
5) To further study the turnover of collagen in the tendons of differing ages of turkeys. A comparison of the levels of ^{3}H-proline incorporated in the tendon and the mineral content would show if there was a correlation between them. This would indicate a possible mechanism for mineralization. Analysis of enzymes responsible for resorption of collagen such as MMP would also prove useful.
6) Characterization of the ^{14}C-Lysine labelled components attained that eluted at the same times as reducible crosslink standards from the foetal bovine bone cell culture experiments. Identification of these components is essential.
7) To repeat the investigation into the lysine hydroxylation state of collagen *in vitro*. The levels of ^{14}C-hydroxylysine, and labelled aldehydes should also be measured for this experiment.

References

References

Arsenault, A.L. (1988) *Calcif. Tissue Int.* **43**, 202-212.

Aresenault, A.L. (1989) *Bone Miner.* **6**, 165-177.

Arsenault, A.L., Frankland, B.W. & Ottensmeyer, F.P. (1991) *Calcif. Tissue Int.* **48**, 46-55.

Ayad, S, Boot-Handford, R.P., Humphries, M.J., Kadler, K.E. & Shuttleworth, C.A. (1994) *The Extracellular Matrix Facts Book.*

Bailey, A.J. & Peach, C.M. (1968) *Biochem. Biophys. Res. Commun.* **33**, 812-819.

Batge, B., Winter, C., Notbohm, H., Acil, Y., Brinckmann, J & Muller, P.K. (1997) *J. Biochem.* **122**, 109-115

Bear, R.S. (1942) *J. Amer. Chem. Soc.* **64**, 727-729.

Bear, R.S. (1944) *J. Amer. Chem. Soc.* **66**, 1297-1301.

Bernstein, P.H. & Mechanic, G.L.(1980) *J. Biol. Chem.* **225**, 10414-10422.

Berthet-Colominas, C., Miller, A. & White, S.W. (1979) *J. Mol. Biol.* **134**, 431-445.

Betts, F., Trotta, R., Goldberg, m.R. & Posner, A.S. (1979) *Orthop. Trans.* **3**, 201-202.

Bianco, P., Silvestrini, G., Termine, J.D. & Bonucci, C. (1988) *Calcif. Tissue Int.* **43**, 155-161.

Bigi, A., Ripamonti, A., Koch, M.H.J., & Roveri, N. (1988) *Int. J. Biol. Macromol.* **10**, 282-286.

Bigi, A., Ripamonti, A., Cojazzi, G., Pizzuto, G., Roveri, N. & Koch, M.H.J., & (1991) *Int. J. Biol. Macromol.* **13**, 110-114.

Boskey, A.L., Wians Jr., F.H. & Hauschka, P.V. (1985) *Calcif. Tissue Int.* **37**, 57-62.

Boskey, A.L., Maresca, M., Ulrich, W., Doty, S.B., Butler, W.T. & Prince, C.W. (1993) *Bone Miner.* **22**, 147-159.

Boskey, A.L. (1994) *Ann. N.Y. Acad. Sci.*, 249-257.

Bruckner, P., Bachinger, H.P., Timpl, R. & Engel, J. (1978) *Eur. J. Biochem.* **90**, 595-603.

Brennan, M. & Davison, P.F. (1980) *Biopolymers* **19**, 1861-1873.

Bulleid, N.J., Dalley, J.A. & Lees, J.C. (1997) *EMBO J.* **16**, 908-916.

Byers, P.H., Click, E.M., Harper, E. & Bornstein, P. (1975*) Proc. Natl. Acad. Sci. USA* **72**, 3009-3013.

Chen, C.C. & Boskey, A.L. (1985) *Calcif. Tissue Int.* **37**, 395-400.

Chen, C.C. & Boskey, A.L. (1986) *Calcif. Tissue Int.* **39**, 324-327.

Christofferson, J. & Landis, W.J. (1991) *Anat. Rec.* **230**, 435-450.

Chu, M.L. & Prockop, D.J. (1993) in *Connective Tissues and its Inheritable Disorders: Molecular, Genetic & Medicinal Aspects.* (Royce, P.M. & Steinmann, B. eds), pp 149-165, Wiley-Liss Inc.

Davis, J.M., Boswell, B.A. & Bachringer, H.P. (1989) *J. Biol. Chem.* **264**, 8956-8962.

de Jong, L., van der Kraan, I. & de Waal, A. (1991) *Biochemistry* **27**, 150-155.

Doane, K.J., Babiarz, J.P., Fitch, J.M., Linsenmayer, T.F. & Birk, D.E. (1992) *Exp.Cell Res.* **202**, 113-124.

Doyle, B.B., Hukins, D.W., Hulmes, D.J., Miller, A., Rattew, C.J. & Woodhead Galloway, J. (1974) *Biochem. Biophys. Res. Commun.* **60**, 858-864.

Eanes, E.D., Lundy, D.R. & Martin, G.N. (1970) *Calcif. Tissue Res.* **6**, 239-248.

Einarsson, S., Josefsson, B. & Largerkvisit, S. (1983) *J. of Chromatography* **282**, 609-618.

Einarsson, S. (1985) *J. of Chromatography* **348**, 213-220.

Endo, A (1987) *J. Jpn. Orthop. Assoc.* **61**, 563-575.

Engel, J. & Prockop, D.J. (1991) *Annu. Rev. Biophys. Biophys. Chem.* **20**, 137-152.

Eyre, D.R. & Glimcher, M.J. (1973) *Biochem. Biophys. Res. Commun.* **52**, 663-671.

Eyre, D.R. & Oguchi, H. (1980)*) Biochem. Biophys. Res. Commun.* **92**, 403-410.

Fernàndez-Moràn, H & Engström, A. (1957) *Biochim. Biophys. Acta* **23**, 260-264.

Fietzek, P.P., Altmann, H., Rauterberg, J. & Wachter, E. (1977*) Proc. Natl. Acad. Sci. USA* **74**, 84-86.

Firschein, H.E. & Shill, J.P. (1966) *Anal* **14**, 296-304.

Fisher, L.W., Termine, J.D., Dejter, S.W., Whitson, S.W., Yanagishita, M., Kimura, J.H., Hascall, V.C., Kleinman, H.K., Hassell, J.R. & Nilsson, B. (1983a) *J. Biol. Chem.* **258**, 6588-6594.

Fisher, L.W., Whitson, S.W., Avioli, L.V. & Termine, J.D (1983b) *J. Biol. Chem.* **258**, 12723-12727.

Fratzl, P., Fratzl-Zelman, N., Klaushofer, K., Vogl, G. & Koller, K. (1991) *Calcif. Tissue Int.* **48**, 407-413.

Fratzl, P., Groschner, M., Vogl, G., Plenk, H., Eschberge, J., Fratzl-Zelman, N., Koller, K., & Klaushofer, K. (1992) *J. Bone Miner. Res.* **7**, 329-334.

Fratzl, P., Fratzl-Zelman, N. & Klaushofer, K. (1993) *Biophys. J.* **64**, 260-266.

Fratzl, P. (1994) *J. Stat. Phys.* **77**, 125-143.

Fratzl, P., Schreiber, S. & Klaushofer, K. (1995) *Proceedings of the 5th International Conferance on the Chemistry and Biology of Mineralized Tissues* (In Press)

Fratzl, P., Schreiber, S. & Klaushofer, K. (1996) *Connect. Tissue Res.* **34**, 247-254.

Frazer, R.D.B. & MacRae, T.P. (1973) in Conformation of Fibrous Proteins, Academic Press, New York.

Frazer, R.D.B., MacRae, T.P., Miller, A. & Suzuki, E. (1983) *J.Mol. Biol.* **167**, 497-521.

Frazer, R.D.B., MacRae, T.P. & Miller, A. (1987) *J.Mol. Biol.* **193**, 115-125.

Fujimoto, D. (1977) *Biochem. Biophys. Res. Commun.* **76**, 1124-1129.

Fujimoto, D. (1980) *Biochem. Biophys. Res. Commun.* **93**, 948-953.

Gadelata, S.J., Camacho, N.P., Mendelsohn, R. & Boskey, A.L. (1996) *Calcif. Tissue Int.* **58**, 17-23.

Glimcher, M.J. (1984) *Philos. Trans. R. Soc. Lond. Biol.* **304**, 479-508.

Hashimoto, Y., Lester, G.E., Caterson, B. & Yamauchi, M. (1995) *Calcif. Tissue Int.* **56**, 398-402.

Hauschka, P.V. & Wians Jr., F.H. (1989) *Anat. Rec.* **224**, 180-188.

Hayashi, T. & Nagai, Y. (1974) *J. Biochem.* **76**, 177-186.

Hodge, A.J. & Petruska, J.A. (1962) in Electron Microscopy (Breese, S.S., Jr, ed.), vol. 1, Paper QQ-1, Academic Press, New York.

Hodge, A.J. & Petruska, J.A. (1963) in Aspects of Protein Structure (Ramachandran, G.N. ed) pp 289-300, Academic Press, New York.

Höhling, H.J., Ashton, B.A. & Koster, H.D. (1974) *Cell Tissue Res.* **148**, 11-26.

Höhling, H.J., Arnold, S., Plate, U., Stratmann, U. & Wiesmann, H.P. (1997) *Adv. Dent. Res.* **11**, 426-466.

Holden, J.L., Clement, J.G. & Phlakey, P.P. (1995) *J. Bone Miner. Res.* **10**, 1400-1409.

Holmes, D.F., Watson, R.B., Chapman, J.A. & Kadler, K.E. (1996) *J. Mol. Biol.* **261**, 93-97.

Hosemann, R., Dreissig, W. & Nemetschek, T. (1974) *J. Mol. Biol.* **83**, 275-280.

Hulmes, D.J.S., Miller, A., Parry, D.A., Piez, K.A. & Woodhead Galloway, J. (1973) *J. Mol. Biol.* **79**, 137-148.

Hulmes, D.J.S., Miller, A., White, S.W. & Doyle, B.B. (1977) *J. Mol. Biol.* **110**, 643-666.

Hulmes, D.J.S. & Miller, A. (1979) *Nature* **282**, 878-880.

Hulmes, D.J.S. & Miller, A. (1981) *Nature* **293**, 239-244.

Hulmes, D.J.S., Holmes, D.F. & Cummings, C. (1985) *J. Mol. Biol.* **184**, 473-477.

Hulmes, D.J.S., Wess, T.J., Prockop, D.J. & Fratzl, P. (1995) *Biophys. J.* **68**, 1661-1670.

Hunter, G.K., Allen, B.L., Grynpas, M.D. & Cheng, P.T. (1985) *Biochem. J.* **228**, 463-469.

Hunter, G.K & Goldberg, H.A. (1993) *Proc. Natl. Acad. Sci. USA* **90**, 8562-8565.

Hunter, G.K. & Szigety, S.K. (1992) *Matrix* **12**, 362-368.

Hunter, G.K. (1991) *Clin. Orthop. Rel. Res.* **262**, 256-280.

Johansen, E. & Parks, H.F. (1960) *J. Biophys. Biochem. Cytol.* **7**, 713-746.

Kadler, K.E., Hulmes, D.J.S., Hojima, Y. & Prockop, D.J. (1990) *Ann. N.Y. Acad. Sci.* **580**, 214-224.

Kadler, K.E. (1994) in Protein Profile, vol 1, pp535-549, Academic Press.

Landis, W.J., Hodgens, K.J., Arena, J., Song, M.J.A. & McEwen, B.F. (1996) *Microscopy Research and Techniques* **33**, 192-202.

Lee, D.D., & Glimcher, M.J. (1989) *Connect. Tissue Res.* **21**, 247-257.

Lee, D.D., & Glimcher, M.J. (1991) *J. Mol. Biol.*. **217**, 487-501.

Lee, S.T., Lee, S. Peters, D.P., Hoffman, C.G., Stacey, A. & Greenspan, D.S. (1992) *J. Biol. Chem.* **267**, 24126-24133.

Lees, S., Bonar, L.C. & Mook, H.A. (1984) *Int. J. Biol. Macromol.* **6**, 321-326.

Lees, S. (1987) *Conn. Tissue Res.* **16**, 281-303.

Lees, S. & Prostak, K.S. (1988) *Connect. Tissue Res.* **18**, 41-54.

Lees, S. & Hukins, D.W.L. (1992) *Bone and Mineral* **17**, 59-63.

Lees, S & Page, E.A. (1992) *Connect. Tissue Res.* **28**, 263-287.

Lees, S., Prostak, K.S., Ingle, V.K. & Kjoller, K. (1994) *Calcif. Tissue Int.* **55**, 180-189.

Lussi, A., Crenshaw, M.A. & Linde, A. (1988) *Arch. Oral Biol.* **33**, 685-691.

Mandelkow, E., Mandelkow, E.M. & Bordas, J. (1981) *Eur. J. Cell Biol.* **24**, 336.

Marchi, F. & Leblond, C.P. (1983) *Am. J. Anat.* **168**, 167-197.

Matsushima, N., Akiyama, M. & Terayama, Y. (1982) *Jpn. J. Appl. Phys.* **21**, 186-189.

Meek, K.M., Chapman, J.A. & Hardcastle, R.A. (1979) *J. Biol. Chem.* **254**, 10710-10714.

Miller, A. & Parry, D.A.D. (1973) *J. Mol. Biol.* **75**, 441-447.

Miyahara, M., Njieha, F.K. & Prockop, D.J. (1982) *J. Biol. Chem.* **257**, 8442-8448.

Mopper, K. & Johnson L. (1983) *J. of Chromatography* **256**, 27-38.

Nagata, K. & Hosokawa, N. (1996) *Cell Struct. Funct.* **21**, 425-430.

Nagata, K. (1998) *Matrix Biol.* **16**, 379-386.

Nakahara, H & Kakei, M. (1984) *Bull. Josai. Dent. Univ.* **13**, 259-263.

Ogawa, T., Ono, T., Tsuda, M. & Kawanishi, Y. (1982) *Biochem. Biophys. Res. Commun.* **107**, 1252-1257.

Otsubo, K., Katz, E.P., Mechanic, G.L., & Yamauchi, M. (1992) *Biochemistry* **31**, 396-402.

Parry, D.A.D. & Craig, A.S. (1984) in Ultrastructure of the Connective Tissue Matrix (Ruggen, A. & Motta, P.M. eds) pp 34-64, Martinus Nijhoff, Boston.

Partridge, S.M. & Elsden, D.F. (1961) *Biochem. J.* **80**, 34p.

Pihlajaniemi, T., Myllyla, R. & Kivirikko, K.I. (1991) *J. Hepatology* **13**, S2-S7

Piez, K.A. & Trus, B.L. (1981) *Biosci. Rep.* **1**, 801-810.

Porod, G. (1951) *Kolloid Zeitschrift* **124**, 83-114.

Posner, A.S. (1985) *Clin. Orthop.* **200**, 87-99.

Posner, A.S. (1987) in Bone and Mineral Research 5 (Peck, W.A. ed) pp 65-116., Elsevier Science Publishers, B.V.

Pratt, D.A., Daniloff, Y., Duncan, A. & Robins, S.P. (1992) *Anal. Biochem.* **207**, 168-175.

Price, R.I., Lees, S. & Kirschner, D.A. (1997) *Int. J. Biol. Macromol.* **20**, 23-33.

Prince, C.W., Oosawa, T., Butler, W.T., Tomana, M., Bhown, A.S., Bhown, M. & Schrohenloher, R.E. (1987) *J. Biol. Chem.* **262**, 2900-2907.

Ramachandran, G.N. & Reddi, A.H. , Eds (1976) Biochemistry of Collagen, pp 45-84 Plenum, New York.

Rey, C., Miquel, J.L., Facchini, L., Legrand, A.P. & Glimcher, M.J. (1995) *Bone* **16**, 583-586.

Robins, S.P. & Bailey, A.J. (1973a) *Biochem. J.* **135**, 657-665.

Robins, S.P. & Bailey, A.J. (1973b) *FEBS Lett.* **33**, 167-171.

Robins, S.P., Shimokomaki, M. & Bailey, A.J. (1973) *Biochem. J.* **131**, 771-780.

Robins, S.P. & Bailey, A.J. (1975) *Biochem. J.* **149**, 381-385.

Robins, S.P. & Duncan, A. (1983) *Biochem. J.* **215**, 175-182.

Robins, S.P. & Duncan, A. (1987) *Biochim. Biophys. Acta* **914**, 233-239.

Robinson, R.A. (1952) *J. Bone Joint Surg.* **34A**, 389-434.

Robinbson, R.A. & Watson, M.L. (1952) *Anat. Rec.* **114**, 383-410.

Romanowski, R., Jundt, G., Termine, J.D., von der Mark, K. & Shultz, A. (1990) *Calcif. Tissue Int.* **43**, 155-161.

Romberg, R.W., Werness, P.G., Riggs, B.L. & Mann, K.G. (1986) *Biochemistry* **25**, 1176-1180.

Roth, M. (1971) *Anal. Chem.* **43**, 880-882.

Roufose, A.H., Landis, W.J., Sabine, W.K. & Glimcher, M.J. (1979) *J. Ultrastruct. Res.* **68**, 235-255.

Sarkar, S.K., Hiyama, Y.,Nin, C.H.,Young, P.E., Gerig, J.T. & Torchia, D.A. (1987) *Biochem.* **26**, 6793-6800.

Siegal, R.C. (1979) *Int. Rev. Conn. Tiss. Res.* **8**, 73-118.

Smedsrod, B., Melkko, J., Risteli, L. & Risteli, J. (1990) *Biochem. J.* **271**, 345-350.

Smith, J.W. (1968) *Nature (London)* **29**, 157-158.

Snigirev, A., Snigireva, I., Riekel, C., Miller, A., Wess, L. & Wess, T. (1993) *Journal de Physique IV* **3**, 443-446.

Speckman, T.W. & Norris, W.P. (1957) *Science* **126**, 753.

Steve-Bocciarelli, D. (1970) *Calcif. Tissue Int.* **5**, 261-269.

Tanzer, M.L., Housley, T., Berube, L., Fairweather, R., Franzblau, C. & Gallop, P.M. (1973) *J. Biol. Chem.* **248**, 393-402.

Termine, J.D., Kleinman, H.D., Whitson, S.W., Conn, K.M., McGarvey, M.L. & Martin, G.R. (1981a) *Cell* **26**, 99-105.

Termine, J.D.,Belcourt, A.B., Conn, K.M & Kleinman, H.D. (1981b) *J. Biochem.* **256**, 10403-10408.

Torchia, D.A. & Sazabo, A. (1985) *J. Magn. Reson.* **64**, 135-141.

Truab, W., Arad, T. & Weiner, S. (1989) *Proc. Natl. Acad. Sci. USA* **86**, 9822-9826.

Traub, W., Arad, T. & Weiner, S. (1992a) *Matrix* **12**, 251-255.

Traub, W., Arad, T. & Weiner, S. (1992b) *Connect. Tissue. Res.* **28**, 99-111.

van der Loo, P.G., Soute, B.A., van Haarlem, L.J. & Vermeer, C. (1987) *Biochem. Biophys. Res. Commun.* **142**, 113-119.

van der Rest, M. & Garrone, R. (1991) *FASEB J.* **5**, 2814-2823.

Veis, A. & Yuan, L. (1975) *Biopolymers* **14**, 895-900.

Volpi, M & Katz, E.P. (1991) J. *Biomech.* **24**, 67-77.

Vuorio, E. & de Crombrugghe, B. (1990) *Ann. Rev. Biochem.* **59**, 837-872.

Wang, C., Eyre, D.R., Clark, R., Kleinberg, D., Newman, C., Iranmanesh, A., Veldhuis, J., Dudley, R.E., Berman, N., Davidson, T., Barstow, T.J., Sinow, R., Alexander, G. & Swerdloff, R.S. (1996) *J. Clin. Endocrinol. Metab.* **81**, 3654-3662.

Weiner, S. & Price, P.A. (1986) *Calcif. Tissue Int.* **39**, 365-375.

Weiner, S. & Traub, W. (1986) *FEBS* **206**, 262-266.

Wess, T.J., Miller, A. & Bradshaw, J.P. (1990) *J. Mol. Biol.* **213**, 1-5.

Wess, T.J., Hammersley, A., Wess, L. & Miller, A. (1995) *J.Mol. Biol.* **248**, 487-493.

Wess, T.J., Hammersley, A., Wess, L. & Miller, A. (1998) *J.Mol. Biol.* **275**, 255-267.

White, S.W., Hulmes, D.J.S., Miller, A. & Timmins, P.A. (1977) *Nature* **266**, 421-425.

Whitson, S.W., Whitson, M.A., Bowers Jr, D.E. & Falk, M.C. (1992) *J. Bone Miner. Res.* **7**, 727-741.

Wilson, R., Lees, J.F. & Bulleid, N.J. (1998) *J. Biol. Chem.* **273**, 9637-9643.

Woodhead Galloway, J., Hukins, D.W.L. & Wray, J.S. (1975) *Biochem. Biophys. Res. Commun.* **64**, 1237-1244.

Woodhead-Galloway, J. & Machin, P.A. (1976) *Acta. Crystallogr.* **A32**, 368-372.

Yamauchi, M., Katz, E.P. & Mechanic, G.L. (1986) *Biochem.* **25**, 4907-4913.

Yamauchi, M., Woodley, D.T. & Mechanic, G.L. (1988a) *Biochem. Biophys. Res. Commun.* **152**, 898-903.

Yamauchi, M., Young, D.R., Chandler, G.S. & Mechanic, G.L. (1988b) *Bone* **9**, 415-418.

Yamauchi, M., Katz, E.P., Kazunori, O., Teraoka, K. & Mechanic, G.L. (1989) *Connect.Tissue Res.* **21**, 159-169.

Yamauchi, M. & Katz, E.P. (1993) *Connect. Tissue Res.* **29**, 81-98.

Ziv, V. & Weiner, S. (1994) *Connect. Tissue Res.* **30**, 165-175.

Appendix 2: Abbreviations List

ASPEC	Automated Sample Preparation with Elution Columns
BSP	Bone Sialoprotein
CPM	Counts Per Minute
DHLNL	Dihydroxylysinonorleucine
DMEM	Dulbeccos Modified Eagles Medium
DPD	Deoxypyridinoline
EM	Electron Microscope
ESRF	European Synchrotron Radiation Facility
FACIT	Fibril Associated Collagens with Interrupted Triple Helices
FCS	Foetal Calf Serum
FMOC	9-Fluorenylmethyl chloroformate
FWHM	Full Width Half Maximum
HHL	Histidino-hydroxylysinonorleucine
HHMD	Histidino-hydroxymerodesmosine
HLNL	Hydroxylysinonorleucine
HNV	Hydroxynorvaline
HPLC	High Pressure Liquid Chromatography
ITS	Insulin, Transferrin and Selenium
MIN	Mineralized
MMP	Matrix Metalloproteinase
NMR	Nuclear Magnetic Resonance
NONMIN	Nonmineralized
OPA	*o*-phthaldialdehyde
PBS	Phosphate Buffered Saline
PYD	Pyridinoline
RP-HPLC	Reversed Phase High Pressure Liquid Chromatography
SAXS	Small Angle X-ray Scattering
SEM	Scanning Electron Microscope
SRP	Signal Recognition Particle
SRS	Synchrotron Radiation Source
TEM	Transmission Electron Microscope
TLT	Turkey Leg Tendon

Appendix 1. Amino Acids

Ala	Alanine
Asx	Asparagine or Aspartic Acid
Cys	Cysteine
Asp	Aspartic Acid
Glu	Glutamic Acid
His	Histidine
Ile	Isoleucine
Lys	Lysine
Hyl	Hydroxylysine
Leu	Leucine
Met	Methionine
Asn	Asparagine
Pro	Proline
Hyp	Hydroxyproline
Gln	Glutamine
Arg	Arginine
Ser	Serine
Thr	Threonine
Val	Valine
Trp	Tryptophan
Tyr	Tyrosine
Glx	Glutamine or Glutamic Acid